Development of Solvent Selection Criteria Based on Diffusion Rate, Mixing Quality, and Solvent Retrieval for Optimal Heavy-Oil and Bitumen Recovery at Different Temperatures

by

Andrea Paola Marciales Ramirez

A thesis submitted in partial fulfillment of the requirements for the degree of

Master of Science

in

Petroleum Engineering

Department of Civil and Environmental Engineering
University of Alberta

Abstract

Heavy-oil and bitumen recovery requires high recovery factors to offset the extreme high cost of the process. Attention has been given to solvent injection for this purpose and it has been observed that high recoveries are achievable when combined with steam injection. Heavier ("liquid") solvents (liquid at ambient conditions) are especially becoming more popular to be used in these processes due to availability and transportation. "Liquid" solvents are advantageous as they yield a better mixing quality (especially with very heavy-oils and bitumen) but a lower diffusion rate than lighter solvents like propane or butane. Despite this understanding, there is still not a clear screening criterion for solvent selection considering both diffusion rate and the quality of the mixture.

Therefore, two main solvent selection criteria parameters—diffusion rate and mixing quality—were proposed to evaluate solvent injection efficiency at different temperatures for a defined set of solvent-heavy oil pairs of varying properties and composition. Diffusion rate, viscosity, and density reduction were among the test carried out through bulk liquid-liquid interaction.

Then, core experiments at different temperatures were performed on Berea sandstone samples using the same set of oil-solvent pairs already defined to obtain the optimum carbon size (solvent type)-heavy oil combination that yields the highest recovery factor and the least asphaltene precipitation. Based on the fluid-fluid (solvent-heavy oil) interaction experiments and heavy-oil saturated rock-solvent interaction tests, the optimal solvent type was determined considering the fastest diffusion and best mixing quality for different oil-solvent combinations.

In all these applications, the retrieval of expensive solvent is essential for the economics of the process. This led to a micro scale analysis to clarify the dynamics of solvent retrieval from matrix under variable temperatures at atmospheric pressure. The reasons of the entrapment of the solvent during this process were investigated for different wettability conditions, solvent type, and heating process carrying out visualization experiments on micromodels.

The experimental and semi-analytical outcome of this research would be useful in determining the best solvent type for a given oil and in understanding the key factors that influence the quality of mixtures, including: (1) viscosity reduction and probable asphaltene precipitation, (2) the optimal solvent type considering the fastest recovery rate and ultimate recovery for different heavy oil-solvent combinations at different temperatures, and, (3) the visualization of the solvent recovery mechanisms at the pore scale.

In loving memory of my beautiful grandma Marlene, who showed me her endless love until her very last day on earth. Love you always, miss you always.

Acknowledgments

First and foremost I am grateful to God for providing me with all the opportunities throughout my life and for giving me the capabilities needed to develop my research.

I would like to offer my sincerest gratitude to my supervisor, Dr. Tayfun Babadagli, for his consistent and effective support full of patience and knowledge. I am thankful for all the time and effort he invested on this work and his guidance in my professional development.

This research was conducted under my supervisor Dr. Tayfun Babadagli´s NSERC Industrial Chair in Unconventional Oil Recovery (Industrial partners are Schlumberger, CNRL, SUNCOR, Petrobank (Touchstone Exploration Inc.), Sherrit Oil, APEX Eng., PEMEX, Husky Energy and Statoil) and NSERC Discovery Grant (RES0011227). The funds for the equipment used in the experiments were obtained from the Canadian Foundation for Innovation (CFI) (Project # 7566) at the University of Alberta. I also extend thanks to them.

I am also thankful to my colleagues and friends, past and present members of EOGRRC group for their support and collaboration. I specially thank Francisco Arguelles-Vivas for his kind support in resolving different technical problems I faced during my experiments. I am also thankful to Georgeta Istratescu and Ly Bui for their technical support, and Pam Keegan for editing my papers and thesis.

CHAPTER 1: INTRODUCTION 1
INTRODUCTION 2
STATEMENT OF THE PROBLEM 3
AIMS AND OBJECTIVES 5
STRUCTURE OF THE THESIS 6
REFERENCES 7
CHAPTER 2: SOLVENT SELECTION CRITERIA BASED ON DIFFUSION RATE AND MIXING QUALITY FOR DIFFERENT TEMPERATURE STEAM/SOLVENT APPLICATIONS IN HEAVY-OIL AND BITUMEN RECOVERY 10
PREFACE 11
1. INTRODUCTION 12
2. EXPERIMENTAL METHODOLOGY 15
3. FREE DIFFUSION EXPERIMENTS 16
4. OBTAINING THE CONCENTRATION PROFILES OF MINERAL OIL SAMPLES 18
5. MIXTURE QUALITY EVALUATION BY VISCOSITY MEASUREMENTS AND ASPHALTENE TITRATION TESTS 21
6. SOLVENT SELECTION CONSIDERING DIFFUSION RATE AND MIXING QUALITY 22
7. CONCLUSIONS 24
REFERENCES 26
CHAPTER 3: SELECTION OF OPTIMAL SOLVENT TYPE FOR HIGH TEMPRATURE SOLVENT APPLICATIONS IN HEAVY-OIL AND BITUMEN RECOVERY 47
PREFACE 48
1. INTRODUCTION 49
2. EXPERIMENTAL METHODOLOGY 50
3. RESULTS 52

4. CONCLUSIONS AND REMARKS 56

APPENDIX 57

REFERENCES 57

CHAPTER 4: PORE SCALE INVESTIGATIONS ON SOLVENT RETRIEVAL DURING HEAVY-OIL RECOVERY AT ELEVATED TEMPERATURES: A MICROMODEL STUDY 73

PREFACE 74

1. INTRODUCTION 75

2. STATEMENT OF THE PROBLEM AND OBJECTIVES 76

3. THEORY: EFFECT OF PORE SIZE IN PHASE EQUILIBRIUM-KELVIN EFFECT: VAPOR PRESSURE AND BOILING POINT 77

4. EXPERIMENTAL METHODOLOGY 79

5. EXPERIMENTAL PROCEDURE 80

6. RESULTS 80

6 EFFECT OF HEAT DISTRIBUTION: EXPERIMENTS 1 AND 3 81

7. CONCLUSIONS AND REMARKS 85

CHAPTER 5: CONTRIBUTION AND RECOMMENDATIONS 102

MAJOR CONCLUSIONS AND CONTRIBUTIONS 103

RECOMMENDATIONS AND FUTURE WORK 105

LIST OF TABLES

CHAPTER 2..... 10
TABLE 1: SOLVENT PROPERTIES 29
TABLE 2: OIL SAMPLE PROPERTIES. LMO: LIGHT MINERAL OIL, HMO: HEAVY MINERAL OIL 29
TABLE 3: OIL SAMPLE PROPERTIES. OIL SAMPLE PROPERTIES. LMO:LIGHT MINERAL OIL, HMO: HEAVY MINERAL OIL 30
TABLE 4: MIXTURE DENSITIES FOR OIL 1 SAMPLE 30
TABLE 5: NORMALIZED PIXEL INTENSITY VS SOLVENT CONCENTRATION ..... **ERROR! BOOKMARK NOT DEFINED.**
CHAPTER 3..... 47
TABLE 1: OIL SAMPLE PROPERTIES 60
TABLE 2: SOLVENT PROPERTIES 60
TABLE 3: SATURATED CORES-SOLVENT EXPERIMENTS 62
CHAPTER 4.....73
TABLE 1. OIL AND SOLVENTS PROPERTIES. 89
TABLE 2. OIL (LMO -LIGHT MINERAL OIL), SOLVENT AND HEATING TYPE COMBINATIONS APPLIED DURING THE EXPERIMENTS. 90

LIST OF FIGURES

CHAPTER 2..... 10
FIGURE 1: BOILING RANGE DISTRIBUTION OF OIL SAMPLE AND DISTILLATE 31
FIGURE 2: MATLAB® APPROACH TO QUANTIFY THE PIXEL INTENSITIES AND EVENTUALLY DETERMINE THE CONCENTRATION PROFILES 32

FIGURE 3: PROFILE CHANGE INSIDE THE CAPILLARY TUBE DURING SOLVENT DIFFUSION 32
FIGURE 4: MICRO CT SCAN FOR THE CASE OF DARK OIL (OIL 2) – DISTILLATE PAIR IN DATAVIEWER® AT T = 0. 33
FIGURE 5: PROFILE CHANGE OVER 18 HOURS 33
FIGURE 6: CONCENTRATION PROFILES FOR CLB-C7 CASE 33
FIGURE 7: PRECIPITATED MATERIAL AT DIFFERENT CONCENTRATIONS OF SOLVENT IN OIL 1. 34
FIGURE 8: PRECIPITATED MATERIAL AT DIFFERENT CONCENTRATIONS OF SOLVENT IN OIL 2. 34
FIGURE 9: PRECIPITATED MATERIAL AT DIFFERENT CONCENTRATIONS OF SOLVENT IN OIL 3. 35
FIGURE 10: DIFFUSION COEFFICIENT VS. TIME FOR LIGHT MINERAL OIL (LMO) 35
FIGURE 11: DIFFUSION COEFFICIENT VS. SOLVENT CONCENTRATION FOR LIGHT MINERAL OIL (LMO) 36
FIGURE 12: DIFFUSION COEFFICIENT VS. TIME FOR HEAVY MINERAL OIL (HMO). 36
FIGURE 13: DIFFUSION COEFFICIENT VS. SOLVENT CONCENTRATION FOR HEAVY MINERAL OIL (HMO). 37
FIGURE 14: DIFFUSION COEFFICIENT VS. TIME FOR DARK OIL (OIL 1) 37
FIGURE 15: DIFFUSION COEFFICIENT VS. SOLVENT CONCENTRATION FOR DARK OIL (OIL 1). 38
FIGURE 16: DIFFUSION COEFFICIENT VS. TIME FOR DARK OIL (OIL 2 38
FIGURE 17: DIFFUSION COEFFICIENT VS. SOLVENT CONCENTRATION FOR DARK OIL (OIL 2). 39
FIGURE 18: DIFFUSION COEFFICIENT VS. TIME FOR DARK OIL (OIL 3) 39
FIGURE 19: DIFFUSION COEFFICIENT VS. SOLVENT CONCENTRATION FOR DARK OIL (OIL 3) 40
FIGURE 20: DIFFUSION RATE AGAINST VISCOSITY AT DIFFERENT CONCENTRATIONS OF SOLVENT IN OIL 1 40

FIGURE 21: DIFFUSION RATE AGAINST VISCOSITY AT DIFFERENT CONCENTRATIONS OF SOLVENT IN OIL 2. 41
FIGURE 22: DIFFUSION RATE AGAINST VISCOSITY AT DIFFERENT CONCENTRATIONS OF SOLVENT IN OIL 3. 41
FIGURE A 1: DENSITY AT DIFFERENT CONCENTRATIONS OF SOLVENT IN OIL..... 142
FIGURE A 2: DENSITY AT DIFFERENT CONCENTRATION OF SOLVENT IN OIL 2. 42
FIGURE A 3: DENSITY AT DIFFERENT CONCENTRATIONS OF SOLVENT IN OIL 3. 43
FIGURE A 4: VISCOSITY AT 25 °C FOR DIFFERENT CONCENTRATIONS OF SOLVENT IN OIL 1 43
FIGURE A 5: VISCOSITY AT 50 °C FOR DIFFERENT CONCENTRATIONS OF SOLVENT IN OIL 3. 44
FIGURE A 6: VISCOSITY AT 25 °C FOR DIFFERENT CONCENTRATIONS OF SOLVENT IN OIL 3 44
FIGURE A 7: VISCOSITY AT 50 °C FOR DIFFERENT CONCENTRATIONS OF SOLVENT IN OIL 1 45
FIGURE A 8: VISCOSITY AT 50 °C FOR DIFFERENT CONCENTRATIONS OF SOLVENT IN OIL 2. 45
FIGURE A 9: VISCOSITY AT 50 °C FOR DIFFERENT CONCENTRATIONS OF SOLVENT IN OIL 3 46
CHAPTER 3..... 47
FIGURE 1: BOILING RANGE DISTRIBUTION OF OIL SAMPLES AND DISTILLATE 60
FIGURE 2: A—BEREA SANDSTONE CORE SATURATED WITH HEAVY OIL, B) BEGINNING OF THE SOLVENT SOAKING EXPERIMENT, AND C) CHANGED IN THE COLOR OF THE SURROUNDING FLUID (OIL SOLVENT MIXTURE) DUE TO DIFFUSION PROCESS AT SOAKING TIMES >150 HOURS. 61

FIGURE 3: CORES AND SOLVENT HEATED TO SETTLED TEMPERATURE, B) MEASURED CORE CHANGE WEIGHT, C) CORE AND SOLVENT PLACED IN CONTACT AT THE SAME TEMPERATURE IN A SEALED IMBIBTION CELL, D) SOAKING TEST RUN AT DETERMINED TEMPERATURE AND REFRACTIVE INDEX TAKEN PERIODICA 61
FIGURE 4: RECOVERY RATES FOR OIL 1: EXPERIMENTS 4,5 AND 6 61
FIGURE 5: RECOVERY RATES FOR OIL 2: EXPERIMENTS 7, 8 AND 9 63
FIGURE 6: RECOVERY RATES FOR OIL 3: EXPERIMENTS 10, 11 AND 12 63
FIGURE 7: RECOVERY RATES FOR MINERAL OIL: EXPERIMENTS 1,2 AND 3. .. 63
FIGURE 8: RECOVERY RATES FOR CORES SATURATED WITH OIL 1 FOR EXPERIMENTS RUN AT A) 25°C, B) 50°C AND C) 80°C 64
FIGURE 11: ULTIMATE RECOVERY SUMMARY 67
FIGURE 13: SOLVENT CONCENTRATION AND SOAKING TIME EFFECT ON EXPERIMENTS RUN AT 25°C FOR CORES SATURATED IN OIL 2 69
FIGURE 15: CORES SATURATED WITH OIL 3 LEFT AFTER EXPERIMENT AT 50°C WERE RUN IN EXPERIMENTS; A) 28, B)29 AND C)30 71
FIGURE A1: MOLECULAR DIFFUSION COEFFICIENT VS. SOLVENT CONCENTRATION FOR MINERAL OIL (MODIFIED FROM FIG. 9 OF MARCIALES AND BABADAGLI 2014). 72
FIGURE A2: MOLECULAR DIFFUSION COEFFICIENT VS. SOLVENT MASS FRACTION FOR OIL 1 (MODIFIED FROM FIG. 10 OF MARCIALES AND BABADAGLI 2014). 72
FIGURE A3: MOLECULAR DIFFUSION COEFFICIENT VS. SOLVENT CONCENTRATION FOR OIL 2 (MODIFIED FROM FIG. 11 OF MARCIALES AND BABADAGLI 2014). 72
CHAPTER 4..... 73
FIGURE 1. MICROMODEL SCHEME AND PICTURE AREA. 90
FIGURE 2. EXPERIMENTAL SET UP. 91
FIGURE 3. BOILING RANGE DISTRIBUTION FOR LMO AND DISTILLATE. 92
FIGURE 4. SCHEMATIC REPRESENTATION OF HEAT DISTRIBUTION: A) MATRIX, B) FRACTURE 92

FIGURE 5. MICROMODEL AFTER SOLVENT SATURATION AND BEFORE STARTING THE HEATING STEP FOR EXPERIMENT 1. 93
FIGURE 6. BUBBLE GROWTH FOR FRACTURE HEATING TYPE IN EXPERIMENT 1. 93
FIGURE 7. MACRO VISUALIZATION OF SOLVENT VAPORIZATION PATTERNS FOR ALL THE EXPERIMENTS AT DIFFERENT TIMES. "0 MIN" CORRESPONDS TO THE POINT FIRST BUBBLE IS OBSERVED 94
FIGURE 8. SOLVENT RETRIEVAL MECHANISM. 95
FIGURE 9. MICROMODEL BEFORE SOLVENT PHASE CHANGE IN EXPERIMENT 3. 95
FIGURE 10. PHASE CHANGE OF SOLVENT WHEN HOMOGENEOUS (WHOLE SYSTEM) HEATING IS APPLIED IN EXPERIMENT 3. 96
FIGURE 11. RECOVERY MECHANISMS AND BUBBLE MIGRATION IN EXPERIMENT 3. 96
FIGURE 12. TIME EFFECT IN HOMOGENEOUS HEATING. 96
FIGURE 13. PORE AND MATRIX OIL-SOLVENT SATURATION BEFORE ANY PHASE CHANGE IN EXPERIMENT 2. 97
FIGURE 14. SOLVENT EVAPORATION AFTER 6 HOURS OF CONSTANT HEATING 97
FIGURE 15. MIXING QUALITY IMPROVED DUE TO TEMPERATURE INCREASE IN EXPERIMENT 4. 97
FIGURE 16. SOLVENT RECOVERY MECHANISM FOR EXPERIMENT 4. 99
FIGURE 17. MATRIX OIL-SOLVENT MIXING BEFORE A) TEMPERATURE INCREASE ANDB) PHASE CHANGE IN EXPERIMENT 5. 99
FIGURE 18. RECOVERY MECHANISM IN EXPERIMENT 5 100
FIGURE 19. WATER-WET VS. OIL-WET CASE 100
FIGURE 20. VAPOR PHASE STABILITY WATER-WET (A AND B) VS. OIL-WET CASE (C AND D). 101

CHAPTER 1: INTRODUCTION

Introduction

Alberta produced 76% of Canada´s oil equivalent production in 2013 with marked bitumen representing 56% of this total. Meanwhile, Alberta's ultimate potential recoverable reserves were estimated to be 315 billion barrels of crude bitumen and only 5.4% of it has been produced since its commercial production started in 1967 (AER 2014).

A great portion of the above-mentioned production (by in-situ recovery) has been achieved by thermal methods, predominantly steam. Due to inefficiency of the steam injection process, the use of different types of solvents (hydrocarbon and CO_2) has been under consideration for several decades as an alternative method to accelerate the viscosity reduction process as well as in-situ upgrading.

The solvent injection was initially suggested as cold injection and different aspects of this method were studied for a specific case called VAPEX (vapor extraction) (Butler and Mokrys 1991, 1993). Due to its inefficiency (mainly cause by its high cost), the idea of improving oil recovery led to combining it with thermal methods, either in the form of co-injection with steam (Allen and Redford 1976; Farouq Ali and Abad 1973; Farouq Ali 1976; Das 1996a-b; Nasr et al. 2003, 2005; Li and Mamora 2011) or by alternate injection (Zhao 2004; Zhao et al. 2005; Al-Bahlani and Babadagli 2011a-b, 2012; Pathak et al. 2011, 2012, 2013).

Despite numerous laboratory and computational analysis of different versions of solvent injection, technical and economic concerns still exist causing delays in its commercialization. An optimization of the process is required to minimize the cost and maximize the recovery and its retrieval (Edmunds et al. 2009; Al-Gosayir et al. 2012a-b, 2013; Mohammed and Babadagli 2013). This complicated exercise is typically done to reduce the amount of solvent used while maximizing its retrieval and oil recovery. Before determining the optimal conditions by applying exhaustive optimization schemes, it is necessary to select the most suitable solvent based on application (temperature, cyclic injection, continuous injection), reservoir type (oil sands, fracture carbonates), and oil

composition (viscosity, asphaltene content, density), as well as the cost and availability of solvent (Naderi and Babadagli 2014a-b; Naderi et al. 2014).

In this optimization process, the primary task is to select the proper solvent for given application conditions (temperature, injected amount), reservoir type, and oil composition (Gupta and Picherack 2003; Naderi and Babadagli 2014a-b; Naderi et al. 2014), as well as to understand the mechanisms for its retrieval after its use. This requires a selection process that optimizes the recovery rate and ultimate recovery.

Statement of the Problem

It is a well-known fact that lower carbon number solvents (typically propane and butane) yield a faster diffusion into oil and oil-saturated rocks (Al-Bahlani and Babadagli 2011a-b). Therefore, higher carbon number solvents (from pentane up to C11-C15 carbon number range distillate oil) are more preferable for better mixing; yielding higher ultimate recovery with less asphaltene deposition (Naderi et al. 2014). But, with this type of "heavy" solvents, the diffusion rate is much slower compared to the "lighter" ones.

Mixing quality is the other factor in solvent-oil systems and was primarily quantified by evaluating the solvent effect on oil viscosity reduction while avoiding asphaltenes precipitation. This standard of solvent evaluation was studied by transport industry, which looks for the best solvent to ease transportation through pipelines by diluting heavy oil to reduce its viscosity. It is recommended to use a diluent with sufficiently effective polar components to reduce oil viscosity with minimal asphaltenes precipitation (Gateau et al. 2004). Correlations are also available for heavy-oil solvent mixtures to be used in different process modeling purposes (Mehrotra 1992). Other works related to the solubility of asphaltenes in n-alkanes were performed through heavy oil titration tests (Kolal et al. 1992; Rassamdana et al. 1996; Buenrostro-Gonzalez et al. 2004). In these experiments, each heavy oil-solvent pair was diluted at several ratios and different soaking times. Then, the resulting mixture was passed through a filter paper that was rinsed with the n-alkanes employed and dried to estimate the precipitated asphaltenes by weight difference.

Then, two critical properties of solvents need to be evaluated in solvent selection processes for in-situ upgrading and effective heavy-oil/bitumen recovery:

(1) Diffusion rate: the solvent's ability to penetrate into the heavy oil, which will affect the oil recovery rate, and;
(2) Mixing quality: the solvent's ability to reduce oil viscosity minimizing asphaltene precipitation, which will eventually affect the ultimate recovery.

In all solvent applications, the retrieval of expensive solvent is essential for the economics of the process. Numerous experimental work at the core scale were presented to clarify the physics (Al-Bahlani and Babadagli, 2011b) and optimal operation conditions (Al-Bahlani and Babadagli, 2011a-b; Pathak et al. 2011, 2012, 2013; Naderi and Goskuner, 2014) of the solvent retrieval process. Visual studies are needed to clarify the dynamics of the solvent recovery at non-isothermal conditions and the reasons behind the solvent entrapment in the matrix.

These aspects of solvent methods for heavy-oil recovery need to be studied from a fluid-fluid (oil-solvent) interaction in porous media point of view. Then, it is prudential to extend the study to core experiments in order to understand how the diffusion rate and mixing quality affect oil recovery (carrying out solvent-rock tests) and to micromodels (micro fluidic devices) in order to clarify the physics of the solvent retrieval process at the pore scale via visualization. In these attempts, the following questions need to be answered:

(1) Temperature effect: Is there any optimal temperature that maximizes oil recovery and minimizes the solvent cost?
(2) Which method is more efficient? Higher solvent concentration that is run for shorter soaking time or higher soaking time with a smaller amount of solvent?
(3) What are the relative contributions of gravity and diffusion rate affecting the recovery?
(4) What are the optimal conditions to minimize solvent entrapment during its retrieval at the pore scale?

This research addresses these questions. In an attempt to provide answers, a step-by-step procedure is established and summarized in the following section.

Aims and Objectives

This research aims to perform the following objectives:

1. Establish a case of study to represent different sets of pairs combining:
   - solvent type
   - oil type

2. Determine bulk diffusion rate for each pair by:
   - developing an optical using UV light
   - applying x-ray cat (computer axial tomography)

3. Evaluate the mixing quality for each pair analyzing the effects of:
   - viscosity and density reduction
   - solvent concentration
   - asphaltene precipitation

4. Examine solvent performance at different temperatures in porous media evaluating:
   - recovery rate
   - ultimate recovery
   - solvent concentration
   - soaking time

5. Cross check solvent bulk properties to porous media efficiency between:
   - recovery rate - diffusion rate
   - ultimate recovery - mixing quality

6. In addition to the above listed aims mainly related to heavy-oil recovery by solvent injection, clarification of the solvent retrieval process at the end of the process using:
   - micro scale investigation of solvent retrieval under variable temperature
   - parametric analysis for different heating conditions and rock wettability

Structure of the Thesis

This is a paper-based thesis and is composed of four chapters. The main body is constructed from three papers that have been submitted or prepared for peer-reviewed journals. Versions of Chapter 2 and Chapter 3 were presented at two conferences. Chapters 2 to 4 contain their own introduction, literature survey, results, conclusions, and references.

CHAPTER 1

This chapter provides an introduction to the thesis and an overview. Here, a brief background about solvent evaluation in bulk and rock experiments are discussed. After this, the statement of the problem, major objectives, and goals are summarized.

CHAPTER 2

This chapter contains a study for fluid-fluid (oil-solvent) interactions. Two main solvent selection criteria parameters—diffusion rate and mixing quality—are considered to evaluate solvent injection efficiency at different temperatures. An optical method under static conditions along with image processing techniques are proposed to determine one-dimensional diffusivity of liquid solvent into a wide range of oil samples. The ideal solvent types for different oil types are determined using the results from the diffusion rate and mixing quality experiments.

CHAPTER 3

As a continuation of Chapter 2, this chapter investigates fluid-rock (solvent-oil-sandstone) interactions. Sandstone samples saturated with three different heavy-oils are exposed to solvent diffusion at static conditions at different temperatures. Recovery rate and ultimate recovery (and asphaltenes left behind) controlled by the diffusion rate and mixing quality are measured. Solvent-rock and liquid-liquid (from Chapter 2) results are correlated. The ideal solvent types, representing the optimal recovery rate and ultimate recovery, are determined for liquid solvents in the carbon number range of C7 to C13, and heavy oil types with a viscosity range on different orders of magnitude.

CHAPTER 4

This chapter provides a pore scale investigation of solvent retrieval for heterogeneous systems. Solvent diffused into tighter matrix from highly permeable medium (fracture, wormholes, high permeability streaks) are retrieved by boiling. The effects of temperature, wettability, and heating conditions on the retrieval efficiency are investigated.

CHAPTER 5

This chapter contains the contributions and achievements of this thesis and also provides recommendations for future work.

References

1. Al-Bahlani, A.M. and Babadagli, T. 2011a. Field Scale Applicability and Efficiency Analysis of Steam-Over-Solvent Injection in Fractured Reservoirs (SOS-FR) Method for Heavy-Oil Recovery. *J. Petr. Sci. and Eng.* **78**: 338-346.
2. Al-Bahlani, A.M. and Babadagli, T. 2011b. SOS-FR (Solvent-Over-Steam Injection in Fractured Reservoir) Technique as a New Approach for Heavy-Oil and Bitumen Recovery: An Overview of the Method. *Energy and Fuels* **25** (10): 4528-4539.
3. Al-Bahlani, A.M. and Babadagli. 2012. Laboratory Scale Experimental Analysis of Steam-Over-Solvent Injection in Fractured Reservoirs (SOS-FR) for Heavy-Oil Recovery. *J. Petr. Sci. and Eng*. **84-85**: 42-56.
4. Al-Bahlani, A.M. and Babadagli, T. 2012. Visual Analysis of Diffusion Process During Oil Recovery Using Hydrocarbon Solvents and Thermal Methods. *Chem. Eng. J*. (181 182): 557-569.
5. Alberta Energy Regulator (AER). ST98-2014: Alberta´s Energy Reserves 2013 and Supply/Demand Outlook 2014-2023.
6. Al-Gosayir, M., Leung, J. and Babadagli, T. 2012a. Design of Solvent-Assisted SAGD Processes in Heterogeneous Reservoirs Using Hybrid Optimization Techniques. *J. Can. Pet. Tech*. **51** (6) 437-44.
7. Al-Gosayir, M., Babadagli, T., and Leung, J. 2012b. Optimization of SAGD and Solvent Additive SAGD Applications: Comparative Analysis of Optimization Techniques with Improved Algorithm Configuration. *J. Petr. Sci. and Eng*. (98-99): 61-68.
8. Al-Gosayir, M., Leung, J., Babadagli, T. et al. 2013. Optimization of SOS-FR (Steam-Over-Solvent Injection in Fractured Reservoirs) Method Using Hybrid Techniques: Testing Cyclic Injection Case. *J. Petr. Sci. and Eng.* **110**: 74-84.
9. Allen, J.C. & Redford, A.D. 1976. Combination Solvent-Noncondensable Gas Injection Method for Recovering Petroleum from Viscous Petroleum-Containing Formations Including Tar Sad Deposits, US Patent No. 4,109,720.
10. Buenrostro-Gonzalez, E., Lira-Galeana,C., Gil-Villegas, A. et al. 2004. Asphaltene Precipitation in Crude Oils: Theory and Experiments. *AIChE Journal*. **50** (10),

2552-2570
11. Butler, A.M and Mokrys, I.J. 1993 Recovery of Heavy Oils Using Vaporized Hydrocarbon Solvents: Further Development of the Vapex Process. *J. of Canadian Petr. Tech*. **32**: 56-62
12. Das, S.K. and Butler, R.M. 1996a. Countercurrent Extraction of Heavy Oil and Bitumen. Paper SPE 37094 presented at the International Conference on Horizontal Well Technology, Calgary, Alberta, Canada, 18-20 November.
13. Das, S.K. and Butler, R.M. 1996b. Diffusion Coefficients of Propane and Butane in Peace River Bitumen. *Can. J. Chem. Eng*. **74**: 986-992.
14. Edmunds, N., Maini, B., and Peterson, J. 2009. Advanced Solvent-Additive Processes via Genetic Optimization. Paper PETSOC 2009-115 presented at Canadian International Petroleum Conference (CIPC) 2009, Calgary, Alberta, Canada, 16-18 June.
15. Farouq, A. and Snyder, S.G. 1973. Miscible Thermal Methods Applied to a Two-Dimensional, Vertical Tar Sand Pack, With Restricted Fluid Entry. *J. Can. Pet. Tech*. **12** (4): 22-26
16. Farouq, A. 1976. Bitumen Recovery from Oil Sands, Using Solvents in Conjunction with Steam. *J. Can. Pet. Tech*. **15** (3).
17. Gateau, P., Hénaut, L., Barré, L. et al. 2004. Heavy Oil Dilution. *Oil & Gas Science and Technology* **59** (5): 503-509.
18. Gupta, S. and Picherack, P. 2003. Insights into Some Key Issues with Solvent Aided Process. *J. Can. Pet. Tech*. **43 (**2): 54-61.
19. Kolal S., Najman J. and Sayegh, S. 1992.Measurement and Correlation of Asphaltene Precipitation from Heavy Oils by Gas Injection. *J. Can. Pet. Technol.* **31** (04): 24-30
20. Li, W. and Mamora, D.D. 2011. Light-and Heavy-Solvent Impacts on solvent-Aided-SAGD Process: A Low-Pressure Experimental Study. *J. Can. Pet. Tech*. **50** (4): 19-30.
21. Mehrotra, A.K., Sheika, H., and Pooladi-Darvish, M. 2006. An Inverse Solution Methodology for Estimating the Diffusion Coefficient of Gases in Athabasca Bitumen from Pressure-Decay Data. *J. Pet. Sci. Eng*. **53** (3-4): 189-202
22. Mohammed, M. and Babadagli, T. 2013. Efficiency of Solvent Retrieval during Steam-Over-Solvent Injection in Fractured Reservoirs (SOS-FR) Method: Core Scale Experimentation. Paper SPE -165528-MS presented at the SPE Heavy Oil Conference, Calgary, AB, 11-13 June.
23. Naderi, K. and Babadagli, T. 2014a. Use of Carbon Dioxide and Hydrocarbon Solvents During the Method of Steam-Over-Solvent Injection in Fractured Reservoirs for Heavy-Oil Recovery From Sandstones and Carbonates. Accepted for publication in SPE *Res. Eval. and Eng*. 2014.
24. Naderi, K. and Babadagli, T. 2014b. An Evaluation of Solvent Selection Criteria and Optimal Application Conditions for the Hybrid Applications of Thermal and Solvent Methods. Submitted to *J. of Canadian Petr. Tech*. 2014b (in review).
25. Naderi, K., Babadagli, T., and Coskuner, G. 2014. Bitumen Recovery by the SOS-FR (Steam-Over-Solvent Injection in Fractured Reservoirs) Method: An Experimental Study on Grosmont Carbonates. *Energy and Fuels* **27** (11): 6501-6517.
26. Naderi, K., Babadagli, T., and Coskuner, G. 2014. Bitumen Recovery by the SOS-

FR (Steam-Over-Solvent Injection in Fractured Reservoirs) Method: An Experimental Study on Grosmont Carbonates. *Energy and Fuels* **27** (11): 6501-6517.
27. Nasr, T.N., Beaulieu, G. Golbeck, H. et al. 2003. Novel Expanding Solvent-SAGD Process "ES-SAGD". *Can. Pet. Tech.* (technical note) **42** (1): 13-16.
28. Nasr, T.N. and Ayodele, O.R. 2005. Thermal Techniques for the Recovery of Heavy Oil and Bitumen. Paper SPE 97488 presented at the SPE Int. Imp. Oil Rec. Conf., Kuala Lumpur, Malaysia, 5-6 December.
29. Pathak, V., Babadagli, T. and Edmunds, N.R. 2011. Heavy Oil and Bitumen Recovery by Hot Solvent Injection. *J. Petr. Sci. and Eng.,* **78**: 637-645.
30. Pathak, V., Babadagli, T. and Edmunds, N.R. 2012. Mechanics of Heavy Oil and Bitumen Recovery by Hot Solvent Injection. *SPE Res. Eval. and Eng.*, **15** (2): 182-194.
31. Pathak, V., Babadagli, T. and Edmunds, N.R. 2013. Experimental Investigation of Bitumen Recovery from Fractured Carbonates Using Hot-Solvents. *J. of Canadian Petr. Tech...* **52** (4): 289-295.
32. Rassamdana H., Dabir B., Nematy, M. et al. 1996. Asphalt Flocculation and Deposition: I. The Onset of Precipitation. *AIChE Journal*. **42** (1): 10-22
33. Zhao, L. 2004. Steam Alternating Solvent Process. Paper SPE 86957 presented at the International Thermal Operations and Heavy Oil and Western Regional meeting, Bakersfield, California, 16-18 March.
34. Zhao, L., Nasr, T., Huang, G., et al. 2005. Steam Alternating Solvent Process: Lab Test and Simulation. *J. Can. Pet. Tech.* **44** (9): 37-43.

CHAPTER 2: SOLVENT SELECTION CRITERIA BASED ON DIFFUSION RATE AND MIXING QUALITY FOR DIFFERENT TEMPERATURE STEAM/SOLVENT APPLICATIONS IN HEAVY-OIL AND BITUMEN RECOVERY

This paper is a modified and improved version of SPE 169291, which was submitted at the SPE Conference held in Maracaibo, Venezuela, 21–23 May 2014. A version of this chapter has been submitted to the Journal of Canadian Petroleum Technology.

Preface

Heavy-oil and bitumen recovery requires high recovery factors to offset the extreme high cost of investments and operations. Attention has been given to solvent injection for this purpose and it has been observed that high recoveries are achievable when combined with steam injection. Heavier ("liquid") solvents (liquid at ambient conditions) are especially becoming more popular due to availability and transportation. High oil prices allow the application of this kind of technique if a proper design is made to retrieve the injected solvent efficiently. "Liquid" solvents are advantageous as they yield a better quality mixing (especially with very heavy-oils and bitumen) but a lower diffusion rate than lighter solvents like propane or butane. Despite this understanding, there still is not a clear screening criterion for solvent selection to mitigate both diffusion rate and the quality of the mixture.

In this study, two main solvent selection criteria parameters—diffusion rate and mixing quality—were considered to evaluate solvent injection efficiency at different temperatures. An optical method under static conditions along with image processing techniques were proposed to determine one-dimensional diffusivity of liquid solvent into a wide range of oil samples in a capillary tube. This sampling range varied from 40 cp oil to 250 cp, for which digital image treatment was developed. X-ray computerized tomography was applied for heavier (and darker) oils (viscosity range of 20,000 cp to 400,000 cp). The diffusion coefficients were then computed through non-linear curve fitting based on an optimization algorithm to assure that the obtained values were in agreement with available analytical solutions. Next, viscosity measurements and asphaltene precipitation for the same heavy-oil/solvent mixtures were performed to determine the mixing quality. The ideal solvent types for different oil types were determined using the results from the diffusion rate and mixing quality experiments.

The experimental and semi-analytical outcome of this research would be useful in determination of the best solvent type for given oil and in understanding the key factors that influence the quality of mixtures including viscosity reduction and probable asphaltene precipitation.

1. Introduction

Solvent injection has been under consideration for several decades as an alternative method for reducing heavy-oil/bitumen viscosity as well as upgrading it in-situ. Initially, it was suggested as cold solvent injection and different studies were carried out considering different types of hydrocarbon solvents (Butler and Mokrys 1991, 1993). Due to its high cost for industrial applications, the idea of improving oil recovery led to combining it with thermal methods either in the form of co-injection with steam (Allen and Redford 1976; Farouq and Abad 1973; Farouq 1976; Das 1996a-b; Nasr et al. 2003, 2005; Li and Mamora 2011) or by alternate injection (Zhao 2004; Zhao et al. 2005; Al-Bahlani and Babadagli 2011a-b, 2012; Pathak et al. 2011, 2012, 2013).

Despite numerous laboratory and computational analysis of different versions of solvent injection, technical and economic concerns still exist causing delays in its commercialization. An optimization of the process is required to minimize the cost and maximize the recovery and its retrieval (Edmunds et al. 2009; Al-Gosayir et al. 2012a-b, 2013; Mohammed and Babadagli 2013). This complicated exercise is typically done to reduce the amount of solvent used while maximizing its retrieval and oil recovery. Before determining the optimal conditions by applying exhaustive optimization schemes, it is necessary to select the most suitable solvent based on application (temperature, cyclic injection, continuous injection), reservoir type (oil sands, fracture carbonates), and oil composition (viscosity, asphaltene content, density) as well as the cost and availability of solvent (Naderi and Babadagli 2014a-b; Naderi et al. 2014).

In the solvent selection process, two factors play a critical role: (1) Diffusion rate, i.e., the rate of solvent mass transfer into heavy oil, and (2) mixing quality, i.e., lowered viscosity with minimal asphaltene precipitation. Historically, the tendency was to use lighter solvents (propane, butane) in the form of gas (Butler and Mokrys 1991, 1993) in heavy-oil recovery. However, despite its high diffusion rate, the mixing quality is low, causing significant asphaltene deposition (Moreno and Babadagli 2014a-b). Because of this fact, higher carbon number has been also tested in the form of gas (Nasr and Ayodele 2005; Ayodele et al. 2010; Keshavarz et al. 2013) or liquid (Naderi et al. 2014). As the carbon number of the solvent increases, the diffusion decreases but mixing be higher quality (Al-

Bahlani and Babadagli 2011b; Coskuner et al. 2013). The mixing quality will be even better if solvents with aromatic content (distillate oil, condensates, light oils) are used rather than single component alkanes (Coskuner et al. 2013; Naderi et al. 2014).

As can be inferred from the above summary, detailed studies combining both factors—i.e., diffusion rate and mixing quality—are needed in the solvent selection process. Attention was paid to the diffusion rate measurement in the past. These techniques are classified by their ability to avoid any disturbance to the system during experimentation and, hence, can be in the form of intrusive or non-intrusive experiments (Guerrero 2009). Non-intrusive experiments were found to be more suitable to determine the solvent rate of penetration since they minimize the errors when solvent concentration was measured (Guerrero and Kantzas 2009). Different free diffusion techniques were developed for this purpose depending on the solvent phase. Riazi (1996) proposed the pressure decay method for diffusion rate calculation in heavy oil that uses an expression of gaseous solvent concentration as a function of pressure decreasing inside the closed system caused by. This method can be named "standard" when low molecular weight solvents are used (Guerrero 2009) and improved versions of this approach were also reported (Ghaderi et al 2011; Zhang et al. 2000; Creux et al. 2005; Upreti and Mehrotra 2000; Mehrotra et al. 2006). More recently, the Pendant Drop Shape Analysis (PDSA) was proposed as an improved methodology, including the effect of oil swelling due to solvent penetration when a drop of oil was pending in a closed medium surrounded by gaseous solvent (Yang and Gu 2003).

For liquid-liquid systems, different optical methods were also proposed. These methods were based on the ability of the source and detectors implemented to register the spatial solvent distribution while the experiment was running. Initially, Oballa and Butler (1989) measured the diffusion rate of toluene into Cold Lake bitumen using laser and reported a value on the order of 10^{-8} cm^2/sec. Nuclear Magnetic Resonance (NMR) was also used for the same purpose (Wen et al. 2005a-b). In this method, the T2 relaxation time of the hydrocarbon samples in the NMR spectra were used to identify the solvent concentration in the mixture, which varied in the range of 5-15% in weight. The reported diffusion rates of heptane (C_7), decane (C_{10}), and distillate solvents in bitumen and heavy oil samples were on the order of 10^{-7} to 10^{-9} cm^2/sec. Recently, the application of X-ray scattering was found to

be useful for measuring the mixing rates (Weng et al. 2004; Afshani and Kantzas 2007; Guerrero 2009; Guerrero and Kantzas 2009).

With the exception of the PDSA (Yang and Gu 2003), all of these non-intrusive methods used a closed system in which the heavy oil component was placed at the bottom and the solvent was carefully injected on top. In this case, the interface of the system can be taken as a reference point for further mathematical analysis in which the data was fitted into the analytical solutions available in the literature. This problem was found to be mathematically described as one dimensional diffusing solvent in a static closed vial. In other words, there is no mass transfer with the environment, the interface between solvent and oil is fixed, there is no change in global volume, and Fickian diffusion occurs only in one direction. This means that the mass flow from the solvent to solute (oil) is only due to the concentration gradient. These statements are summarized mathematically as mass transfer problem in an extended initial distribution medium as follows-(Crank 1975; Bird et al. 2001):

$$\left(\frac{\partial C}{\partial t}\right)_x = D\left(\frac{\partial^2 C}{\partial x^2}\right)_t \tag{1}$$

where:

At t = 0

$C = C_o$ For $x < 0$ (above the oil interface) and $C = 0$ for $x > 0$,

For t > 0, $C = \frac{1}{2}Co$ at $x = 0$,

x direction is increasing downwards.

The analytical solution to this system leads to the following (Crank 1975):

$$C = \frac{1}{2}Co * erfc\left(\frac{x}{2\sqrt{Dt}}\right) \tag{2}$$

This equation describes the concentration profile along the axial axe of the vial at different times with an average diffusion coefficient and gives an idea about the rate or ability of the specified solvent to penetrate into heavier hydrocarbon. The magnitude of this parameter is [length^2/ time] and for the solvents employed in this study, the diffusion coefficient values

fall into a range between 10^{-5} to 10^{-8} cm^2/sec (Guerrero 2009; Wen et al 2005a; Wen et al. 2005b) at 25 °C, depending on the system in consideration.

Mixing quality is the other factor in solvent-oil systems and was primarily quantified by evaluating the solvent effect on oil viscosity reduction while avoiding asphaltenes precipitation. This standard of solvent evaluation was studied by transport industry, which looks for the best solvent to transport heavy oil through pipelines by reducing viscosity. It is recommended to use a diluent with sufficiently effective polar components to reduce oil viscosity with minimal asphaltenes precipitation (Gateau et al. 2004). Correlations are also available for heavy-oil solvent mixtures to be used in different process modeling purposes (Mehrotra 1992). Other works related to the solubility of asphaltenes in n-alkanes were performed through heavy oil titration tests (Kolal et al. 1992; Rassamdana et al. 1996; Buenrostro-Gonzalez et al. 2004). In these experiments, each heavy oil-solvent pair was diluted at several ratios and different soaking times. Then, the resulting mixture was passed through a filter paper that was rinsed with the n-alkanes employed and dried to estimate the precipitated asphaltenes by weight difference.

The present study focuses on selection of proper solvents by cross-checking the diffusion (mixing) rate and mixing quality. A combination of four heavy oil types and three solvents with a wide range of viscosities and densities were used to provide a general framework. Diffusion experiments were performed using UV lights and X-ray CAT. To test the mixing quality, viscosity and asphaltene precipitation measurements were carried out for different oil-solvent mixtures. Using this data with diffusion rate measurements, a selection of proper solvent type for a wide variety of heavy oils is presented.

2. Experimental Methodology

2.1 *Materials*.

A case of study was established to understand and evaluate solvent selection criteria for heavy-oil recovery processes. Three different solvents and four different oil samples were selected to achieve this objective: Light mineral oils (LMO) and heavy mineral oils (HMO) and three crude oils (Oil 1, Oil 2, and Oil 3) obtained from three different fields in Alberta,

Canada. The solvent and oil samples are summarized in **Tables 1 to 3.** The viscosity data for heptane and decane given in Table 1 were taken from literature (Dymond and Oye 1993). **Figure 1** shows their boiling range distribution obtained through gas chromatograph (GC) analysis under specified standards, which is also specified in Table 3.

3. Free Diffusion Experiments

Diffusion experiments are designed to generate the change in the concentration profile when two miscible fluids are in contact and require proper visualization technique. Because the processed oil samples (mineral oils in **Table 2**) are transparent, optical techniques are applicable. For heavy oil samples (Oil 1, Oil 2, and Oil 3 in Table 2), however, one has to take advantage of advanced visualization techniques such as X-ray CAT or nuclear magnetic resonance (NMR). The procedure and observations are summarized below.

3.1 *Free diffusion experiments with mineral oil samples.*

When the mineral oil was employed inside a capillary tube, the concentration of the -dyed-solvent inside the mixture was tracked by measuring its pixel intensity using a digital camera. For these experiments, the solvents were dyed with yellow fluorescent color DFSB-K43 (Risk Reactor Inc. 2005) composed of n-butyl-4-(butylamino) 1, 8-naphthalalimide – FUROL 555 (Curtis and Nikiforos 2006), which was excited by a 405 nm UV LED of 5610 lumen inside a dark box. A CANON 7D camera with a 50 mm lens was set at a 3’’2 shutter speed and 4.5 aperture. To avoid possible noises, a S-W 040 - Orange 550 (Schneider Optische 2007) filter was used to simply block possible blue lights allowing only red and yellow lights to pass through the lens.

Initially, the standard patterns of different pixel intensities were created for various solvent concentrations. In this process, 0wt%, 30wt%, 50wt%, 70wt%, and 100wt% solvent concentrations in the mixtures were registered and the pixel intensities in red, green, blue (RGB) colors were measured using MATLAB®. Then, statistical analyses were performed to minimize the standard deviation in quantification of pixel values for various solvent concentrations. Next, the capillary tubes were filled with mineral oil from the bottom by capillary imbibition until its level reached a certain height. The solvent was injected very carefully at the top of the capillary tube using a 29G needle to assure it comprises 20wt% of

the total amount of fluids in the tube. Finally, the tubes were sealed with epoxy resin to avoid any solvent loss and were placed carefully in the dark box in vertical position. The camera was programmed to take images every hour for a minimum of 10 hours. Further analysis of the images collected was carried out in the MATLAB® environment.

3.2 *Free diffusion experiments with dark oil samples.*

As a quick and nondestructive method for three-dimensional visualization and characterization of opaque objects, high-resolution X-ray computed tomography (CT) was selected as a methodology to determine the diffusion rate for crude oil samples. This technique differs from conventional medical CAT scanning in the resolution of the information obtained, which is up to a few microns in size. This technique has been applied successfully in medicine and further extended to geosciences (Ketcham 2001). The success of the–application of this methodology requires the proper configuration of micro-CT scanner, in terms of X-ray energy, image resolution, and attenuation vs. density calibration.

In our experiments, a SkyScan1176 micro CT scanner was employed using image pixel size 35 μm at 35kv to obtain the average attenuation coefficient for each pure sample. The X-ray attenuation was calibrated using a commercially standardized phantom (a material made of calcium hydroxyapatite (CaHA) of known density (SkyScan 2013)). The equation that relates equivalent bone mineral density (BMD) with X-ray attenuation coefficient under these specifications is expressed as follows:

$$BMD\ \left[\frac{g}{cm^3}\right] = \frac{AC - 0.060945}{-0.05065} \tag{3}$$

where:

AC = attenuation coefficient

To run the free diffusion tests, dark oil samples (Oil 1, Oil 2, and Oil 3) were placed inside a plastic vial and solvent was carefully added at the top until the total concentration of solvent was 20wt% in the vial. Then, the sample was closed and scanned during the first 10 hours in order to obtain its attenuation coefficient through each slide (of average length of 35 μm) at every hour.

4. Obtaining the Concentration Profiles of Mineral Oil Samples

To calculate the diffusion rate, it is necessary to obtain the concentration profiles. This depends on the ability of the employed technique to differentiate the solvent from the oil in the system while it is diffusing into each other.

4. 1 *Mineral oil samples (optical method).*

In order to quantify the concentration profile, the images obtained from the experiments at different times were treated by applying the following steps:

1. The entire capillary tube was selected from the picture.
2. The green pixel intensity was averaged for each line in the abscissa along the length of the tube.
3. Each averaged value was normalized between 0 and 1 after using the following equation (Spotfire 2012):

$$(ei)_{norm} = \frac{e_i - \min(Ei)}{\max(Ei) - \min(Ei)} \tag{4}$$

where:

$e_i =$ original pixel intensity (G)
$(ei)_{norm} =$ normalized value (scaled between 0 and 1)
$\min(Ei) =$ minimum value for obtained pixel intensity
$\max(Ei) =$ maximum value for obtained pixel intensity

4. Each normalized value was transformed into weight percent solvent concentration. **Table 4** summarizes the obtained values through this procedure.
5. The units from coordinate axis were transformed from pixel scale to centimeter scale based on the distance from the camera to the objectives.
6. Finally, the concentration profiles were obtained.

Note that proper combination of camera filter and dye color was chosen to obtain the best color identification of the present phases. **Figure 2** shows the capillary tube and the intensity-concentration profiles of the LMO-C_7 case after applying steps 1 to 6 using MATLAB®. In this particular example, the red and blue distributions are also shown with

their corresponding colors. The green trend is more useful to recognize the solvent from oil compared to the blue and red trends as the wavelength emission of this dye is around 500 nm (Curtis and Nikiforos 2006), showing a green-yellow color shade (Risk Reactor Inc. 2005), and the filter used blocks mainly all light emissions below 500 nm (Schneider Optische 2007).

4. 2 ***Dark (crude) oil samples (X-ray CAT).***

All scanned samples were initially reconstructed using the standardized phantom as reference. Subsequently, the portion of the vial to be analyzed was selected in the DataViewer® software (**Figs. 4 and 5**) and the equivalent density was obtained for sections of 0.1 mm length. Eq. (3) was applied on a group of 33 slices inside the vial, each 35 μm in average, using the CTan® software. The equivalent density was then transformed into mixture density by correlating the BMD to the oil-solvent pair. Table 4 describes the BMD-Oil density correlation employed for Oil 1**. Figure 6** shows the concentration profile change for the Oil 3-C7 pair. After evaluating the sample density, the additive volume mixing rule was applied through Eq. (5) to calculate the mass fraction of solvent concentration:

$$X_{vs} = \frac{\rho_{mix} - \rho_o}{\rho_s - \rho_o} \tag{5}$$

where:

$X_{v\,s}$= solvent volume fraction (0-1)
ρ_{mix} = mixture density (g/cm^3)
ρ_o = bulk oil density (g/cm^3)
ρ_s = bulk solvent density (g/cm^3)

After obtaining the concentration profiles for each dark oil-solvent pair, the average diffusion rate values were calculated at different times using an algorithm developed in the MATLAB® environment. This algorithm is an unconstrained non-linear optimization model that minimizes the error between the experimental data and the analytical solution of Eq. (2), subject to the restriction of the fitting parameters (diffusion rate [cm^2/sec] and time [sec]). The optimization model is described as follows:

Min err = $\left(y_{i-lab} - y_{i-eqn2}\right)^2$

s.t. $\begin{cases} \text{1e-8} \leq D \leq \text{1e-3} \\ t_{exp-c} \leq t \leq t_{exp+c} \end{cases}$

where:

err = error function,

y_{i-lab} = concentration profile; i.e., solvent mass fraction vs. x-cm data obtained from the experiments,

y_{i-eqn2} = concentration profile in the same units as y_{i-lab} calculated from the optimized D and t,

t = time - sec from the start of the experiment that better fits the analytical solution for objective function minimization, which can vary from a very short period –c or +c, less than 10% of the time from which the data was obtained,

D = diffusion rate - cm^2/sec that better fits the analytical solution in Eq. (2). For this case, diffusion rate boundaries were left as wide as possible for less biased data.

After finding the average diffusion rate at each time, the concentration dependency of diffusion rate was determined applying the procedure proposed by Sarafianos (1996) and Guerrero (2009) using the following equations:

$$\frac{C}{C_\infty} = \frac{1}{2} * erfc(u) \tag{6}$$

$$erfc(u) = 1 - \text{erf}\,(u) \tag{7}$$

$$u = hx + k \tag{8}$$

$$\text{erf}(u) = \frac{2}{\pi}\int_0^\infty \exp\,(-z^2)\,dz \tag{9}$$

$$D = \frac{1}{4h^2 t}\left(1 - k\pi^{\frac{1}{2}} exp(u^2) erfc(u)\right) \tag{10}$$

Sarafianos (1996) indicated that C_∞ in Eq. (6) correspond to 100% of the diffusing component, which was metal for his experiments. Guerrero (2009) proposed a methodology

using Eqs. (6) through (10) to obtain the diffusion rate as a function of solvent concentration. The first step in this procedure is to obtain the concentration profile to estimate the $erfc(u)$ term in Eq. (6). Here, u is an introduced function that relates the spatial distribution of the concentration profile and can be obtained from the inverse calculation of the error function using Eq. (6) or by the employment of Eq. (7). At the next step, it is necessary to plot u against the spatial distribution (x) in order to find the relationship described by Eq. (8). In this equation, h is the slope and k is the tangent intercepting the ordinate axis and they should be determined at each point of u *vs.* x pair. Finally, Eq. (10) is used to estimate the diffusion coefficient for different solvent concentrations.

5. Mixture Quality Evaluation by Viscosity Measurements and Asphaltene Titration Tests

The efficiency of solvent was evaluated through its ability to reduce oil density and viscosity with minimum asphaltene precipitation. The precipitated asphaltene by each solvent was measured with titration tests as described in literature (Kokal et al. 1992; Rassamdana et al. 1996; Buenrostro-Gonzalez et al. 2004). In our case, 5 grams of each dark oil sample were mixed at room conditions and different proportions with specified solvents in Table 2. The resulting mixture went through 24 hrs of soaking in a closed system and then was filtered under vacuum using a filter paper Watman No. 42. The paper was rinsed with the corresponding n-alkane in order to isolate the insoluble material from oil and further dried for solvent evaporation. The weight difference in the filter paper was correlated to the precipitated material associated with asphaltenes. The distillate used to rinse the oil mixtures was filtered through a column employed for SARA analysis to remove the aromatic composition and better evaluate its impact on minimizing asphaltene precipitation. **Figures 7 to 9** show the results for Oil 1, 2, and 3 with solvents at different proportions.

The density and viscosity of dark oil solutions (20, 40, 60, and 80 wt% of solvent) were also measured. Densities were obtained at 25°C by a DDM 2910 Density Meter while the viscosities were measured at different temperatures using a Brookfield Programmable

LVDV-II+ Viscometer. Examples of density and viscosity changes with solvent concentrations in the mixture are given in the Appendix.

6. Solvent Selection Considering Diffusion Rate and Mixing Quality

Figures 10 to 19 illustrate the calculated values of diffusion rate at different times using Eq. (2) and its variation with concentration in accordance to the set of Eqs. (6) through (10). The single component cases (C7 and C10) followed a typical trend (an exponential change of the diffusion coefficient with time and solvent concentration) and, as expected, the lower the carbon number of solvent, the faster the solvent diffusion. These results are in agreement with the observations of Wen (2004), Guerrero (2009), and Guerrero and Kantzas (2009). A similar trend was also observed for the distillate cases with LMO and HMO (Figs. 10 through 13). However, in the cases of dark oil (Oil 1 and Oil 2), though the lightest solvent (C7) followed an exponential trend, the heavier solvents (C10 and distillate) yielded very weak diffusion responses with respect to time (Figs. 13 and 16). Diffusion coefficient did not change for Oil 1 (14) as time passed. As illustrated in Figures 14 and 15, C10 did not show any changes in the diffusion process even at high solvent concentrations. The same behavior was observed for the distillate case at early times; however, in this case, increasing solvent concentration resulted in an increase in the diffusion coefficient at late times. This could be attributed to the multi component nature of the distillate. In fact, this particular solvent contains aromatic compounds that are capable of dissolving asphaltenes, which eventually provides better mixing conditions. For the case of Oil 3, C7 and distillate diffusion rates were observed to be close to each other (Fig. 18), but distillate showed a faster diffusion than C7 at high solvent concentrations, as seen in Figure 19.

This characteristic behavior implies that distillate can be as effective as light hydrocarbon solvents (C7 in our case) in the long run. It might also be suggested to start the process with lighter solvents to take advantage of its high diffusion capability and subsequently continue with distillate type solvent, which is relatively inexpensive and readily available.

Another important issue to be addressed is the soaking time. It was observed that diffusion rate decreases as the soaking time increases. This is mainly due to a significant change in the quality of the present solvent at its interface with heavy oil, as the global concentration of solvent is constant during our experiment. This is in agreement with other observations (Zhang 2000; Wen 2004) and might necessitate the replenishing of solvent in cyclic stimulation type applications for a more effective diffusion process.

Figures 7 to 9 show the solvent efficiency in terms of asphaltene precipitation. This, in turn, would affect ultimate recovery when implemented in the reservoir. In our case, the least viscous dark Oil (Oil 1, Fig. 7) was found to precipitate the same amount of asphaltenes compared to the most viscous one (Oil 3, Fig. 9) at identical solvent ratios. This phenomenon might be explained with the proportional presence of resins/asphaltenes in the oil, which would determine the effect of crude composition and make the oil prone to precipitation as suggested by Kokal (1992).

It can also be observed that after the concentration of solvent in the mixture is higher than 10 cm^3/g oil, the precipitated amount increased. This is also in line with previous observations (Kolal et al. 1992; Rassamdana et al. 1996; Buenrostro-Gonzalez et al. 2004). Although experiments were carried out at atmospheric pressure, this asymptotic behavior at different solvent ratios was also observed at higher pressures (Akbarzadeh et al. 2004; Sabbagh et al. 2006). This would imply that when the solvent is applied inside the reservoir, there could be regions of high solvent concentration in which asphaltene precipitation would be at maximum and could cause pore blockage and reservoir impairment. Therefore, it is important to take asphaltene precipitation as an index of solvent quality into consideration.

As a general trend for the n-alkane case, it was found that C7 precipitates less material compared to C10; i.e., the lower the carbon number, the lower the precipitated material as in agreement with earlier observations (Kokal et al. 1992; Rassamdana et al. 1996; Buenrostro-Gonzalez et al. 2004; Moreno and Babadagli 2014a-b). In this study, the distillate was found to be the best solvent in terms of minimum asphaltene precipitation.

Again, this is due to the presence of aromatic components, which would lead to better asphaltene dilution in the mixtures.

As iteratively mentioned throughout the paper, the two characteristics that are critically important in solvent applications are (1) diffusion rate and (2) mixing quality. **Figures 20 to 22** present a cross-plot to indicate the impact of solvent concentration on both diffusion rate and viscosity reduction. As can be observed, an exponentially declining trend in viscosity accompanies the decreasing trend of diffusion coefficients, which is in agreement with previous observations by Das and Butler (1996b). The desirable region is high diffusion rate, low mixture viscosity, and low solvent concentrations. Initially, C7 appears to be the best solvent considering all three parameters but the distillate exhibits a similar trend to C7. The plots given in Figures 20 and 22 also verify the previous suggestion of starting the process with a light solvent and continuing with less expensive distillate.

7. Conclusions

(1) An image processing and analysis scheme was developed to measure the diffusion rate for different heavy-oil-solvent pairs. Optical and high resolution X-ray CAT methods were applied for transparent (mineral oils) and opaque (crude -dark- oil) oil samples, respectively. For both cases, the diffusion rate decreased when the carbon number of the solvent increased while also depending on time. In fact, the diffusion rate dropped down two orders of magnitude in later times suggesting that the most effective solvent application would occur in the early stages and the solvent should be replenished after this period.

(2) For the light (LMO and HMO) and dark (Oil 1 and Oil 2) oil cases, the diffusion rate was found to be strongly dependent on solvent concentration; i.e., it is an increasing monotonic function of solvent concentration, indicating that higher amounts of solvent would be needed for higher diffusion rates.

(3) Solvent concentration affects not only the diffusion rate but also the quality of mixture. It was observed as an exponentially declining trend in viscosity when diffusion coefficient was in a decreasing trend.

(4) For the light mineral oil cases, diffusion rate was not found to be strongly dependent on solvent concentration, contrary to the dark oil case, in which a different trend was obtained.

(5) Additionally, for the dark oil cases (Oil 1 and Oil 2), it was found that when solvent concentration increases up to 0.2 mass fraction at the interface of the mixture, diffusion rate increases up to one order of magnitude, suggesting that the most effective solvent application would be through the short periods of solvent replenish in which overall solvent concentration in the mixture is quite low.

(6) Distillate is as fast as C7 in Oil 3, especially at high solvent concentrations.

(7) In general, it was found for our cases that optimal solvent concentration falls in the range of 0.2 to 0.4 volume in the mixture because, at this concentration of solvent in the mixture, oil viscosity decreases dramatically (about half of the original value), diffusion rate is quite high and asphaltene precipitation is minimum.

(8) The distillate and C7 are the best candidates to be used as solvents when both diffusion rate and mixing quality were considered. However, considering the asphaltene dissolving capability, distillate could be as effective as light single component solvents at late stages. Then, one may suggest starting the process with lighter solvents to take advantage of its high diffusion capability and continue with distillate type solvent, which is relatively inexpensive and readily available.

Acknowledgements

This research was conducted under the second author's (TB) NSERC Industrial Research Chair in Unconventional Oil Recovery (industrial partners are CNRL, SUNCOR, Petrobank, Sherritt Oil, APEX Eng., PEMEX, Husky Energy, and Statoil). A partial support was also obtained from an NSERC Discovery grant (No: RES0011227). We gratefully acknowledge these supports.

Appendix

Examples of density and viscosity changes with solvent concentrations in the mixture

Figures A1-A9.

References

1. Akbarzadeh, K., Sabbagh, O. , Beck, J. et al. 2004. Asphaltene Precipitation from Bitumen Diluted With n-Alkanes. Paper presented at the Canadian International Petroleum Conf., Calgary, Alberta, Canada, 8-10 June.
2. Allen, J.C. and Redford, A.D. 1976. Combination Solvent-Noncondensable Gas Injection Method for Recovering Petroleum from Viscous Petroleum-Containing Formations including Tar Sad Deposits. US Patent No. 4,109,720.
3. Afshani, B. and Kantzas, A. 2007. Advances in Diffusivity Measurement of Solvents in Oil Sands. *J. Can. Pet. Tech.* **46** (11): 56-61.
4. Al-Bahlani, A.M. and Babadagli, T. 2011a. Field Scale Applicability and Efficiency Analysis of Steam-Over-Solvent Injection in Fractured Reservoirs (SOS-FR) Method for Heavy-Oil Recovery. *J. Petr. Sci. and Eng.* **78**: 338-346.
5. Al-Bahlani, A.M. and Babadagli, T. 2011b. SOS-FR (Solvent-Over-Steam Injection in Fractured Reservoir) Technique as a New Approach for Heavy-Oil and Bitumen Recovery: An Overview of the Method. *Energy and Fuels* **25** (10): 4528-4539.
6. Al-Gosayir, M., Leung, J. and Babadagli, T. 2012a. Design of Solvent-Assisted SAGD Processes in Heterogeneous Reservoirs Using Hybrid Optimization Techniques. *J. Can. Pet. Tech*. **51** (6) 437-44.
7. Al-Gosayir, M., Babadagli, T., and Leung, J. 2012b. Optimization of SAGD and Solvent Additive SAGD Applications: Comparative Analysis of Optimization Techniques with Improved Algorithm Configuration. *J. Petr. Sci. and Eng*. (98-99): 61-68.
8. Al-Gosayir, M., Leung, J., Babadagli, T. et al. 2013. Optimization of SOS-FR (Steam-Over-Solvent Injection in Fractured Reservoirs) Method Using Hybrid Techniques: Testing Cyclic Injection Case. J. *Petr. Sci. and Eng.* **110**: 74-84.
9. Ayodele, O. R., Nasr, T.N., Ivory, J. et al. 2010. Testing and History Matching ES-SAGD (Using Hexane). Paper SPE 134002 presented at the SPE West. Reg. Meet., Anaheim, California, 27-29 May.
10. Bird, R.B., Stewart, W.E., and Lightfool, E.N. 2001. *Transport Phenomena*, second Edition. New York: Wiley & Sons.
11. Buenrostro-Gonzalez, E., Lira-Galeana,C., Gil-Villegas, A. et al. 2004. Asphaltene Precipitation in Crude Oils: Theory and Experiments. *AIChE Journal*. **50** (10), 2552-2570
12. Curtis, C. and Nikiforos, K. 2006. Topical Composition Fluorescence Detection. US Patent No. 2,275,177 A1.
13. Coskuner, G., Naderi, K. and Babadagli, T. 2013. An Enhanced Oil Recovery Technology as a Follow Up to Cold Heavy Oil Production with Sand. Paper SPE 165385 presented at the SPE Heavy Oil Conf., Calgary, Alberta, and Canada11-13 June.
14. Crank, J. 1975. *The Mathematics of Diffusion*, second edition. Oxford: Clarendon Press.

15. Creux, P., Meyer, V., Cordelier, P. R., et al. 2005. Diffusivity in Heavy Oils. Paper SPE 97798 presented at the SPE International Thermal Operations and Heavy Oil Symposium, Calgary, Alberta, Canada, 1-3 November.
16. Das, S.K. and Butler, R.M. 1996a. Countercurrent Extraction of Heavy Oil and Bitumen. Paper SPE 37094 presented at the International Conference on Horizontal Well Technology, Calgary, Alberta, Canada, 18-20 November.
17. Das, S.K. and Butler, R.M. 1996b. Diffusion Coefficients of Propane and Butane in Peace River Bitumen. *Can. J. Chem. Eng*. **74**: 986-992.
18. Dymond, J.H. and Oye, H.A. 1994. Viscosity of Selected Liquid n-alkanes. *J. Phys. Chem. Ref. Data* **23**, 41.
19. Edmunds, N., Maini, B., and Peterson, J. 2009. Advanced Solvent-Additive Processes via Genetic Optimization. Paper PETSOC 2009-115 presented at Canadian International Petroleum Conference (CIPC) 2009, Calgary, Alberta, Canada, 16-18 June.
20. Farouq, A. 1976. Bitumen Recovery from Oil Sands, Using Solvents in Conjunction with Steam. *J. Can. Pet. Tech*. **3** (11).
21. Farouq, A. and Snyder, S.G. 1973. Miscible Thermal Methods Applied to a Two-Dimensional, Vertical Tar Sand Pack, With Restricted Fluid Entry. *J. Can. Pet. Tech*. **12 (**4): 22-26
22. Gateau, P., Hénaut, L., Barré, L. et al. 2004. Heavy Oil Dilution. *Oil & Gas Science and Technology* **59** (5): 503-509.
23. Ghaderi, S.M., Tabatabaie, S.H., Hassanzadeh, H. et al. 2011. Estimation of Concentration-Dependent Diffusion Coefficient in Pressure-Decay Experiment of Heavy Oils and Bitumen. *Fluid Phase Equilibria* **305** (2): 132-144.
24. Guerrero, U. 2009. The Diffusion Coefficient of Liquid and Gaseous solvents in Heavy Oil and Bitumen. MSC thesis, University of Calgary, Calgary, Alberta, Canada (September 2009).
25. Guerrero, U and Kantzas, A. 2009. Diffusion of Hydrocarbon Gases in Heavy Oil and Bitumen. Paper SPE 122783 presented at the SPE Latin American and Caribbean Petroleum Engineering Conference, Cartagena, Colombia, 31 May – 3 June.
26. Keshavarz, M., Okuno, R., and Babadagli, T. 2013. Optimal Application Conditions for Steam-Solvent Coinjection. Paper SPE 165471 presented at the SPE Heavy Oil Conference, Calgary, Alberta, Canada, 11-13 June.
27. Ketcham, R.A. 2001. Acquisition, Optimization and Interpretation of X-ray Computed Tomographic Imagery: Applications to the Geosciences. *Computers & Geosciences* **27**(4): 381-400.
28. Kolal S., Najman J. and Sayegh, S. 1992.Measurement and Correlation of Asphaltene Precipitation from Heavy Oils by Gas Injection. *J. Can. Pet. Technol.* **31** (04): 24-30
29. Li, W. and Mamora, D.D. 2011. Light-and Heavy-Solvent Impacts on solvent-Aided-SAGD Process: A Low-Pressure Experimental Study. *J. Can. Pet. Tech*. **50** (4): 19-30.
30. Mehrotra, A.K., Sheika, H., and Pooladi-Darvish, M. 2006. An Inverse Solution Methodology for Estimating the Diffusion Coefficient of Gases in Athabasca Bitumen from Pressure-Decay Data. *J. Pet. Sci. Eng*. **53** (3-4): 189-202
31. Mehrotra, A. 1992. A Model for the Viscosity of Bitumen/Bitumen Fractions-

Diluent Blends. *J. Can. Pet. Tech.* **31** (9): 28-32.
32. Mohammed, M. and Babadagli, T. 2013. Efficiency of Solvent Retrieval during Steam-Over-Solvent Injection in Fractured Reservoirs (SOS-FR) Method: Core Scale Experimentation. Paper SPE -165528-MS presented at the SPE Heavy Oil Conference, Calgary, Alberta, 11-13 June.
33. Moreno, L. and Babadagli, T. 2014a. Asphaltene Precipitation, Flocculation and Deposition During Solvent Injection at Elevated Temperatures for Heavy Oil Recovery. Accepted for publication in *Fuel* 2014.
34. Moreno, L. and Babadagli, T. 2014b.Quantitative and Visual Characterization of Asphaltenic Components of Heavy-Oil and Bitumen Samples after Solvent Interaction at Different Temperatures and Pressures. *Fluid Phase Equilibria* **366**: 74-87.
35. Naderi, K. and Babadagli, T. 2014a.Use of Carbon Dioxide and Hydrocarbon Solvents During the Method of Steam-Over-Solvent Injection in Fractured Reservoirs for Heavy-Oil Recovery From Sandstones and Carbonates. Accepted for publication in SPE *Res. Eval and Eng*. 2014.
36. Naderi, K., Babadagli, T. 2014b. An Evaluation of Solvent Selection Criteria and Optimal Application Conditions for the Hybrid Applications of Thermal and Solvent Methods. Submitted to *J. of Canadian Petr. Tech*. 2014b (in review).
37. Naderi, K., Babadagli, T., and Coskuner, G. 2014. Bitumen Recovery by the SOS-FR (Steam-Over-Solvent Injection in Fractured Reservoirs) Method: An Experimental Study on Grosmont Carbonates. *Energy and Fuels* **27** (11): 6501-6517.
38. Nasr, T.N. and Ayodele, O.R. 2005. Thermal Techniques for the Recovery of Heavy Oil and Bitumen. Paper SPE 97488 presented at the SPE Int. Imp. Oil Rec. Conf., Kuala Lumpur, Malaysia, 5-6 December.
39. Nasr, T.N., Beaulieu, G. Golbeck, H. et al. 2003. Novel Expanding Solvent-SAGD Process "ES-SAGD". *Can. Pet. Tech.* (technical note) **42** (1): 13-16.
40. Oballa, V. and Butler, R.M. 1989. An Experimental Study of Diffusion in the Bitumen-Toluene System. *Can. Pet. Tech.* **28** (2).
41. Rassamdana H., Dabir B., Nematy, M. et al. 1996. Asphalt Flocculation and Deposition: I. The Onset of Precipitation. *AIChE Journal*. **42** (1): 10-22
42. Riazi, M. R. 1996. A New Method for Experimental Measurement of Diffusion Coefficients in Reservoir Fluids. *J. Pet. Sci. Eng*. **14** (3): 235-250.
43. Risk Reactor Inc. 2005. Translucent Yellow Fluorescent Dye, http://www.riskreactor.com/translucent-yellow-fluorescent-dye-2/ (accessed 8 February 2014).
44. Sabbagh, O. Akbarzadeh, K. Badamchi-Zadeh, W.Y. et al. 2006. Applying the PR-EoS to Asphaltene Precipitation from n-Alkane Diluted Heavy Oils and Bitumens. *Energy & Fuels* **20**: 625-634
45. Sarafianos, N. 1996. An Analytical Method of Calculating Variable Diffusion Coefficients. *Journal of Materials and Science* **21** (7): 2283-2288.
46. Schneider Optische Werke GmbH. 2007. B + W Filters Professional Line,
47. http://www.schneiderkreuznach.com/fileadmin/user_upload/bu_photo_imaging/fotofilter/Produktfinder/Tipps_und_Tricks/B_W_Filter_Info_UEbersicht_Filtertypen_de.pdf (accessed 8 February 2014).
48. SkyScan. 2013. CT-Analyzer Version 1.13. The User's Guide,

http://www.skyscan.be/next/ctan_usermanual.pdf (accessed 15 October 2013).
49. Spotfire. 2012. Normalization by Scaling between 0 and 1, http://stn.spotfire.com/spotfire_client_help/norm/norm_scale_between_0_and_1.htm (accessed 1 December 2013).
50. Upreti, R. and Mehrotra A.K. 2000. Experimental Measurement of Gas Diffusivity in Bitumen: Results for Carbon Dioxide. *Ind. Eng. Chem. Res.* **39** (4): 1080-1087.
51. Wen, Y., Bryan, J., and Kantzas, A. 2005a. Evaluation of Bitumen-Solvent Properties Using Low Field NMR. *J. Can. Pet. Tech.* **44** (4): 22-28.
52. Wen, Y., Bryan, J., and Kantzas, A. 2005b. Estimation of Diffusion Coefficients in Bitumen Solvent Mixtures as Derived from Low Field NMR Spectra. *J. Can. Pet. Tech*. **44** (4): 29-35
53. Weng, Y., Kantzas, A., and Wang, G.J. 2004. Estimation of Diffusion Coefficients in Bitumen Solvent Mixtures Using X-Ray CAT Scanning and Low Field NMR. Paper PETSOC-2004-064 presented at the Canadian International Petroleum Conference, Calgary, Alberta, 8-10 June.
54. Yang, C. and Gu, Y. 2003. A New Method for Measuring Solvent Diffusivity in Heavy Oil by Dynamic Pendant Drop Shape Analysis (DPDSA). Paper SPE-84202-PA presented at the SPE Annual Technical Conference and Exhibition, Denver, Colorado, 5-8 October.
55. Zhang, Y.P., Hyndam, C.L., and Maini, B.B. 2000. Measurement of Gas Diffusivity in Heavy Oils. *J. Pet. Sci. Eng*. **25** (1-2): 37-47.
56. Zhao, L. 2004. Steam Alternating Solvent Process. Paper SPE 86957 presented at the International Thermal Operations and Heavy Oil and Western Regional Meeting, Bakersfield, California, 16-18 March.
57. Zhao, L., Nasr, T., Huang, G. et al. 2005. Steam Alternating Solvent Process: Lab Test and Simulation. *J. Can. Pet. Tech.* **44** (9): 37-43.

Table 1: Solvent Properties

Solvent	Specific Gravity	Viscosity, cP @ 25°C
Heptane	0.683	0.294
Decane	0.735	0.848
Distillate	0.738	0.742

Table 1: Oil sample properties. LMO: Light Mineral Oil, HMO: Heavy Mineral Oil

Oil samples	Density g/ml @ 25 °C	Viscosity, cP @ 25 °C
LMO	0.8529	44.1
HMO	0.8734	250
Oil 1	0.9818	20,675
Oil 2	1.0035	153,000
Oil 3	1.0156	476,353

Table 2: Oil Sample properties. OIL SAMPLE PROPERTIES. LMO: Light Mineral Oil, HMO: Heavy Mineral Oil

Carbon size number range	FBP°C	Mass Composition%					
		Distillate	LMO	HMO	Oil 1	Oil2	Oil3
IBP-C_5	36.1	1.918	---	---	---	---	---
C_6 -C_{10}	173.9	56.122	---	---	0.686	---	---
C_{11}- C_{13}	235	40.937	---	---	4.239	2.77	---
C_{14}-C_{20}	344	---	6.775	1.478	18.22	12.222	9.006
C_{21}-C_{30}	449	---	74.282	55.882	21.177	14.982	25.593
C_{31}-C_{40}	522	---	17.849	40.248	13.491	10.038	17.408
C_{41}-C_{50}	575	---	---	---	8.401	6.543	10.059
C_{51}-C_{60}	615	---	---	---	5.863	4.812	7.631
C_{61}-C_{70}	647	---	---	---	3.426	3.412	4.114
C_{71}-C_{80}	675	---	---	---	2.639	2.317	3.425
C_{81}-C_{90}	700	---	---	---	1.52	1.366	2.001
C_{91}-C_{100}	720	---	---	---	0.724	0.746	0.916
C_{100+}	720+	---	---	---	19.614	40.792	19.847

Table 3: Mixture densities for Oil 1 sample

Mixture	**Mixture density g/cm^3**
Oil1-C_7	-3.200*BMD + 4.313
Oil1-C_{10}	-3.5057*BMD + 4.6247
Oil1-D	-2.8756*BMD + 3.97

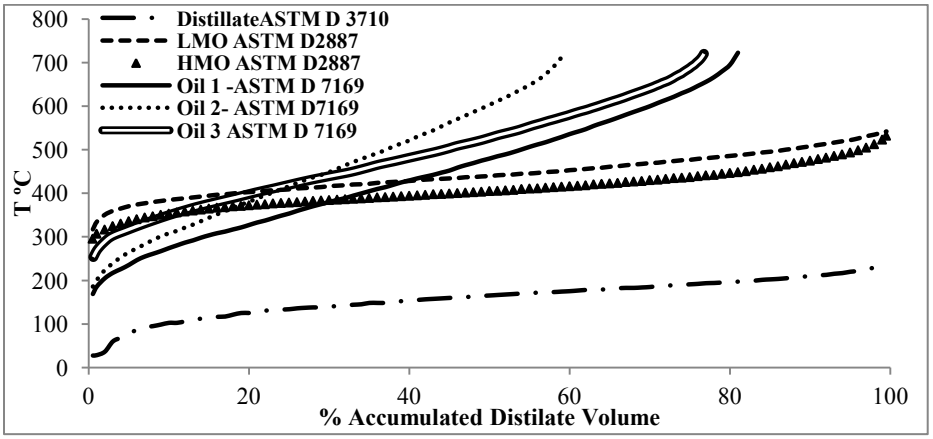

Fig. 1: Boiling range distribution of oil sample and distillate.

Table 4: Normalized pixel intensity vs. solvent concentration

Mineral oil – solvent sample	Normalized pixel intensity value	C_7 concentration equal to in weight in G
LMO & C_7	$0 \leq (ei)_{norm} \leq 0.5658$	$0.5302(ei)_{norm}$
	$0.56586 < (ei)_{norm} \leq 0.6812$	$3.4672(ei)_{norm}$ - 1.661
	$0.6812 < (ei)_{norm} \leq 1$	$0.941(ei)_{norm}$ + 0.059
LMO & C_{10}	$0 \leq (ei)_{norm} \leq 0.8616$	$0.3482(ei)_{norm}$
	$0.8616 < (ei)_{norm} \leq 0.8969$	$3.7707(ei)_{norm}$ - 2.9223
	$0.8969 < (ei)_{norm} \leq 1$	$8.4048(ei)_{norm}$ - 7.4048
LMO & D	$0 \leq (ei)_{norm} \leq 0.9026$	$0.3324(ei)_{norm}$
	$0.9026 < (ei)_{norm} \leq 0.9967$	$0.0003\exp(7.8038(ei)_{norm})$
	$0.9967 < (ei)_{norm} \leq 1$	$90.432(ei)_{norm}$ - 89.432
HMO & C_7	$0 \leq (ei)_{norm} \leq 0.6636$	$0.4521(ei)_{norm}$ - 6E-17
	$0.6636 < (ei)_{norm} \leq 0.8150$	$2.6407(ei)_{norm}$ - 1.454
	$0.8150 < (ei)_{norm} \leq 1$	$1.6215(ei)_{norm}$ - 0.6215
HMO & C_{10}	$0 \leq (ei)_{norm} \leq 0.6109$	$0.4911(ei)_{norm}$ + 4E-17
	$0.6109 < (ei)_{norm} \leq 0.8486$	$1.6457(ei)_{norm}$ - 0.6839
	$0.8486 < (ei)_{norm} \leq 1$	$1.9809(ei)_{norm}$ - 0.9809
HMO & D	$0 \leq (ei)_{norm} \leq 0.97507$	$0.3077(ei)_{norm}$
	$0.97507 < (ei)_{norm} \leq 0.9965418$	$15.597(ei)_{norm}$ - 14.918
	$0.9965418 < (ei)_{norm} \leq 1$	$87.062(ei)_{norm}$ - 86.062

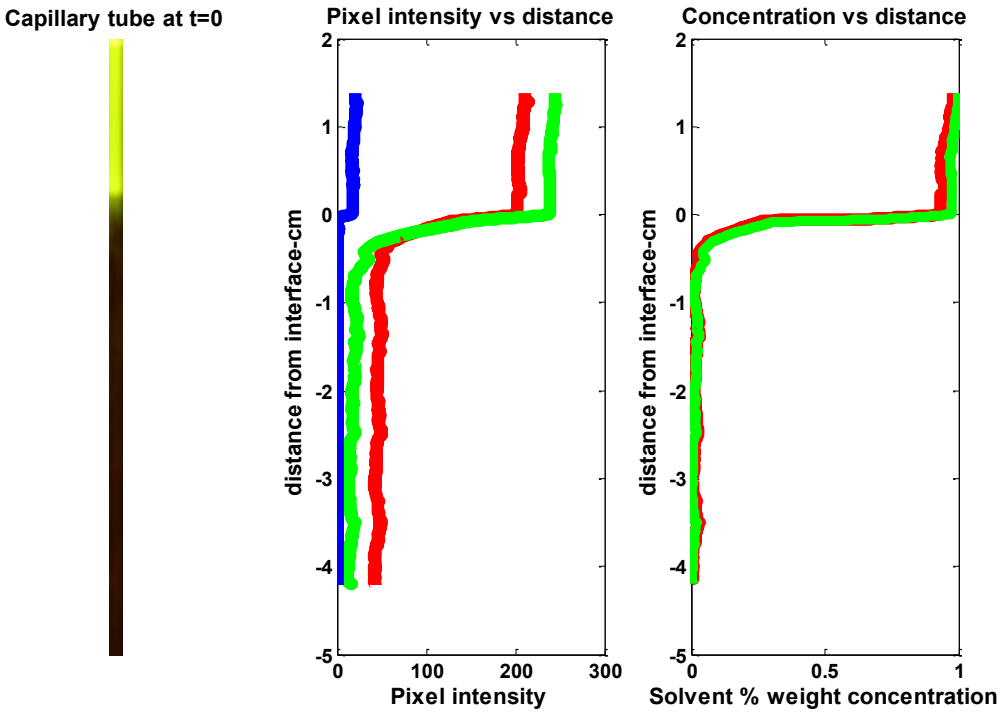

Fig. 2: MATLAB® approach to quantify the pixel intensities and eventually determine the concentration profiles.

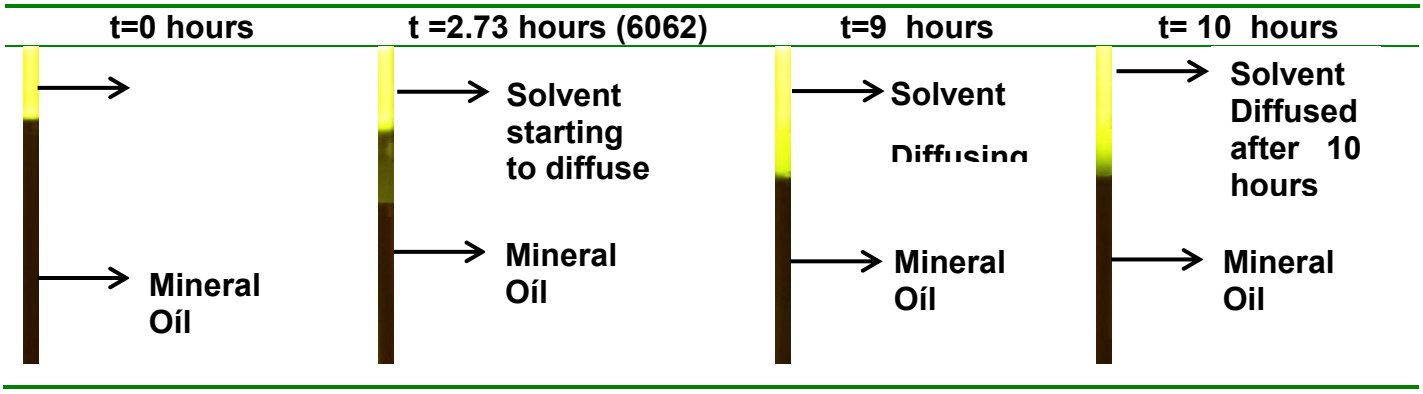

Fig. 3: Profile change inside the capillary tube during solvent diffusion.

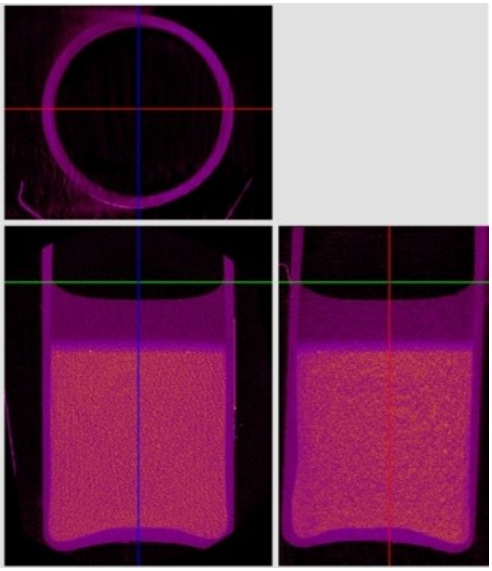

Fig. 4: Micro CT scan for the case of dark oil (Oil 2) – distillate pair in DataViewer® at t = 0.

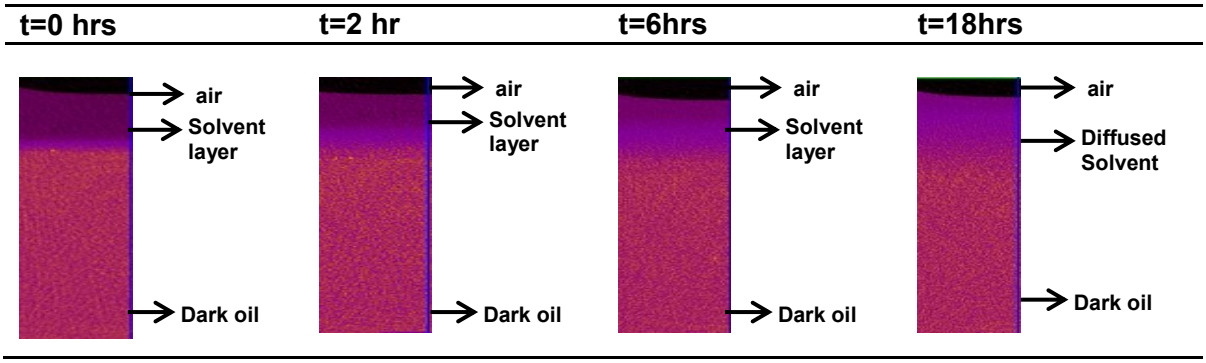

Fig. 5: Profile change over 18 hours.

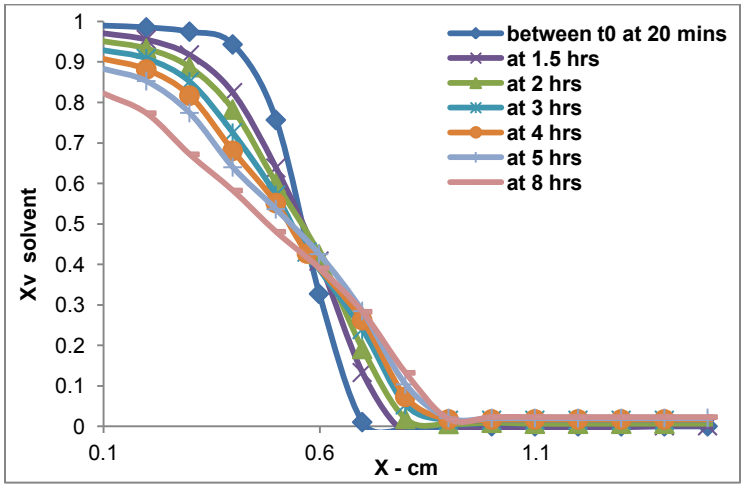

Fig. 6: Concentration profiles for CLB-C7 case.

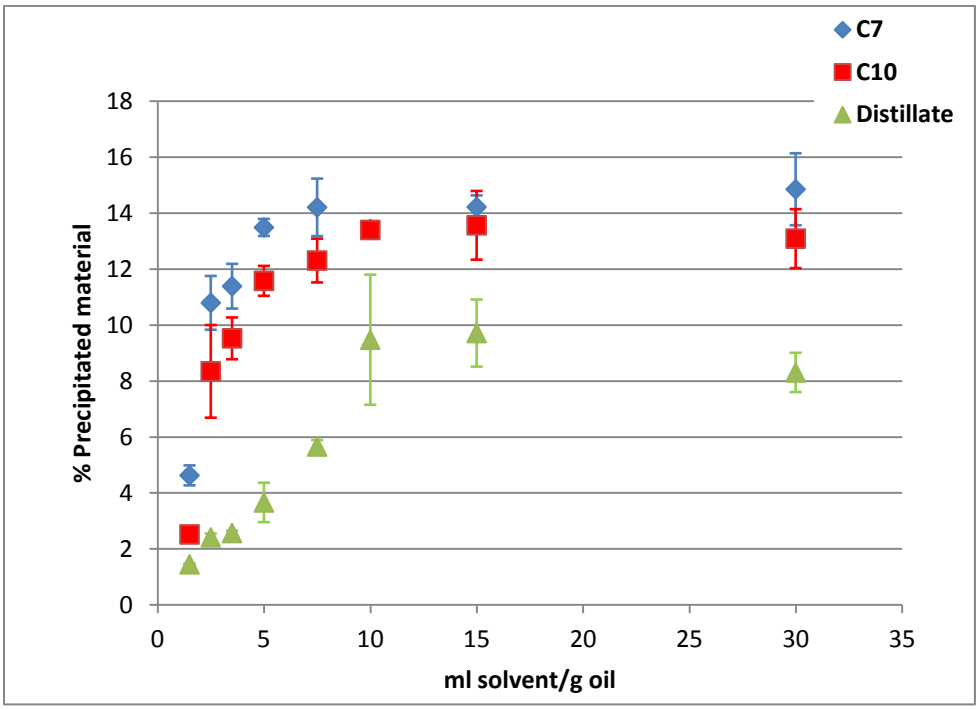

Fig. 7: Precipitated material at different concentrations of solvent in Oil 1.

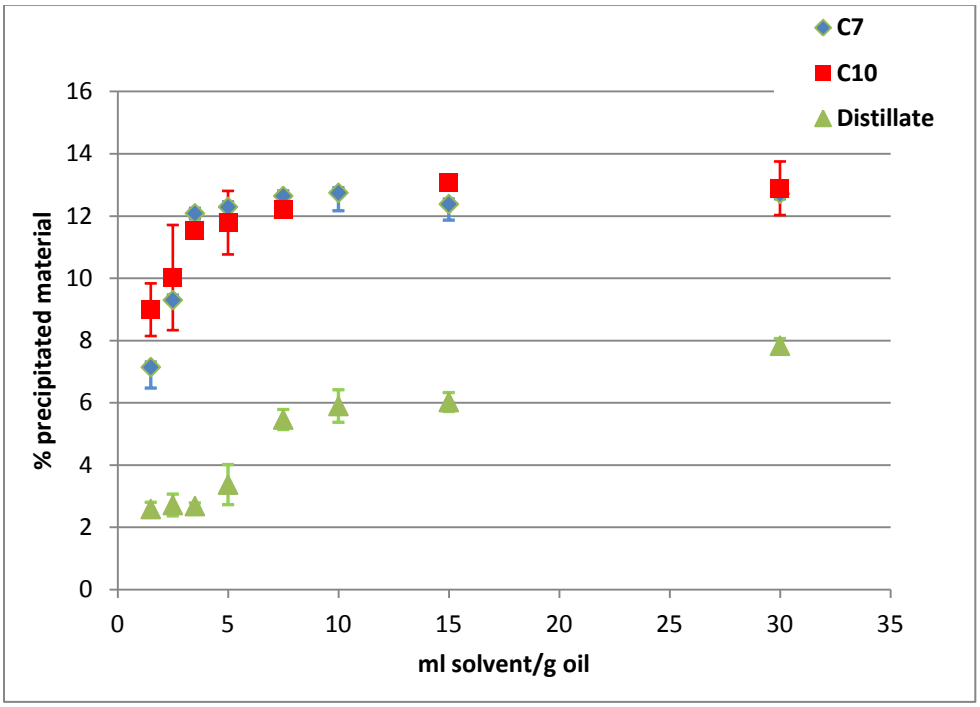

Fig. 8: Precipitated material at different concentrations of solvent in Oil 2.

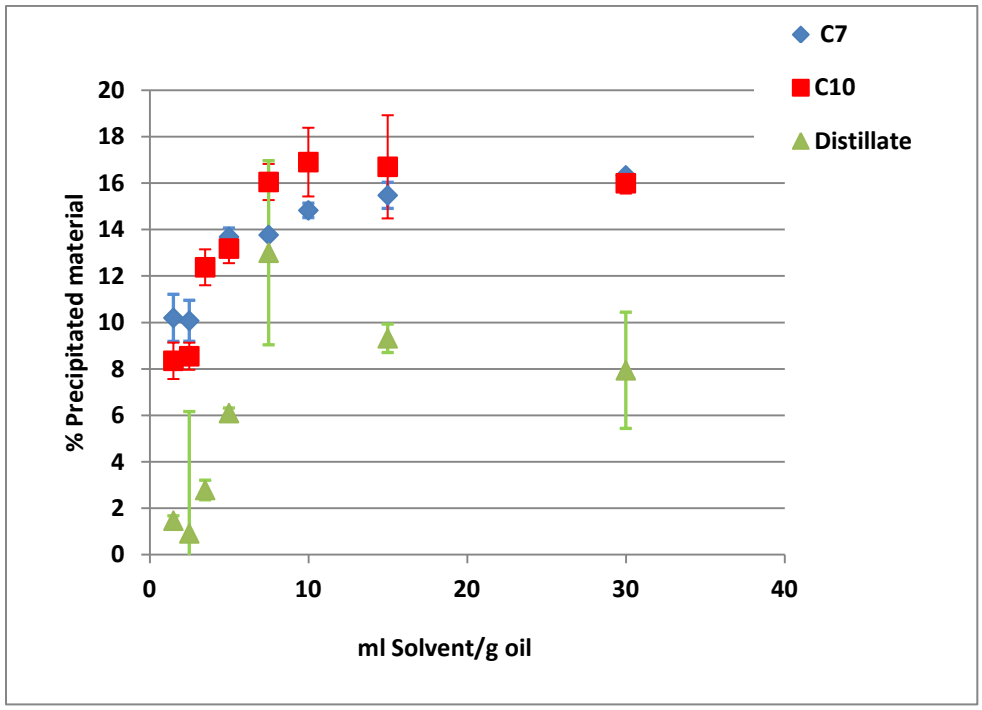

Fig. 9: Precipitated material at different concentrations of solvent in Oil 3.

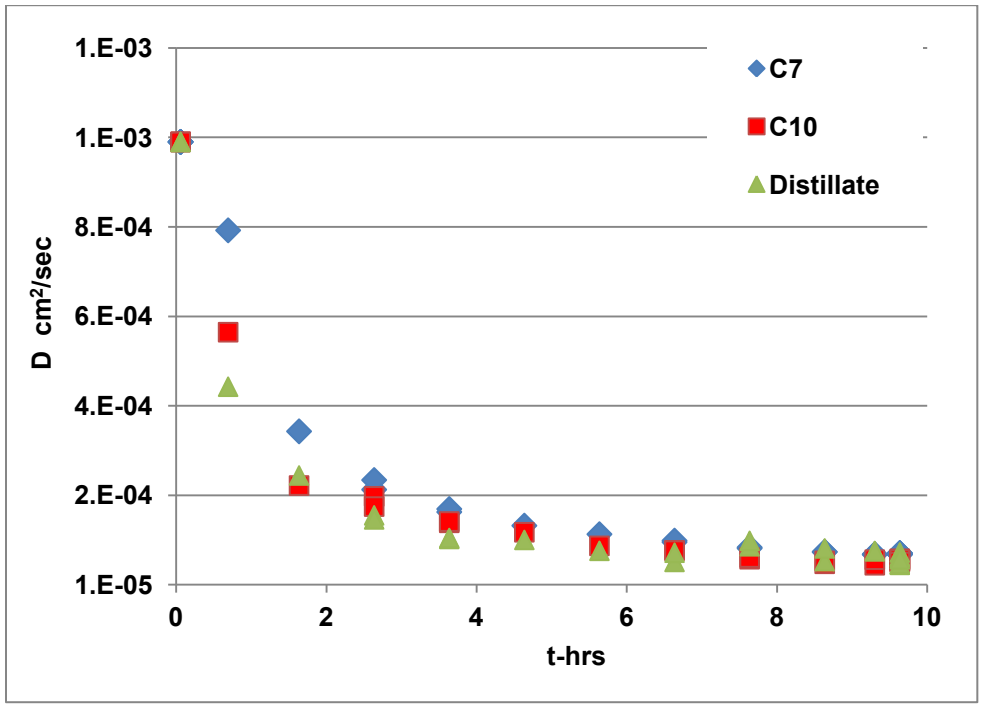

Fig. 10: Diffusion coefficient vs. time for light mineral oil (LMO).

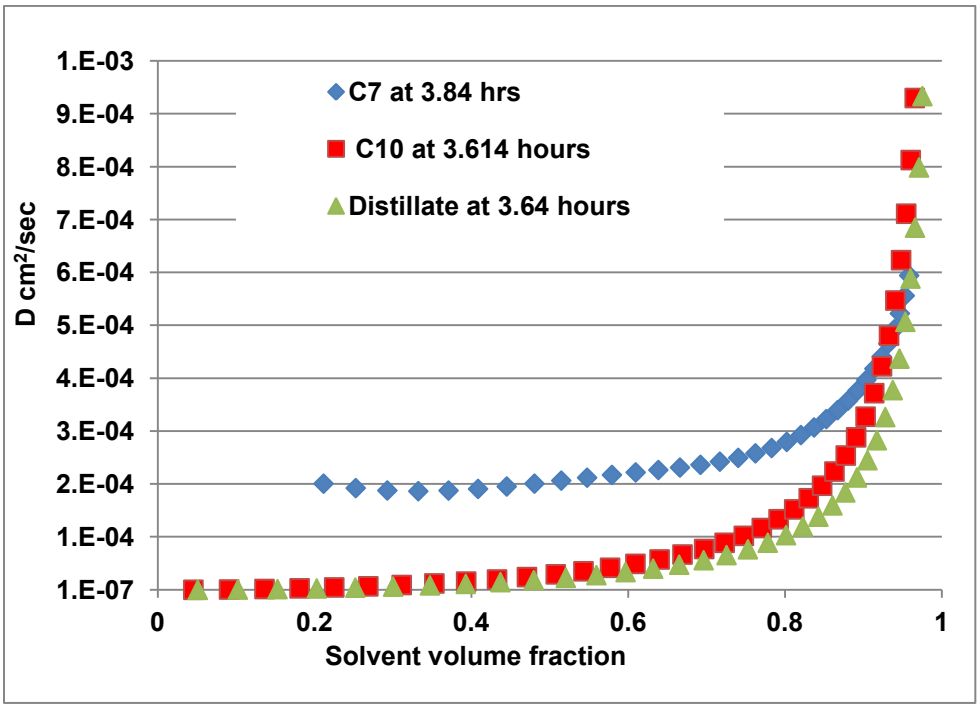

Fig. 11: Diffusion coefficient vs. solvent concentration for light mineral oil (LMO).

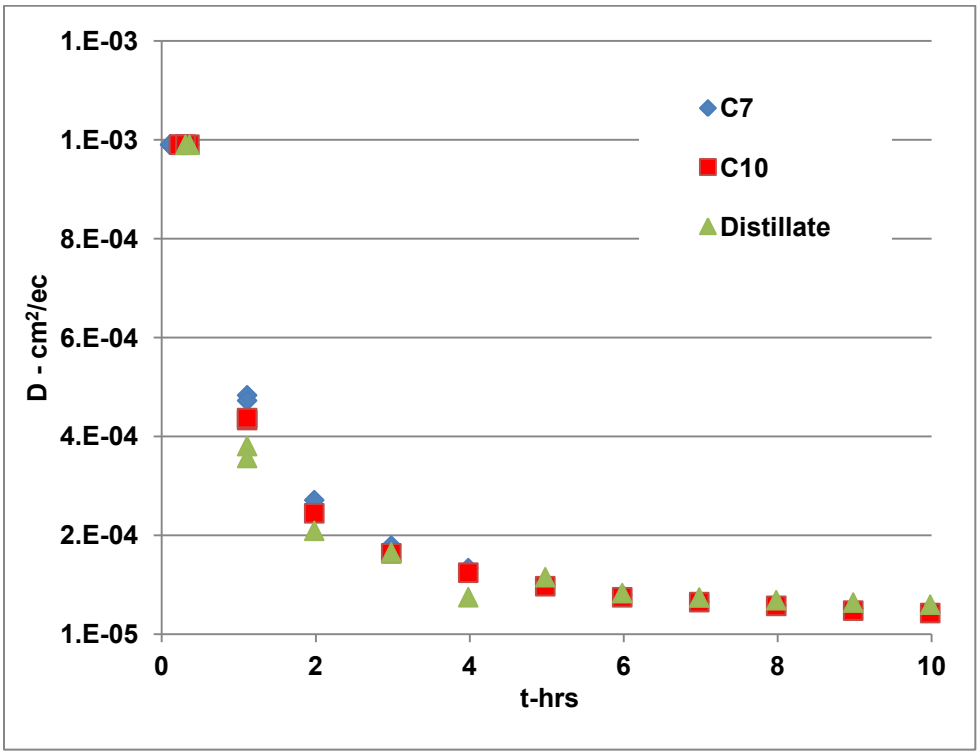

Fig. 12: Diffusion coefficient vs. time for heavy mineral oil (HMO).

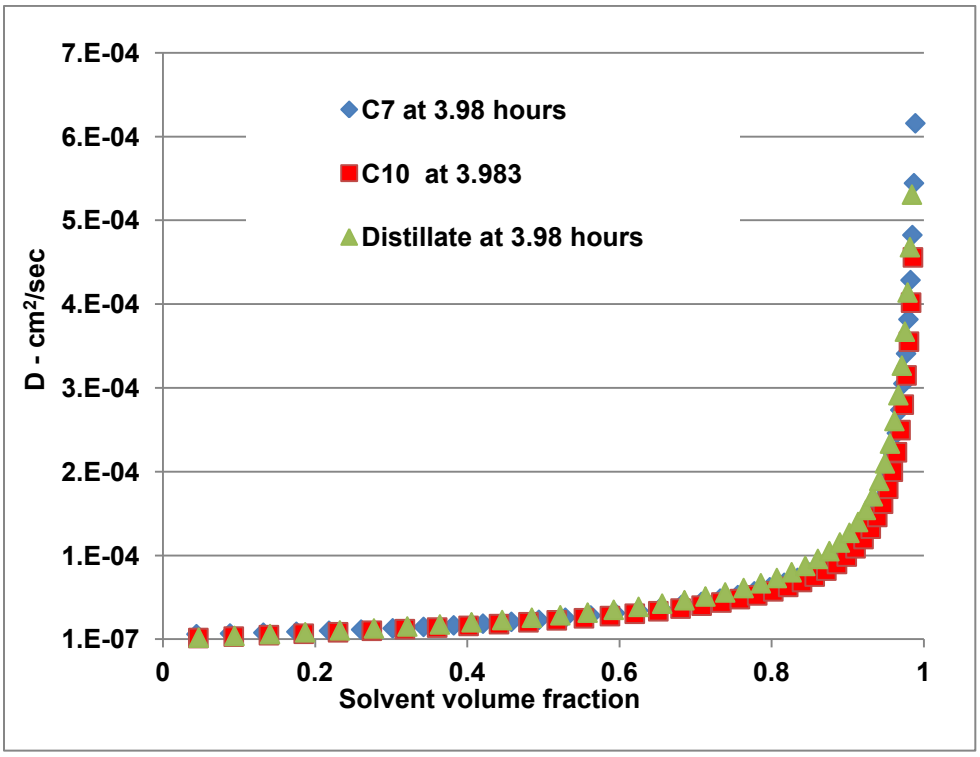

Fig. 13: Diffusion coefficient vs. solvent concentration for heavy mineral oil (HMO).

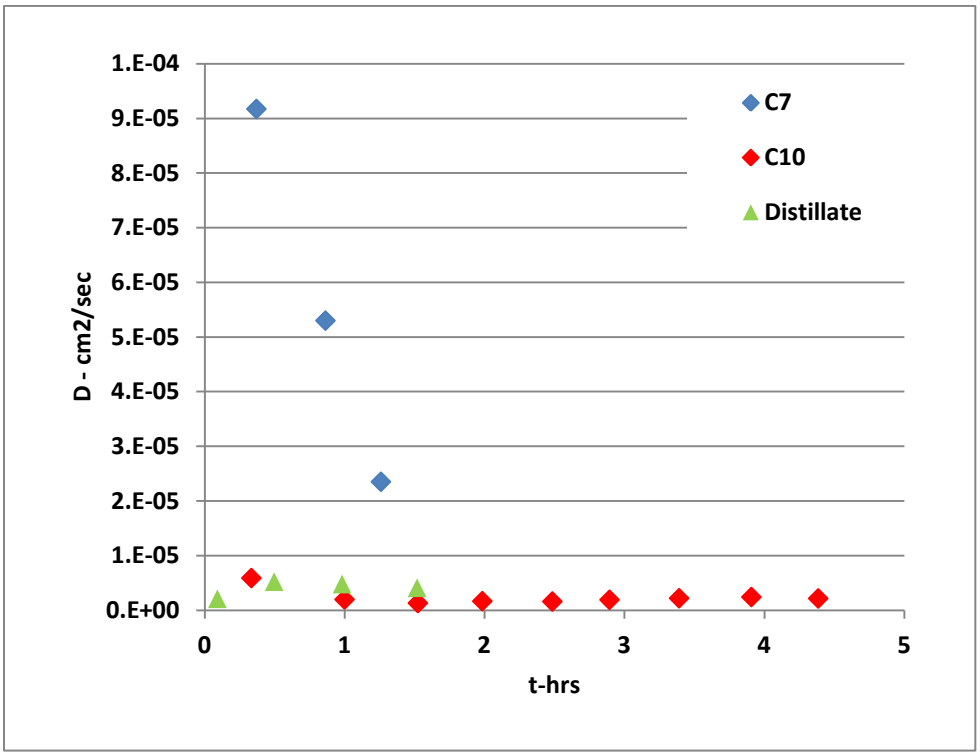

Fig. 14: Diffusion coefficient vs. time for dark oil (Oil 1).

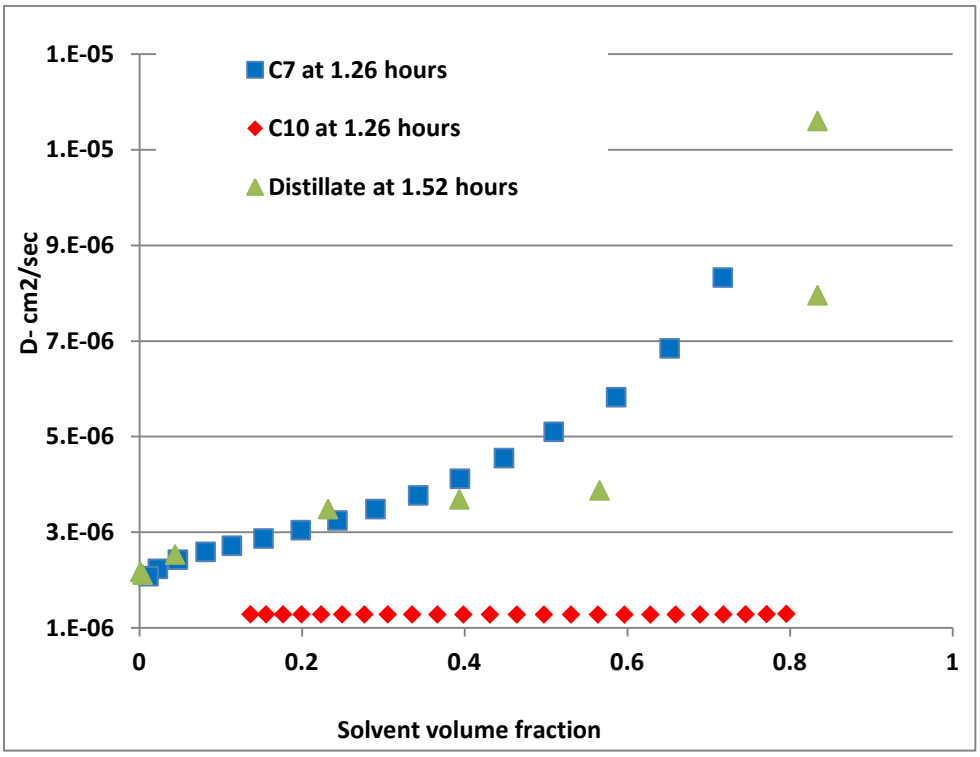

Fig. 15: Diffusion coefficient vs. solvent concentration for dark oil (Oil 1).

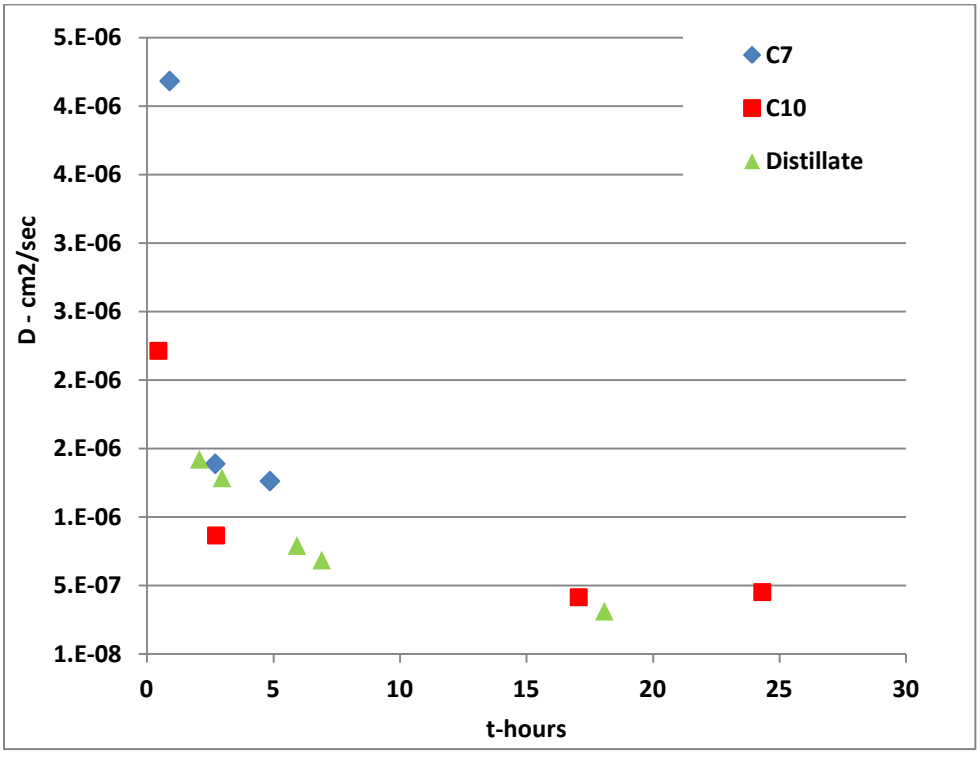

Fig. 16: Diffusion coefficient vs. time for dark oil (Oil 2).

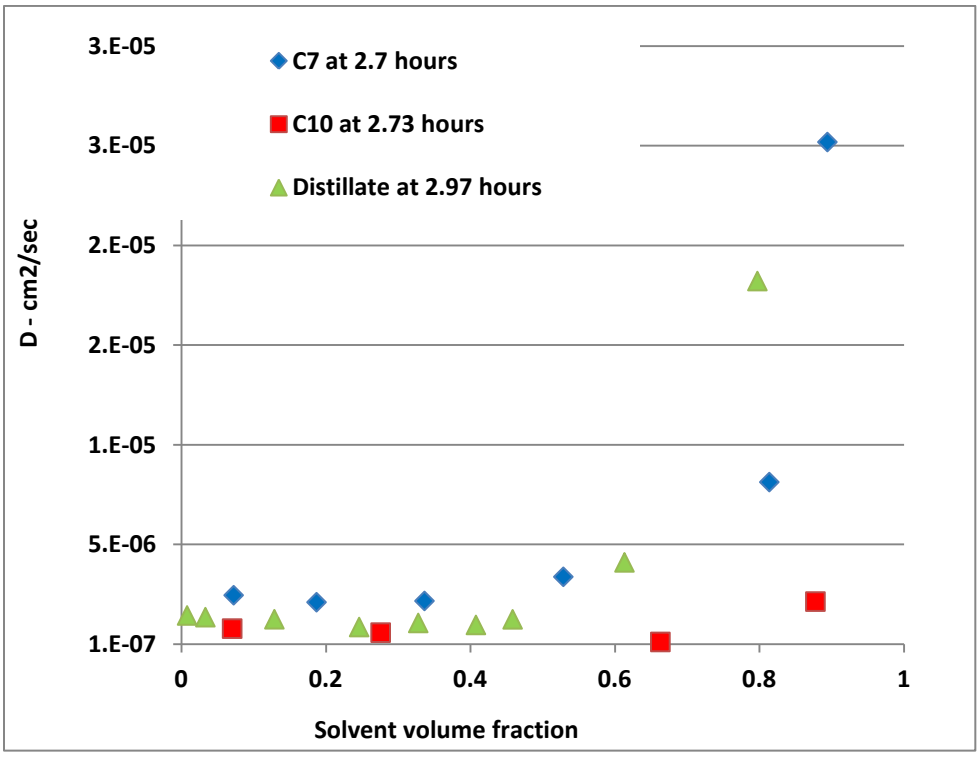

Fig. 17: Diffusion coefficient vs. solvent concentration for dark oil (Oil 2).

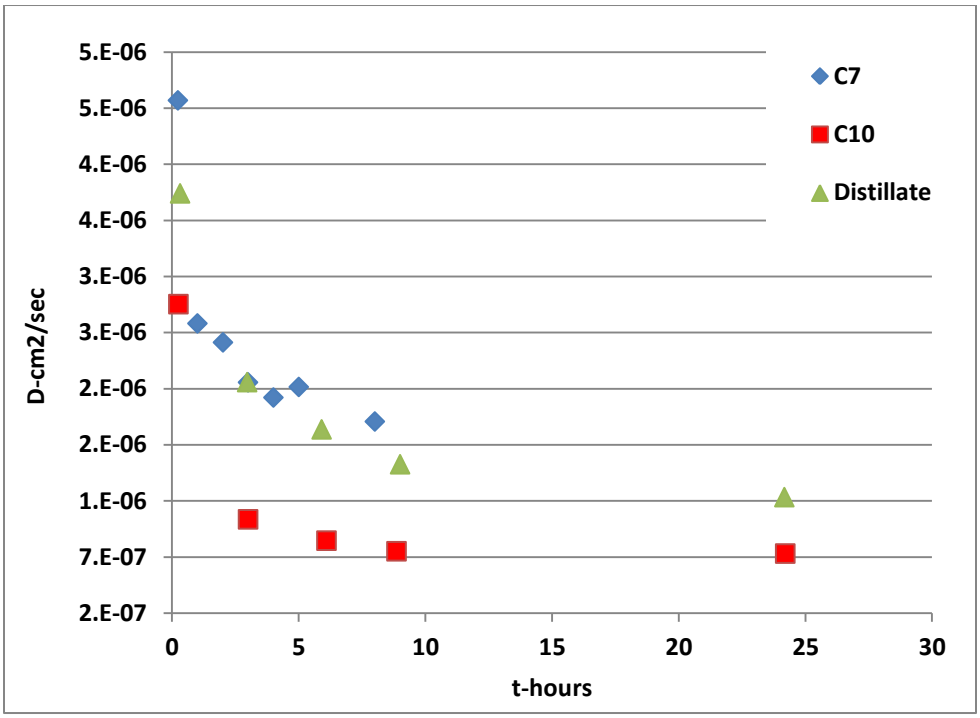

Fig. 18: Diffusion coefficient vs. time for dark oil (Oil 3).

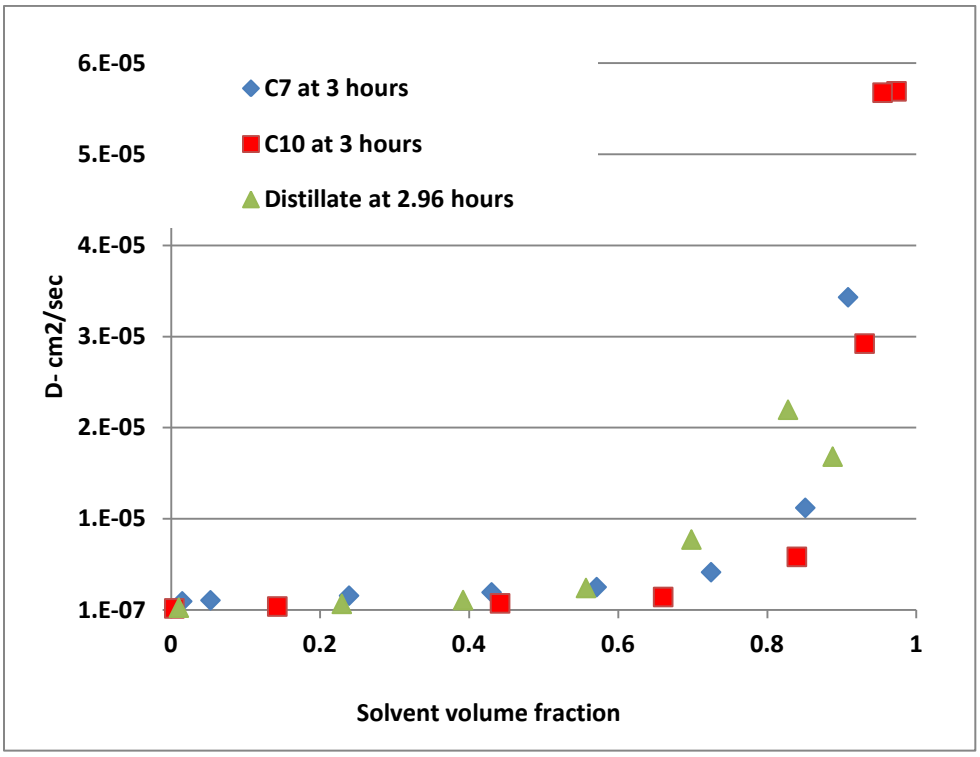

Fig. 19: Diffusion coefficient vs. solvent concentration for dark oil (Oil 3).

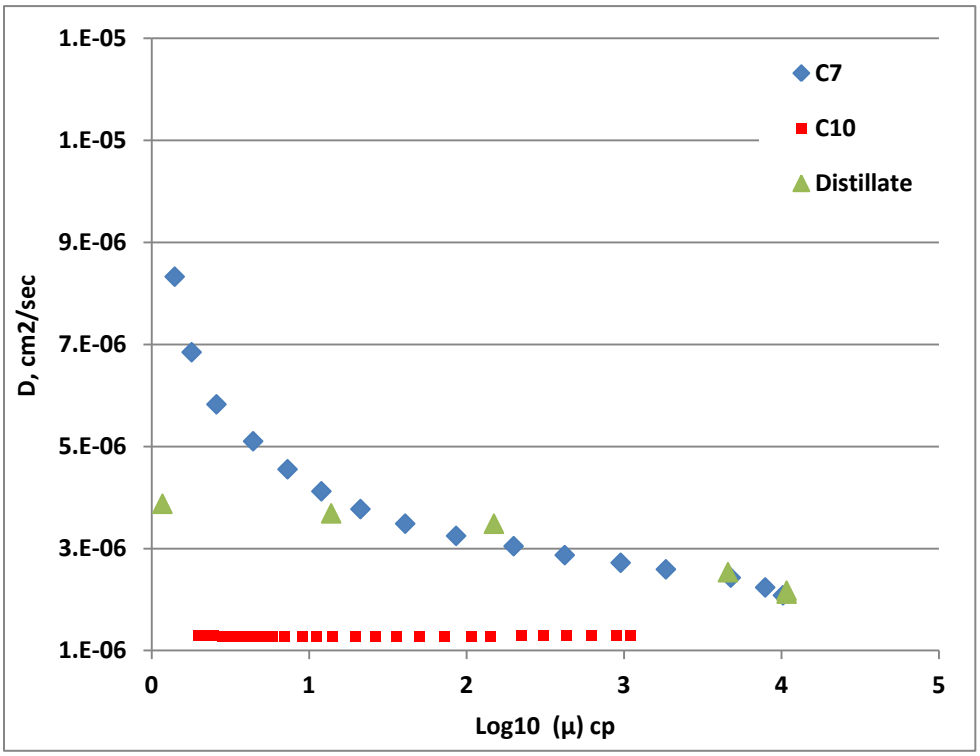

Fig. 20 Diffusion rate against viscosity at different concentrations of solvent in Oil 1

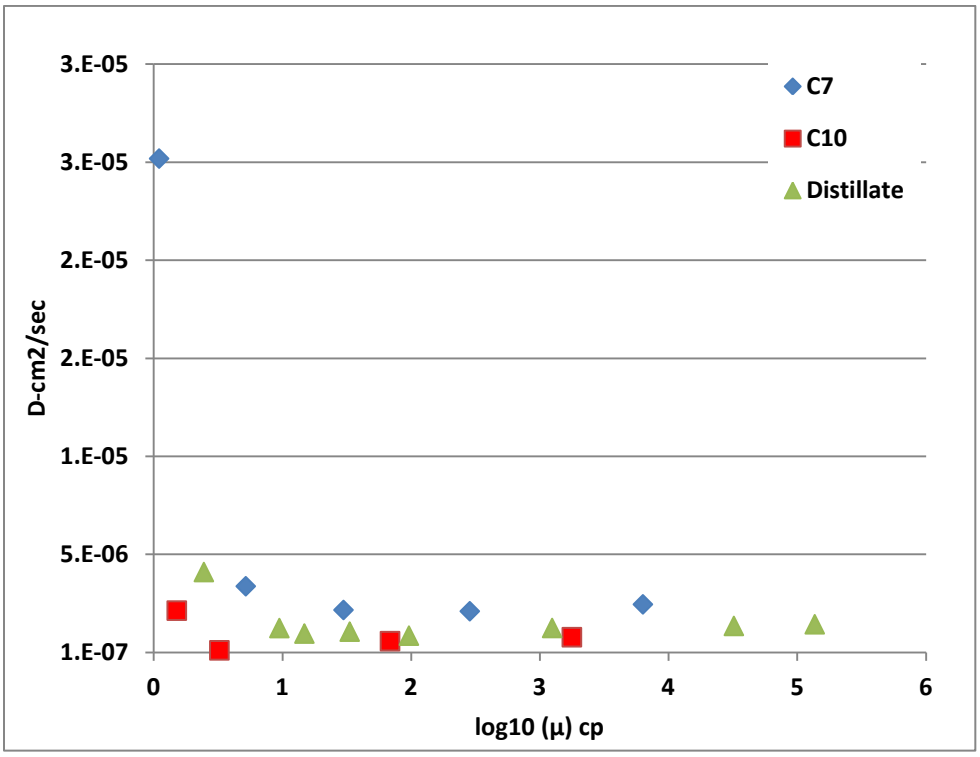

Fig. 21: Diffusion rate against viscosity at different concentrations of solvent in Oil 2.

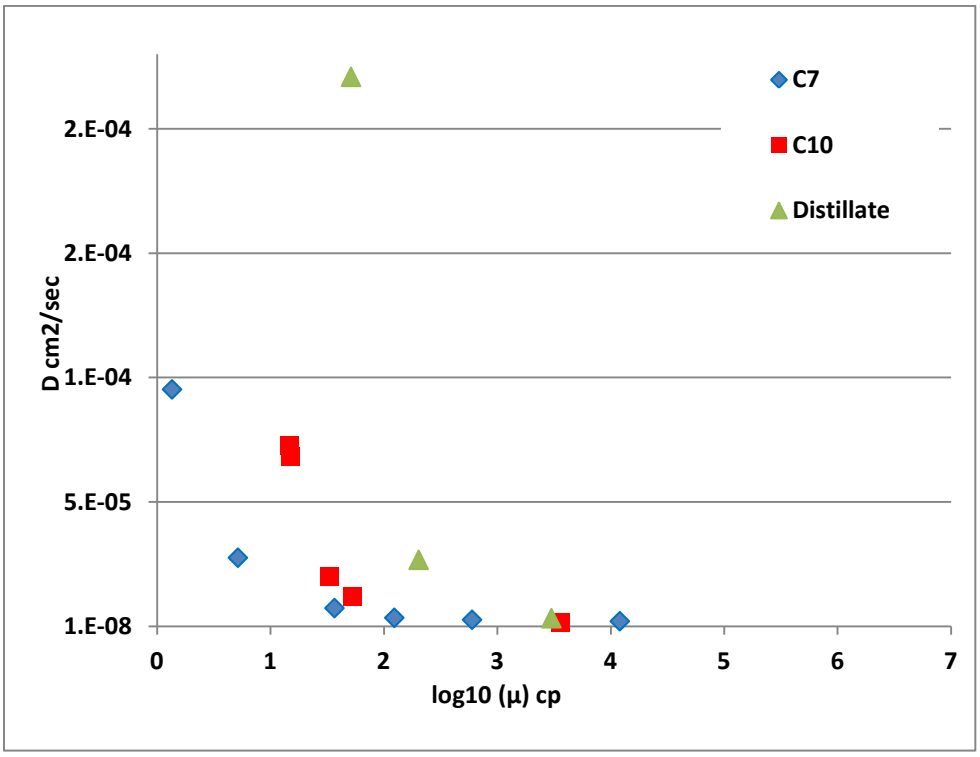

Fig. 22: Diffusion rate against viscosity at different concentrations of solvent in Oil 3.

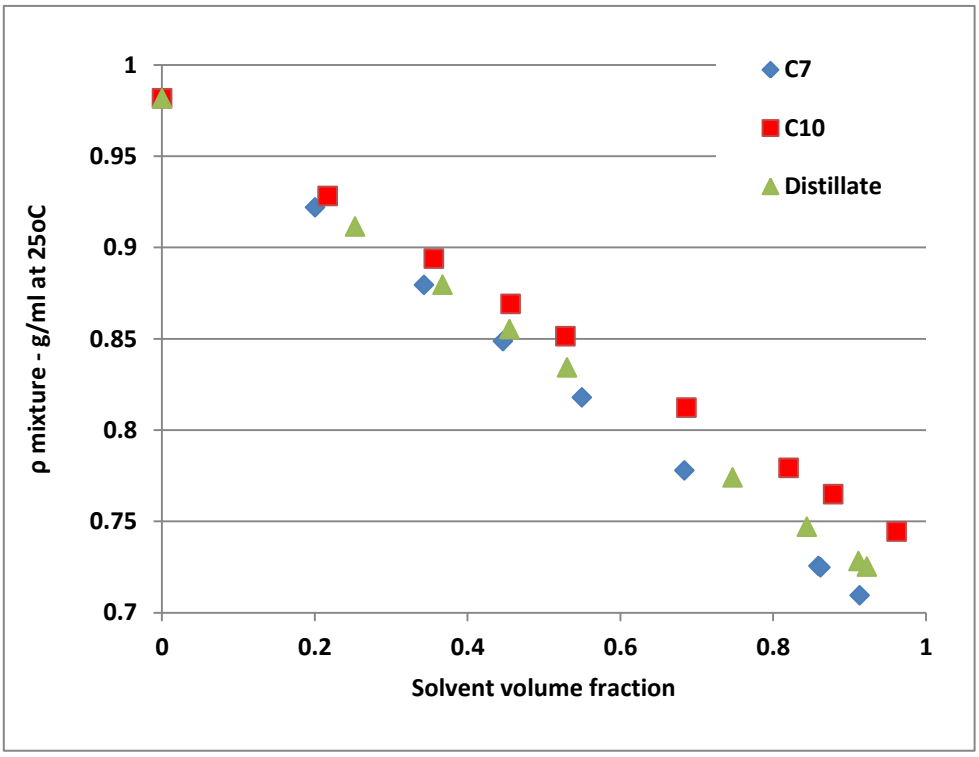

Fig A 1: Density at different concentrations of solvent in Oil 1.

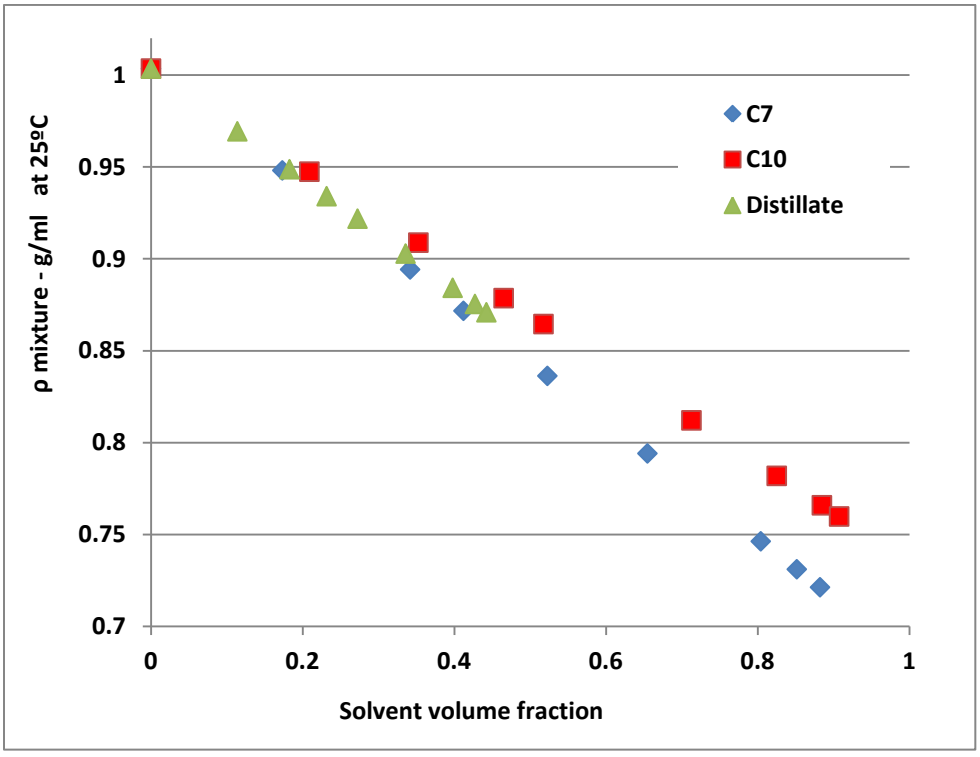

Fig A 2: Density at different concentration of solvent in Oil 2.

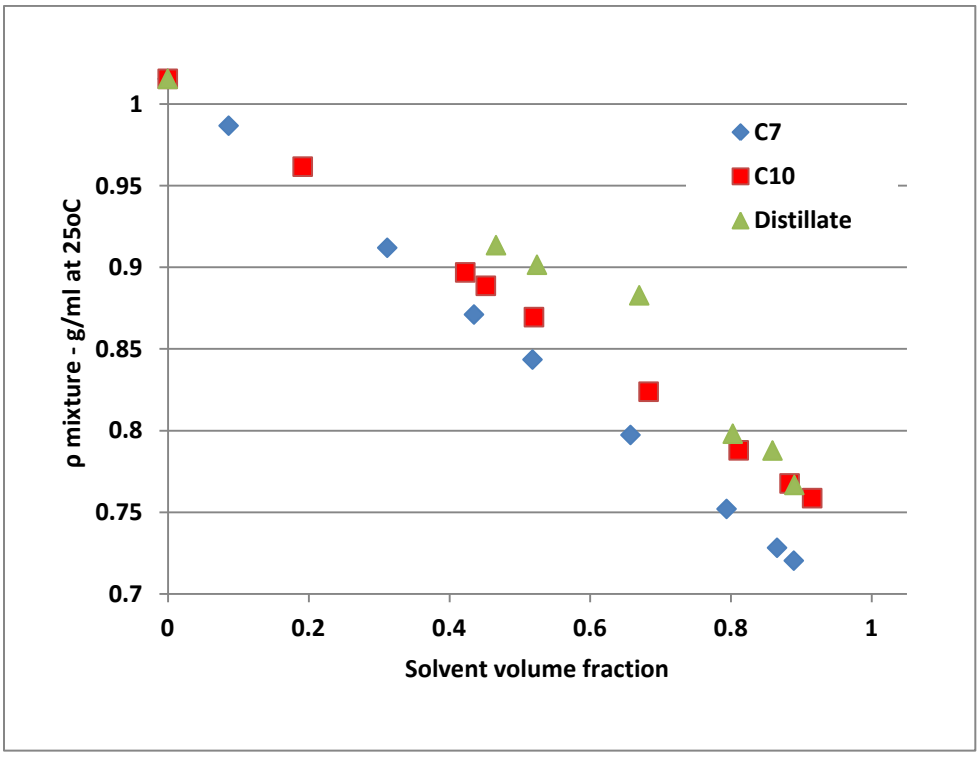

Fig A 3: Density at different concentrations of solvent in Oil 3.

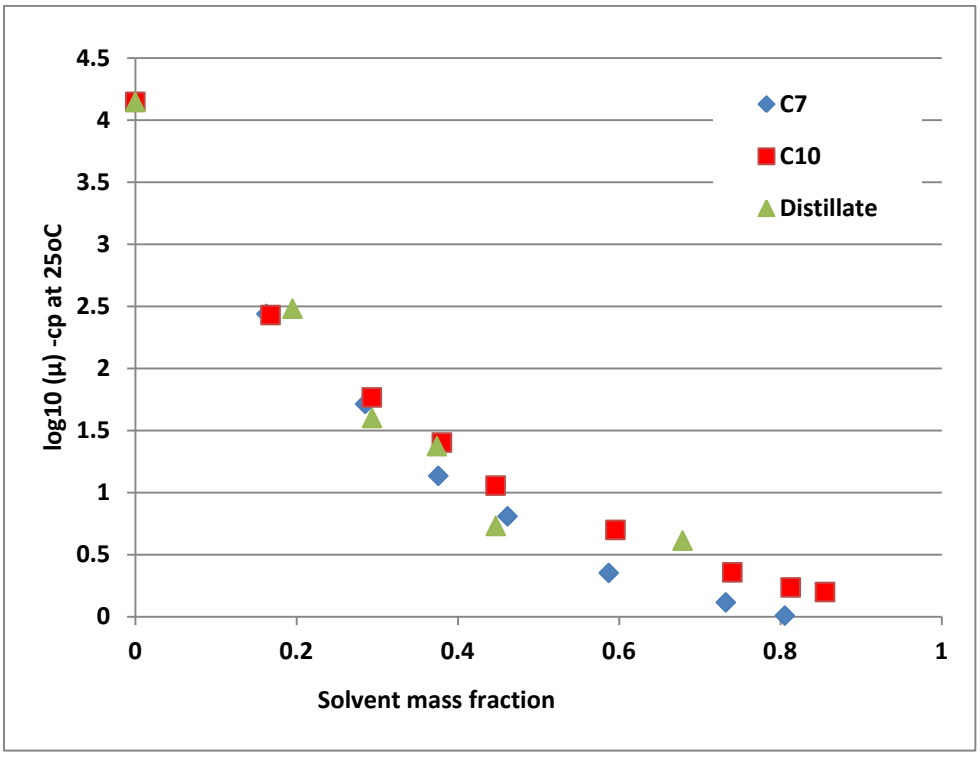

Fig A 4: Viscosity at 25 °C for different concentrations of solvent in Oil 1.

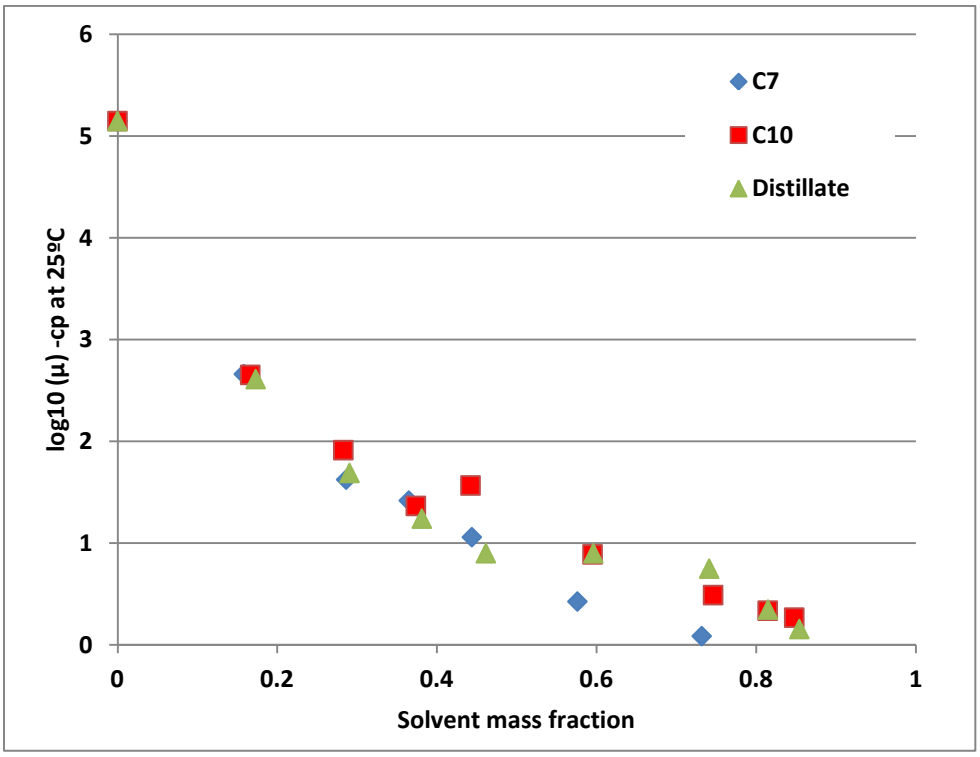

Fig A 5: Viscosity at 50 °C for different concentrations of solvent in Oil 2.

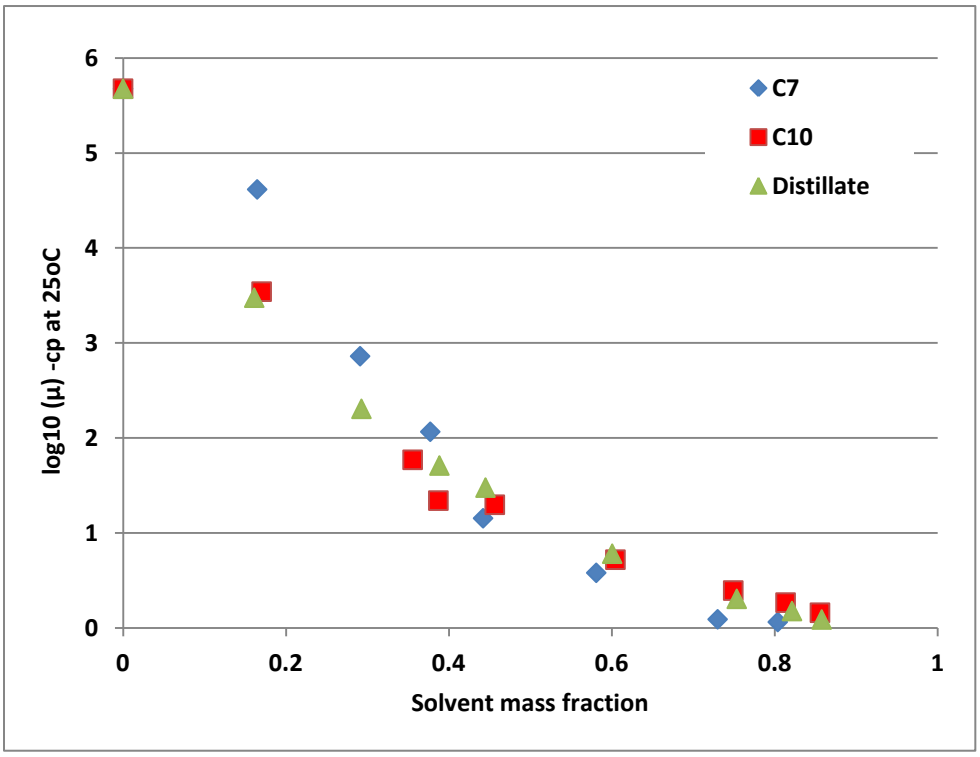

Fig A 6: Viscosity at 25 °C for different concentrations of solvent in Oil 3.

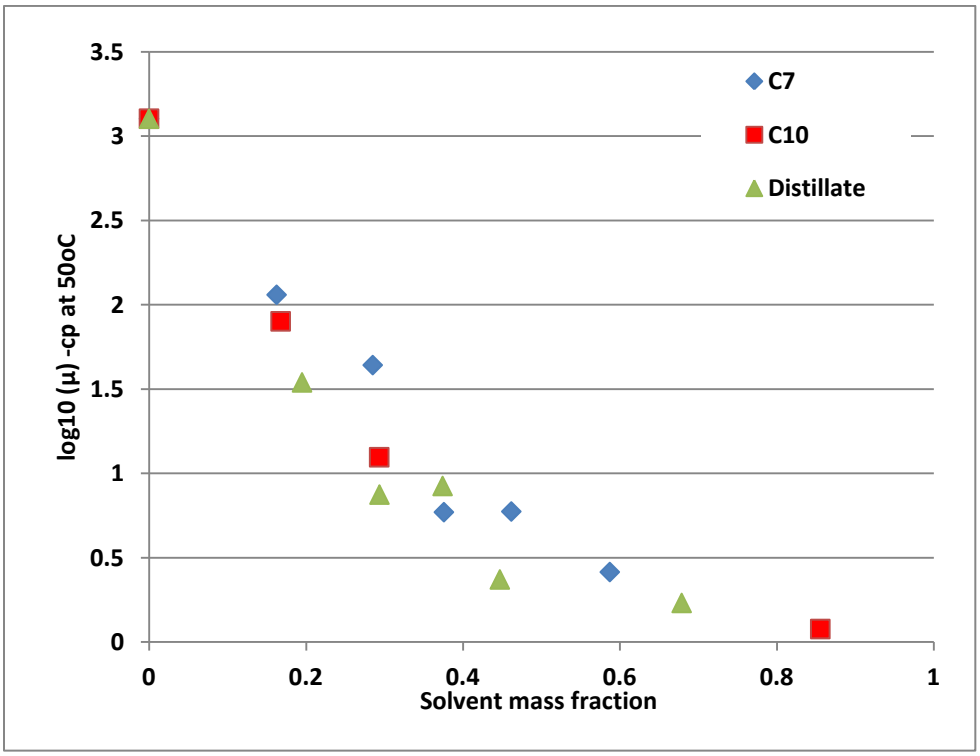

Fig A 7: Viscosity at 50 °C for different concentrations of solvent in Oil 1.

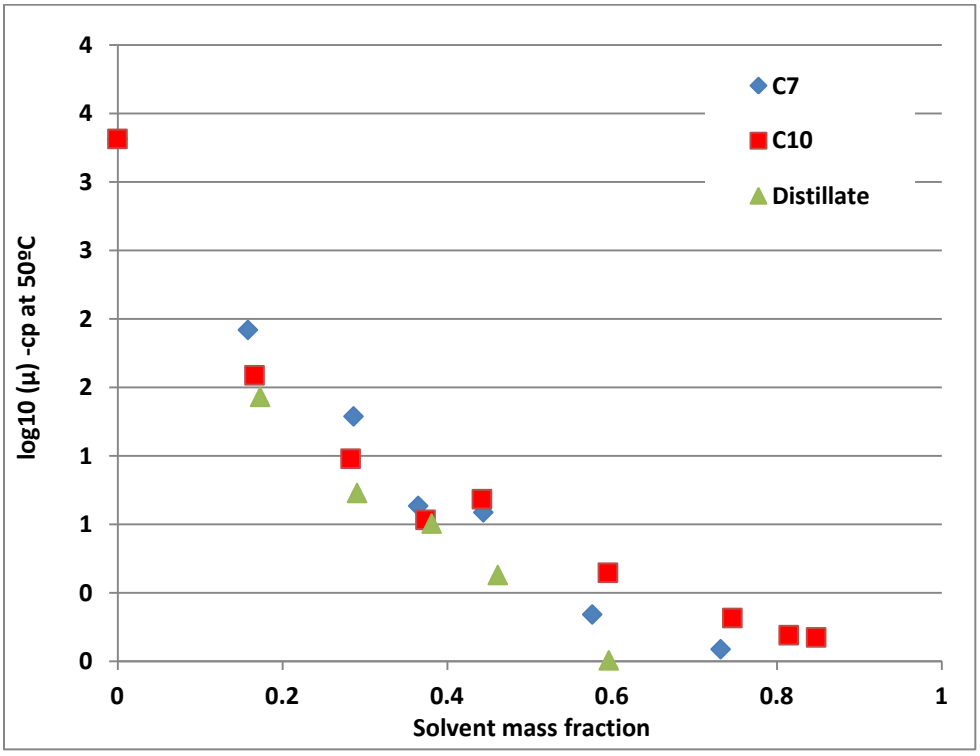

Fig A 8: Viscosity at 50 °C for different concentrations of solvent in Oil 2.

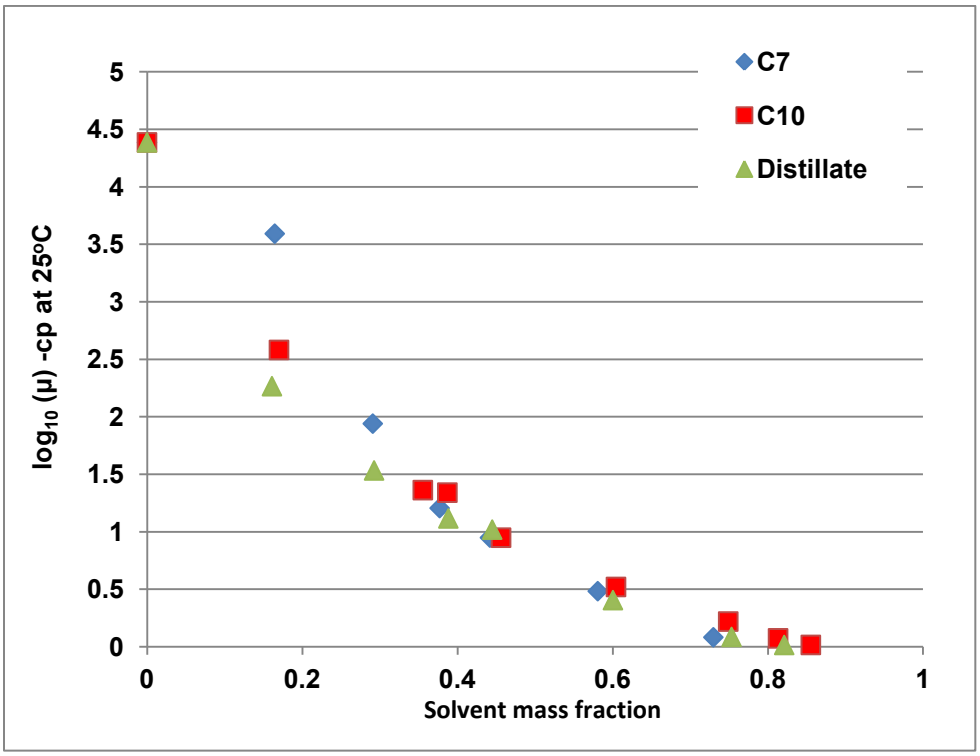

Fig A 9: Viscosity at 50 °C for different concentrations of solvent in Oil 3.

CHAPTER 3: SELECTION OF OPTIMAL SOLVENT TYPE FOR HIGH TEMPRATURE SOLVENT APPLICATIONS IN HEAVY-OIL AND BITUMEN RECOVERY

This paper is a modified and improved version of SPE 170021, which was presented at the SPE Conference held in Calgary, Alberta, 10–12 June 2014. A version of this chapter has been submitted to The Science and Technology of Fuel and Energy

Preface

The selection of most suitable solvent for an efficient heavy-oil recovery process is a critical task. Low carbon number solvents yield faster diffusion but the mixing quality may not be high. Also, high carbon number solvents yield a better quality mixing (much less asphaltene precipitation) but the mixing process is rather slow. Hence, the understanding of solvent selection criteria for solvent-aided recovery processes has established two main aspects of oil-solvent interaction: (1) Oil-solvent mixture quality and (2) rate of mixture formation.

Oil-solvent mixture quality is determined by two parameters: (1) Viscosity and (2) asphaltene precipitation. The rate of mixture formation is quantified by the diffusion rate. These two parameters need to be quantitatively and qualitatively determined to select the suitable solvent for heavy-oil recovery also supported by static experiments that measure solvent diffusion (and oil recovery) from a rock saturated with heavy-oil and exposed to solvent diffusion at static conditions.

This paper focuses on these tests and uses three oil samples with a wide range of viscosities (250-476,000cp), and three liquid solvents with different carbon numbers varying between C7 and C13. The methodologies applied for diffusion rate measurement were optical applying image analysis under UV light (for processed -mineral- oil) and CT scanning (for heavy-oil obtained from fields). Next, viscosity and asphaltene precipitation measurements were conducted after mixing the crude oil and solvents to quantify the mixing quality.

Then, core experiments at different temperatures were performed on Berea sandstone samples using the same solvent-heavy oil pairs to obtain the optimum carbon size (solvent type)-heavy oil combination that yields the highest recovery factor and the least asphaltene precipitation. Based on the fluid-fluid (solvent-heavy oil) interaction experiments and heavy-oil saturated rock-solvent interaction tests, the optimal solvent type was determined considering the fastest diffusion and best mixing quality for different oil-solvent combinations.

1. Introduction

After the pioneering works documented in the 1970s (Farouq and Synder 1973; Allen and Redford 1976; Farouq 1976) and the introduction of the VAPEX (vapor extraction) process (Butler and Mokrys 1993), different versions of solvent aided processes for heavy-oil recovery have been proposed (Das 1996a-b; Nasr et al. 2003; Nasr and Ayodele 2005; Zhao 2004; Zhao et al. 2005; Li and Mamora 2011; Pathak et al. 2011, 2012, 2013).

Due to high cost of the solvents, its industrial applications requires a better understanding of solvent performance through extensive laboratory and computational efforts to optimize its use by minimizing its cost through maximized its retrieval (Al-Bahlani and Babadagli 2011a-b, Mohammed and Babadagli 2013), and maximized oil recovery (Edmunds et al. 2009; Al-Gosayir et al. 2012, 2013). In this optimization process, the primary task is to select the proper solvent for given application conditions (temperature, injected amount), reservoir type and oil composition (Gupta and Picherack 2003; Naderi and Babadagli 2014a-b; Naderi et al. 2014).

It is a well-known fact that lower carbon number solvents (typically propane and butane) yield a faster diffusion into oil and oil saturated rocks (Al-Bahlani and Babadagli 2011a-b). Therefore, higher carbon number solvents (from pentane up to C11-C15 carbon number range distillate oil) are more preferable for a better mixing, yielding higher ultimate recovery with less asphaltene deposition (Naderi et al. 2014). But, with this type of "heavy" solvents, the diffusion rate is much slower compared to the "lighter" ones. This requires a selection process that optimizes the recovery rate and ultimate recovery. Two critical properties of solvents need to be evaluated in solvent selection processes (Marciales and Babadagli 2014):

(1) Diffusion rate: the solvent's ability to penetrate into the heavy oil, which will affect the oil recovery rate, and
(2) Mixing quality: the solvent's ability to reduce oil viscosity minimizing asphaltene precipitation, which will eventually affect the ultimate recovery.

Attempts have been made to measure these two characteristics of oil-solvent pairs and literature offers some insights on solvent preferences in heavy oil recovery. Initially, a low

carbon number solvent application at its dew point was suggested (Butler and Mokrys 1993; Gupta and Picherack 2003). On the other hand, it was found that significant asphaltene deposition may occur under these conditions (Moreno and Babadagli 2014a-b). Then, heavier solvents in gas (Nasr and Ayodele 2005; Ayodele et al. 2010; Keshavarz et al. 2013) and liquid phase (Naderi et al. 2014) where found to be more convenient.

The objective of this work is to propose solvent selection criteria based on their performance on oil recovery rate and ultimate recovery. In an attempt for this, sandstone samples saturated with three different heavy-oils were exposed to solvent diffusion at static conditions at different temperatures and the recovery rate and ultimate recovery (and asphaltenes left behind), controlled by the diffusion rate and mixing quality, respectively, were measured. Parallel to this work representing solvent-oil saturated rock (solvent-rock tests) interaction, the mixing quality and diffusion rates were determined through viscosity measurements and "free" diffusion tests for the same bulk oil and solvents pairs (liquid-liquid tests). By correlating the results of these two types of tests (solvent-rock and liquid-liquid), the ideal solvent types, representing the optimal recovery rate and ultimate recovery, were determined for liquid solvents in the carbon number range of C7 to C13, and heavy oil types with a viscosity range on different orders of magnitude.

2. Experimental Methodology

2.1 *Materials and experimental procedure.*

Berea sandstone cores (ϕ_{ave}=22% and k_{ave}=500 md) with a diameter of ~~2.5~~ 1.5 inch and ~~10~~ 9.5 cm length were saturated with heavy-oil samples given in **Table 1**. Then, the cores were exposed to three different solvents detailed in Table 1. **Figure 1** shows the distillation curves and carbon size distribution for the oils and distillate solvent used in the experiments under their respective ASTM standards.

The core saturation was accomplished through different steps. After cutting the sandstone rock, all of them were washed with sink water and dried at 140 °C in an oven inside a dessicator under vacuum for approximately three days. Subsequently, the cores were placed vertically in a container filled with its respective oil inside a closed dessicator connected to a vacuum line inside an oven settled at 75 °C. At this point, weight was registered daily for

about a week and the process was stopped when the change in weight was less than 1%. **Figure 2a** shows a core saturated with heavy oil and its dimensions.

A set of experiments, as listed in **Table 3**, were carried out at different temperatures by placing the core samples into a container filled with solvent for the soaking period. In all the cases, the refractive index of the resulting mixture was measured periodically. **Figures 2b and c** show the scheme for the set of the first twelve experiments carried out at room conditions indicating the change in color of the solvent surrounding the core at the beginning and later times, respectively. For this case, a stirrer was used to homogenize the oil-solvent mixture before taking samples for refractometer readings. **Figure 3** shows the procedure followed for the experiments step-by-step.

For safety reasons, it was necessary to roto-evaporate the distillate employed in the experiments performed at 80°C (Exp. No. 33, 36 and 39 in Table 3). Thus, this distillate would not have the hydrocarbon components with boiling point below 80°C at atmospheric pressure compared to the original one in Fig. 1.

2.2 ***Recovery rate evaluation by refractive index measurement.***

The refractive index is defined as the ratio of velocity of light in a vacuum to the velocity of light in the substance (fluid). It is a dimensionless quantity and a temperature- and pressure-dependent quantity. The calculation of refractive index for hydrocarbon mixture is volume based (Riazi 2005) and it eventually reflects the amount of the solvent in the whole mixture.

The oil volume fraction is calculated from the refractive mixture using the following equation:

$$X_{vol-oil} = \frac{n_{mixture} - n_{solv}}{n_{oil} - n_{solv}} \quad (1)$$

where

$X_{vol-oil}$: Volumetric fraction of oil

$n_{mixture}$: Refractive index of the mixture at 25 °C

n_{solv}: Refractive index of pure solvent at 25 °C

n_{oil}: Refractive index of pure oil at 25 °C

This can be related to the recovery rates by applying the following relationship:

$$\%RF = X_{vol-oil} * (V_{total-mixture})/V_{oil\ initially\ inside\ the\ core} \quad (2)$$

where

$\%RF$: Recovery factor

$V_{total-mixture}$: Total volume of the mixture

$V_{oil\ initially\ inside\ the\ core}$: Volume of oil initially inside the core

While applying Eqs. 1 and 2, the following assumptions were made:

1. The total volume change of the system due to mixing is negligible.
2. The refractive index obtained from each sample obtained represents the average value of the mixture.
3. The volume of oil encountered inside the solvent phase is equal to the volume of solvent inside the porous media.

At the end of each experiment, the obtained recovery factor through refractive index was validated with the weight change of core from steps e and b in Figure 3. Then, the ultimate recovery factor and recovery curves were obtained.

3. Results

3.1 *Temperature effect.*

Figures 4 through 7 show cumulative oil recovery for four oil types when the volume proportion of solvent to oil is high which corresponds to the first 12 experiments in Table 3. In this set of experiments, distillate was found to have the highest oil recovery in all employed oil samples except for Oil 3. In the latter, heptane was found to be the best solvent. This could be explained by the lower diffusion rate of distillate in Oil 3, which is the heaviest sample used in our experiments.

Figures 8 through 10 show the effect of temperature on recovery curves for the experiments run at low volume solvent/oil ratio and for nine different oil-solvent pairs. Figures 8a-c display the change of the solvent behavior for the experiments run with Oil 1. At room conditions (Fig. 8a), distillate and heptane show similar results; however, at the end of the experiments, distillate reaches a slightly higher recovery. The difference between

this pair of recovery curves is very different when high amount of solvent is employed (Fig. 4). In the latter, distillate is more efficient than heptane. This could be attributed to the pore blockage of the core surface by asphaltenes on the surface of the core when heptane was introduced. That is because the change in concentration at the interface between the core and the solvent is high; this leads to a faster asphaltenes deposition. For the experiments run at 50°C (Fig. 8b), the results were different; heptane showed better recovery than distillate. In this case, a higher temperature would decrease the asphaltene precipitation expectedly. Also, some components of the original distillate would be in vapor phase, leading to a lower mixture quality. This phenomenon would change for the 80°C case (Fig. 8c), which distillate efficiency is better than heptane.

Figures 9a-c illustrate the results obtained with Oil 2. Distillate was more efficient at 25°C and 80°C; while at 50°C, it barely shows higher recovery than distillate. The reason for this behavior would be the same as explained for Oil 1.

The results achieved with Oil 3 are shown in **Figures 10a-c**. For this set of experiments, distillate shows better performance in general, confirming its greater ability to recover more oil and to provide a better mixture quality with heavy-component oil samples such as the ones found in sample 3 (Fig. 1).

Figures 11a-c summarize the final recoveries measured at the end of the experiments based on the change of the weight of each core employed. In general, heptane and distillate reach higher recoveries than decane when experiments were run at 25 and 50°C. Decane and distillate were the better options at 80°C. Also, it was found that increasing the temperature from 25°C to 50°C improves heptane efficiency in all oil samples, but the recovery does not only improve, but even decreases when this is employed closer to its boiling point (80°C), concluding that the best performance for heptane was accomplished at 50°C. On the other hand, the increase in temperature increased the recovery when decane and distillate were used. However, this trend is more obvious for the decane trend. Finally, distillate obtained the highest recovery for each oil at each temperature except by Oil 1 at 50°C (Fig. 11a), when is marginally overcome by heptane; followed very close to the obtained by heptane for Oil 2 and 3 (**Fig. 11b-c**), at 50°C.

3.2 ***Solvent concentration vs. soaking time in recovery effect.***

Figures 12 to 14 evaluate the solvent efficiency when this is used at low and high concentration as well as soaking time effect in the ultimate recovery for experiments run at 25°C after a period surrounding 300 hours. Based on the overall concentration of solvent employed in the soaking tests, its molecular diffusion rate was obtained and plotted for the data set in the x-axes of figures a and b of Figures 12-14. These values were calculated from our earlier experiments that used the same oil-solvent pairs (Marciales and Babadagli 2014) as explained in Appendix. Since the diffusion rate would eventually affect oil recovery rate, each of the values found was paired with its ultimate recovery in order to evaluate the best solvent based on these two criteria. As a general rule, it was observed that the higher the concentration of solvent, the higher the diffusion rate and hence, the higher the oil recovery (Gupta and Picherack 2003). However, this increase was found not to be proportional in all cases in our study. Figures 12 a-b show close recovery values for Oil 1 when our three solvents were used at low concentration and had small diffusion rate, but the difference in terms of ultimate recovery was greater when the solvent amount increased. For these cases, the distillate - heptane - decane decreasing production trend was kept in both cases and diffusion rate was similar for distillate and heptane.

Figures 13a-b shows the values for Oil 2. Here, again the distillate - heptane - decane decreasing production trend was followed, but distillate diffusion rate at high solvent concentration is closer to decane than heptane. The results for Oil 3 gave different trend. The distillate is more efficient than heptane if employed at lower concentration even though the diffusion rate is slightly higher (**Fig. 14a**). This is in contrast to the high concentration case where heptane showed better efficiency (**Figure 14b**).

Since the solvent was not replenished in these experiments, soaking time effect in solvent efficiency was tested experimentally to find how much would compensate doubling the time of the runs when low concentration of solvent was used, or if the prolonged time of contact between the oil-solvent pairs would reach the same recovery as the high concentration cases in the long term. This is shown in Figures 12c, 13c and 14c, with the numbers over the bars indicate the soaking hours. This result indicates that a longer solvent exposure leads to a higher recovery for most cases; however, doubling the time of the tests

was not enough to reach the same recovery as if higher concentration of solvent was employed in half period of time. Nevertheless, a longer period of time than the employed here would eventually drive to this point.

3.3 *Recovery mechanisms.*

The main purpose of solvent injection in heavy-oil recovery processes is to reduce in-situ oil viscosity (Butler and Mokrys 1993,Gupta and Picherack 2003). However, the success of this method depends on the "driving force" or mass transfer between the solvent and the oil inside the matrix (Kahrobaei et al. 2012, Nenniger and Dunn 2008) and hence other forces as gravity and viscous forces along with pure solvent diffusion may contribute to oil recovery at different regions in the same core. This would explain the appearance of the cores left behind after; *e.g.*, the results of the experiments 28, 29 and 30 defined in Table 3 and shown in **Figure 15.** Figures 15 a-b show how organic material was deposited mainly at the top of each sample. This is expected to be asphaltene since the solvents used in both cases are paraffinic, while this material was not observed in Fig. c, where distillate with high aromatic components was employed.

Another important observation here is the visual aspect of the bottom of the cores and why the precipitated material is mainly found at the top. Due to the high difference between the viscosity and density of the solvent and oil employed, gravity rather than diffusion may govern the displacement from the bottom of the cores leading to a faster recovery at this section, as discussed by Kahrobaei et al. (2012), and also viscous fingering could occur inside the lower section of the core, when buoyant forces enhance the mixture formation, as described by Hatiboglu and Babadagli (2006).

As seen, the diffusion rate and mixing quality should be considered simultaneously in the selection of optimal solvent type and application procedure. Based on our observations presented in this paper, starting the solvent treatment with light solvents (low carbon number) for a short period of time and continuing it with distillate type may yield technically and economically feasible processes. Note, however, that we used “liquid” solvents in the experiments whereas “gas” solvents such as propane and butane are suggested (Das and Butler 1996a-b) in practice. Recent studies have shown that small carbon number solvents may yield inefficient mixing (Moreno and Babadagli 2013, 2104a-

b) or low mixing quality (with high asphaltene precipitation), mid-carbon numbers are more efficient (hexane-heptane) yielding optimal mixing quality. Therefore, it might be more preferable to start the process with this carbon number range (C6-C7) alkanes before switching to distillate.

4. Conclusions and Remarks

Oil recovery rate by solvent diffusion was found to be dependent on diffusion rate at early stages of the experiments when the solvent concentration in the mixture (oil and solvent) surrounding the core was high. In this study, it was observed that lower solvent concentration (half for instance) needs more exposure (soaking) time (more than twice) to compensate the effect of high amount of solvent to obtain the same oil recovery.

The results showed that heptane yielded the highest recovery -diffusion- rate followed by the distillate and decane at early times. However, at late times, distillate and heptane showed similar ultimate recoveries that can translate into a better mixing than decane. This could be explained by the aromatic content of the distillate that dissolves the heavier fractions more successfully than single component alkanes.

The distillate employed for these sets of experiments was found to be the most efficient solvent when both the diffusion rate and mixing quality were considered as well as the availability. However, it would be plausible to start the process with light single component solvents for a short period of time and continue with distillate type -heavier- solvents for a better efficiency.

The temperature, at which the liquid-liquid heavy oil/solvent mixture is formed, would possibly affect the ultimate recovery. For these experiments, as the oil and solvent were placed in contact at the same temperature, it was found that the closest the solvents are to their boiling points, the lower the recovery would be. Heptane optimum temperature application was found at 50°C and distillate gave good results when is used all in liquid phase (25 and 80°C).

Along with mass transfer due to solvent diffusion, it was found that gravity and viscous forces would enhance the recovery at the bottom of the cores since the buoyancy force would lead to a faster and better sweep section inside the oil matrix.

Acknowledgements

This research was conducted under the second author's (TB) NSERC Industrial Research Chair in Unconventional Oil Recovery (industrial partners are CNRL, SUNCOR, Petrobank, Sherritt Oil, APEX Eng., PEMEX, Husky Energy, and Statoil). A partial support was also obtained from an NSERC Discovery Grant (No: RES0011227). We gratefully acknowledge these supports.

Appendix

To generate the values of the y-axes of Figs. 6, 7, and 8, we used our previous data given in Figs. 9, 11, and 13 of Marciales and Babadagli (2014). Figs. A1, A2, and A3 illustrate the re-plots of these three figures. The very beginning of the experiments with high solvent concentration around the rock sample was taken to obtain the diffusion rates. Due to high solvent concentration around the rock sample, the diffusion rate is at its highest value. As seen in Figs. A2 and A3, diffusion rates corresponding to ~90% solvent concentration (mass fraction) were obtained (illustrated by the arrows) for three solvents. The solvent concentration value is 96% for the mineral oil cases (Fig. A1), at which point the asymptotic behavior begins. The obtained diffusion coefficient values were used as the y-axes of Figs. 6, 7 and 8.

References

1. Allen, J.C. and Redford, A.D. 1976. Combination Solvent-Noncondensable Gas Injection Method for Recovering Petroleum from Viscous Petroleum-Containing Formations including Tar Sad Deposits. US Patent No. 4,109,720.
2. Al-Bahlani, A.M. and Babadagli, T. 2011a. Field Scale Applicability and Efficiency Analysis of Steam-Over-Solvent Injection in Fractured Reservoirs (SOS-FR) Method for Heavy-Oil Recovery. *J. Petr. Sci. and Eng.* **78**: 338-346.
3. Al-Bahlani, A.M. and Babadagli, T. 2011b. SOS-FR (Solvent-Over-Steam Injection in Fractured Reservoir) Technique as a New Approach for Heavy-Oil and Bitumen Recovery: An Overview of the Method. Accepted for publication in *Energy and Fuels*, 2011.
4. Al-Gosayir, M., Leung, J. and Babadagli, T. 2012. Design of Solvent-Assisted SAGD Processes in Heterogeneous Reservoirs Using Hybrid Optimization

Techniques. *J. Can. Pet. Tech*. **51** (6) 437-44.
5. Al-Gosayir, M., Leung, J., Babadagli, T., and Al-Bahlani, A.M. 2013. Optimization of SOS-FR (Steam-Over-Solvent Injection in Fractured Reservoirs) Method Using Hybrid Techniques: Testing Cyclic Injection Case. J. *Petr. Sci. and Eng.* **110**: 74-84.
6. Ayodele, O. R., Nasr, T.N., Ivory, J., et al. 2010. Testing and History Matching ES-SAGD (Using Hexane). Paper SPE 134002 presented at the SPE West. Reg. Meet., Anaheim, CA, 27-29 May.
7. Butler, A.M and Mokrys, I.J. 1993 Recovery of Heavy Oils Using Vaporized Hydrocarbon Solvents: Further Development of the Vapex Process. *J. of Canadian Petr. Tech*. **32**: 56-62
8. Das, S.K. and Butler, R.M. 1996a. Countercurrent Extraction of Heavy Oil and Bitumen. Paper SPE 37094 presented at the International Conference on Horizontal Well Technology, Calgary, Alberta, Canada, 18-20 November.
9. Das, S.K. and Butler, R.M. 1996b. Diffusion Coefficients of Propane and Butane in Peace River Bitumen. *Can. J. Chem. Eng*. **74**: 986-992.
10. Edmunds, N., Maini, B., and Peterson, J. 2009. Advanced Solvent-Additive Processes via Genetic Optimization. Paper PETSOC 2009-115 presented at Canadian International Petroleum Conference (CIPC) 2009, Calgary, Alberta, Canada, 16-18 June.
11. Farouq, A. 1976. Bitumen Recovery from Oil Sands, Using Solvents in Conjunction with Steam. *J. Can. Pet. Tech*. **3** (11).
12. Farouq, A. and Snyder, S.G. 1973. Miscible Thermal Methods Applied to a Two-Dimensional, Vertical Tar Sand Pack, With Restricted Fluid Entry. *J. Can. Pet. Tech*. **12 (**4): 22-26
13. Gupta, S. and Picherack, P. 2003. Insights into Some Key Issues with Solvent Aided Process. *J. Can. Pet. Tech*. **43 (**2): 54-61.
14. Hatiboglu, C. and T. Babadagli, "Diffusion Mass Transfer in Miscible Oil Recovery: Visual Experiments and Simulation". Transport in Porous Media. **74**(2): 169-184 (2008).
15. Kahrobaei, S.; Farajzadeh, R., Suicmez, V.S. and Bruining, J. 2012. Gravity-Enhanced Transfer between Fracture and Matrix in Solvent-Based Enhanced Oil Recovery. Paper SPE 154171 presented at the SPE Improved Oil Recovery Symposium, Tulsa, Oklahoma, USA, 14-18 April.
16. Keshavarz, M., Okuno, R., and Babadagli, T. 2013. Optimal Application Conditions for Steam-Solvent Coinjection. Paper SPE 165471 presented at the SPE Heavy Oil Conference, Calgary, Alberta, Canada, 11-13 June.
17. Li, W. and Mamora, D.D. 2011. Light-and Heavy-Solvent Impacts on solvent-Aided-SAGD Process: A Low-Pressure Experimental Study. *J. Can. Pet. Tech*. **50** (4): 19-30.
18. Marciales, A. and Babadagli, T. 2014. Solvent Selection Criteria Based on Diffusion Rate and Mixing Quality for Different Temperature Steam/Solvent Applications in Heavy Oil and Bitumen Recovery. Paper SPE 16921 presented at the SPE Heavy Oil Conference, Maracaibo, Venezuela, 21-23 May.
19. Mohammed, M. and Babadagli, T. 2013. Efficiency of Solvent Retrieval during Steam-Over-Solvent Injection in Fractured Reservoirs (SOS-FR) Method: Core Scale Experimentation. Paper SPE -165528-MS presented at the SPE Heavy Oil

Conference, Calgary, AB, 11-13 June.
20. Moreno, L. and Babadagli, T. 2013a. Optimal Application Conditions of Solvent Injection into Oil Sands to Minimize the Effect of Asphaltene Deposition: An Experimental Investigation," SPE 165531, 2013 SPE Heavy Oil Conf., Calgary, AB, Canada, 11-13 June.
21. Moreno, L. and Babadagli, T. 2014a. Quantitative and Visual Characterization of Asphaltenic Components of Heavy-Oil and Bitumen Samples after Solvent Interaction at Different Temperatures and Pressures. *Fluid Phase Equilibria* **366**: 74-87
22. Moreno, L. and Babadagli, T. 2014b. Asphaltene Precipitation, Flocculation and Deposition During Solvent Injection at Elevated Temperatures for Heavy Oil Recovery. *Fuel* **124**: 202-211.
23. Naderi, K. and Babadagli, T. 2014a. Use of Carbon Dioxide and Hydrocarbon Solvents During the Method of Steam-Over-Solvent Injection in Fractured Reservoirs for Heavy-Oil Recovery From Sandstones and Carbonates. Accepted for publication in SPE *Res. Eval. and Eng*. 2014.
24. Naderi, K. and Babadagli, T. 2014b. An Evaluation of Solvent Selection Criteria and Optimal Application Conditions for the Hybrid Applications of Thermal and Solvent Methods. Submitted to *J. of Canadian Petr. Tech*. 2014b (in review).
25. Naderi, K., Babadagli, T., and Coskuner, G. 2014. Bitumen Recovery by the SOS-FR (Steam-Over-Solvent Injection in Fractured Reservoirs) Method: An Experimental Study on Grosmont Carbonates. *Energy and Fuels* **27** (11): 6501-6517.
26. Nasr, T. N. and Ayodele, O.R. 2005. Thermal Techniques for the Recovery of Heavy Oil and Bitumen. Paper SPE 97488 presented at the SPE Int. Imp. Oil Rec. Conf., Kuala Lumpur, Malaysia, 5-6 December.
27. Nasr, T.N., Beaulieu, G. Golbeck, H. et al. 2003. Novel Expanding Solvent-SAGD Process "ES-SAGD". *Can. Pet. Tech.* (technical note) **42** (1): 13-16.
28. Nenniger, J.E. and Dunn, S.G., 2008. How Fast is Solvent Based Gravity Drainage? Paper PETSOC 2008-139 presented at the Canadian International Petroleum Conference/SPE Gas Technology Symposium, Calgary, AB, Canada , 17-19 June.
29. Pathak, V., Babadagli, T. and Edmunds, N.R. 2013. Experimental Investigation of Bitumen Recovery from Fractured Carbonates Using Hot-Solvents. *J. of Canadian Petr. Tech...* **52** (4): 289-295.
30. Pathak, V., Babadagli, T. and Edmunds, N.R. 2012. Mechanics of Heavy Oil and Bitumen Recovery by Hot Solvent Injection. *SPE Res. Eval. and Eng.*, **15** (2): 182-194.
31. Pathak, V., Babadagli, T. and Edmunds, N.R. 2011. Heavy Oil and Bitumen Recovery by Hot Solvent Injection. *J. Petr. Sci. and Eng.,* **78**: 637-645.
32. Riazi, M.R. 2005. *Characterization and Properties of Petroleum Fractions*.1st Ed. Philadelphia, PA: ASTM Manual Series: MNL50
33. Zhao, L. 2004. Steam Alternating Solvent Process. Paper SPE 86957 presented at the International Thermal Operations and Heavy Oil and Western Regional meeting, Bakersfield, California, 16-18 March.
34. Zhao, L., Nasr, T., Huang, G., et al. 2005. Steam Alternating Solvent Process: Lab Test and Simulation. *J. Can. Pet. Tech.* **44** (9): 37-43.

Table 1: Oil sample properties

Oil samples	Density g/ml @ 25 °C	Viscosity, cP @ 25 °C	Refractive index, *n* @25°C
Mineral Oil	0.8734	250	1.47635
Oil 1	0.9818	20,675	1.55118
Oil 2	1.0035	153,000	1.53835
Oil 3	1.0156	476,353	1.58425

Table 2: Solvent Properties

Solvent	Specific Gravity	Viscosity, cP @ 25°C	Refractive index, *n* @25°C
Heptane	0.683	0.294	1.38418
Decane	0.735	0.848	1.40851
Distillate	0.738	0.742	1.41025

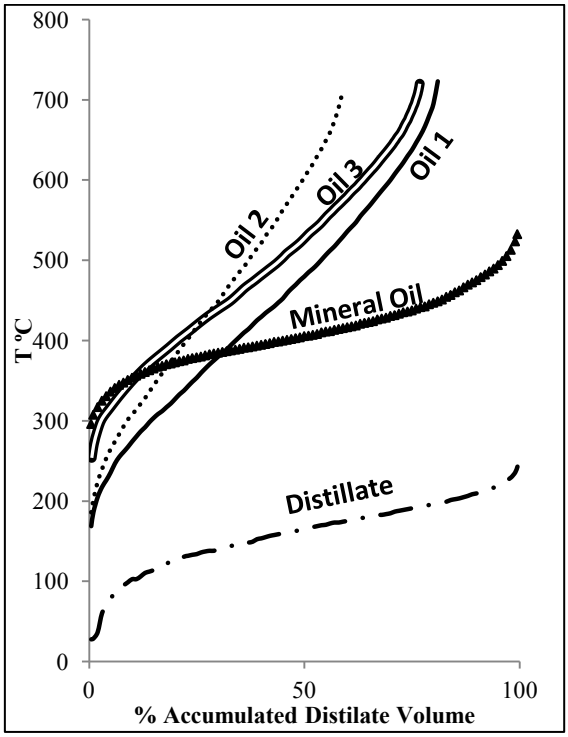

Carbon size number	FBP °C	Distillate	MO	Oil 1	Oil2	Oil3
IBP-C_5	36.1	1.918	---	---	---	---
C_6 -C_{10}	173.9	56.122	---	0.68	---	---
C_{11}- C_{13}	235	40.937	---	4.24	2.77	---
C_{14}-C_{20}	344	---	1.5	18.22	12.22	9.01
C_{21}-C_{30}	449	---	55.9	21.18	14.98	25.59
C_{31}-C_{40}	522	---	40.3	13.49	10.04	17.401
C_{41}-C_{50}	575	---	---	8.40	6.54	10.06
C_{51}-C_{60}	615	---	---	5.86	4.81	7.63
C_{61}-C_{70}	647	---	---	3.43	3.41	4.114
C_{71}-C_{80}	675	---	---	2.64	2.33	3.43
C_{81}-C_{90}	700	---	---	1.52	1.37	2.00
C_{91}-C_{100}	720	---	---	0.72	0.75	0.92
C_{100+}	720+	---	---	19.6	40.79	19.85

Fig. 1: Boiling range distribution of oil samples and distillate.

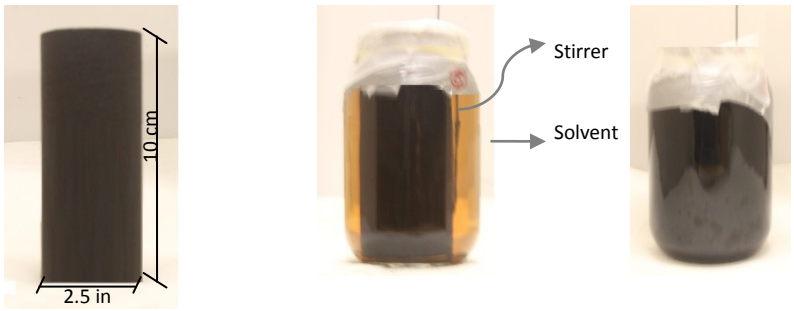

a) b) c)

Fig. 2 a:Berea sandstone core saturated with heavy oil, b) beginning of the solvent soaking experiment, and c) changed in the color of the surrounding fluid (oil solvent mixture) due to diffusion process at soaking times >150 hours.

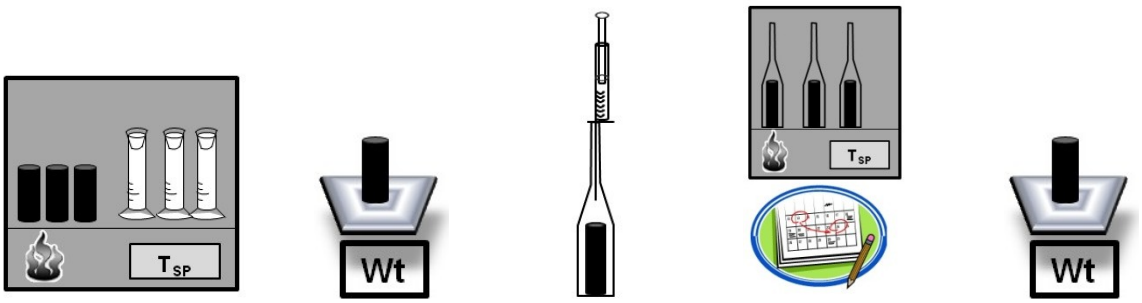

a b c d e

Fig. 3: Cores and solvent heated to settled temperature, b) Measured core change weight, c) Core and solvent placed in contact at the same temperature in a sealed imbibition cell, d) Soaking test run at determined temperature and refractive index taken periodically.

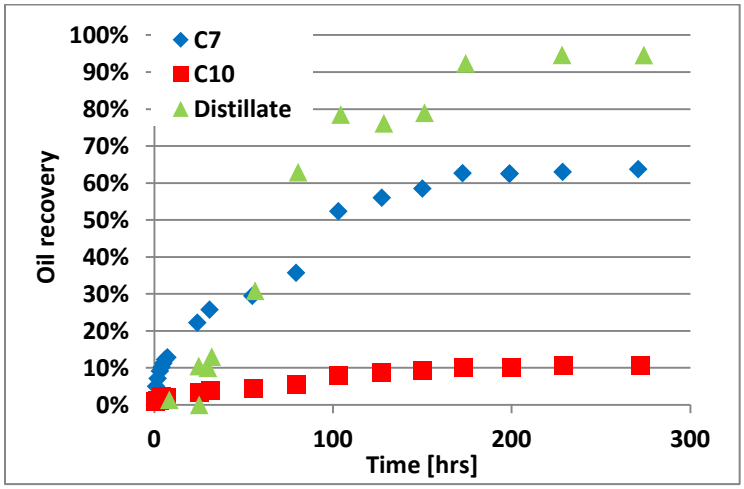

Fig. 4: Recovery rates for Oil 1: Experiments 4, 5 and 6.

Table 3: Saturated Cores-Solvent Experiments

Exp. No.	Temp. [°C]	Vol. Solvent/ Vol. Oil	Oil	Solvent
1	25	14.06	Mineral Oil	C7
2	25	15.91	Mineral Oil	C10
3	25	15.82	Mineral Oil	Distillate
4	25	14.06	Oil 1	C7
5	25	13.98	Oil 1	C10
6	25	13.95	Oil 1	Distillate
7	25	13.95	Oil 2	C7
8	25	14.16	Oil 2	C10
9	25	14.16	Oil 2	Distillate
10	25	18.72	Oil 3	C7
11	25	21.38	Oil 3	C10
12	25	18.52	Oil 3	Distillate
13	25	2.84	Oil 1	C7
14	25	2.66	Oil 1	C10
15	25	2.88	Oil 1	Distillate
16	25	2.57	Oil 2	C7
17	25	2.89	Oil 2	C10
18	25	2.76	Oil 2	Distillate
19	25	2.99	Oil 3	C7
20	25	3.16	Oil 3	C10
21	25	2.86	Oil 3	Distillate
22	50	3.54	Oil 1	C7
23	50	2.84	Oil 1	C10
24	50	2.842	Oil 1	Distillate
25	50	2.78	Oil 2	C7
26	50	3.99	Oil 2	C10
27	50	2.94	Oil 2	Distillate
28	50	3.89	Oil 3	C7
29	50	3.43	Oil 3	C10
30	50	3.12	Oil 3	Distillate
31	80	2.96	Oil 1	C7
32	80	2.63	Oil 1	C10
33	80	2.83	Oil 1	Distillate
34	80	2.67	Oil 2	C7
35	80	2.79	Oil 2	C10
36	80	2.31	Oil 2	Distillate
37	80	2.75	Oil 3	C7
38	80	2.83	Oil 3	C10
39	80	2.47	Oil 3	Distillate

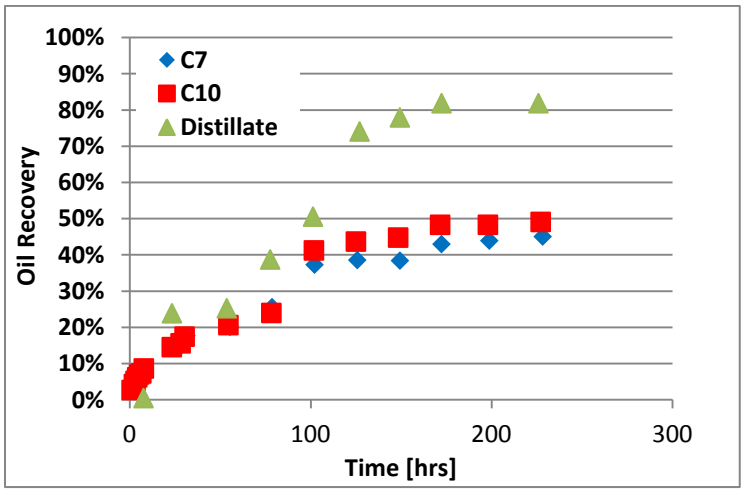

Fig. 5: Recovery rates for Oil 2: Experiments 7, 8, and 9.

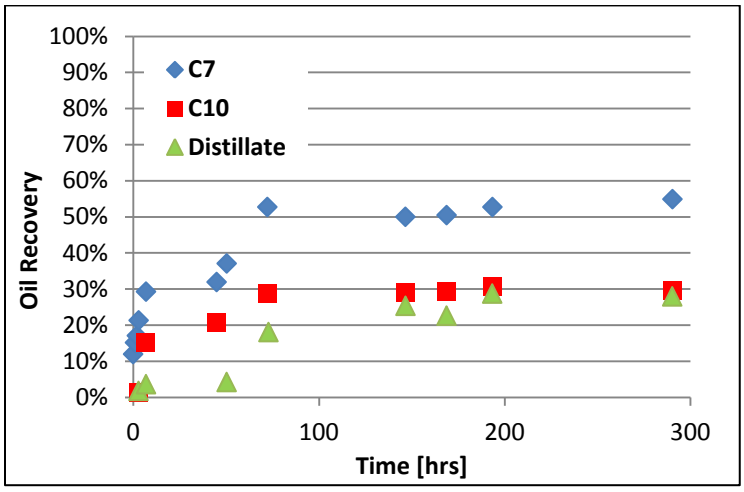

Fig. 6: Recovery rates for Oil 3: Experiments 10, 11, and 12.

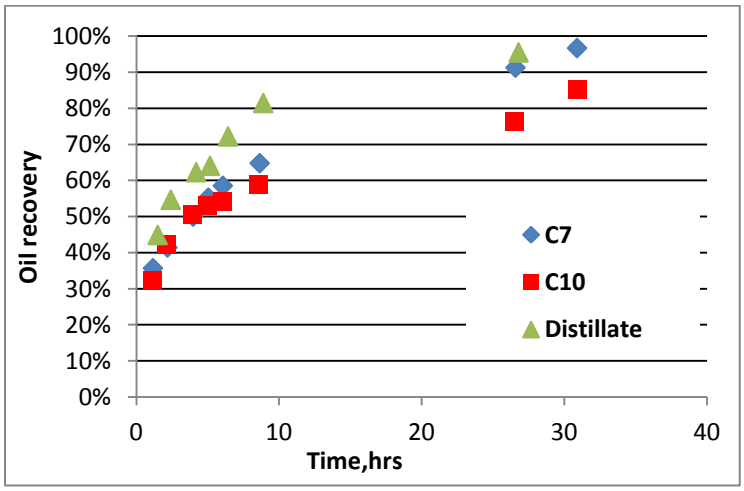

Fig. 7: Recovery rates for Mineral Oil: Experiments 1, 2, and 3.

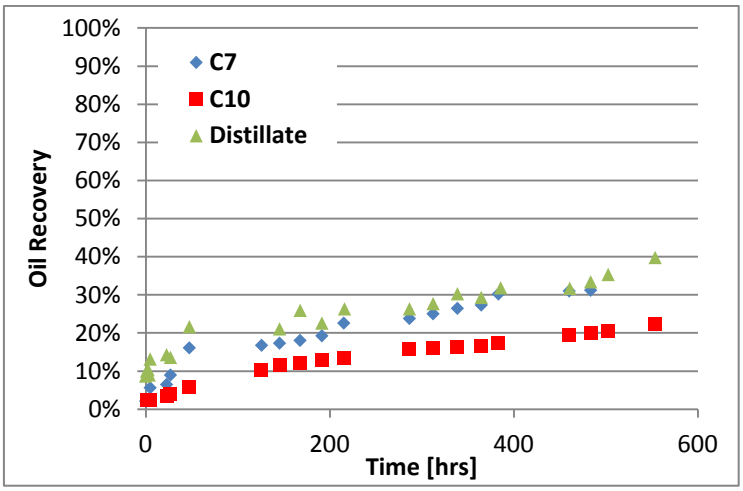

a) experiments 13, 14 and 15

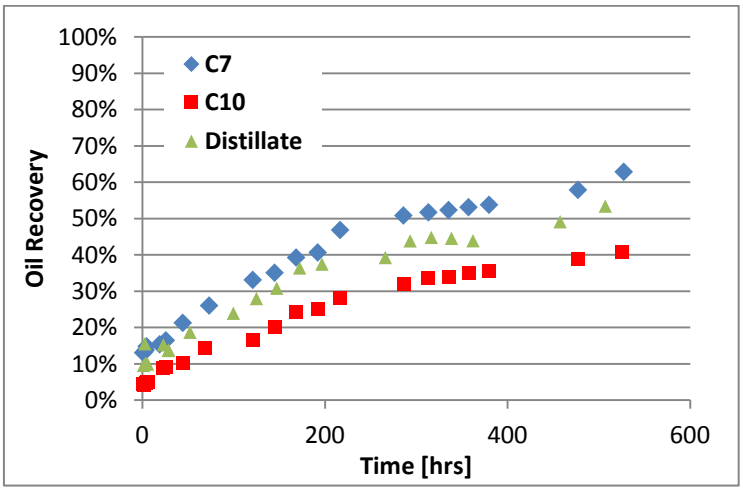

b) experiments 22, 23 and 24

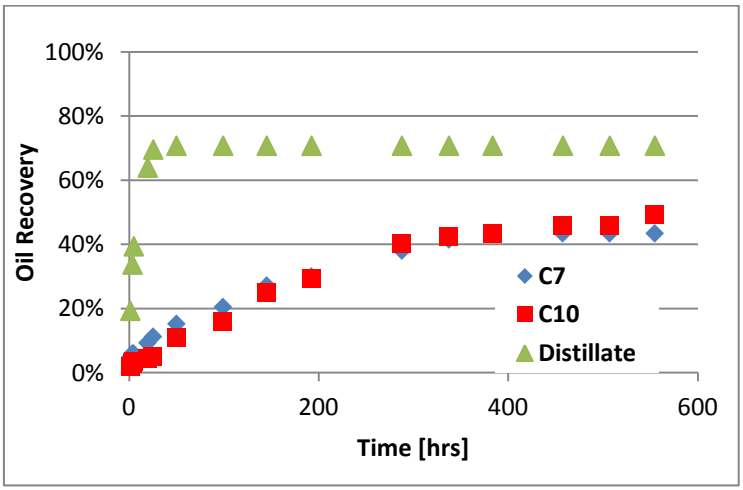

c) experiments 31, 32 and 33

Fig. 8: Recovery rates for cores saturated with Oil 1 for experiments run at a) 25°C, b) 50°C, and c) 80°C.

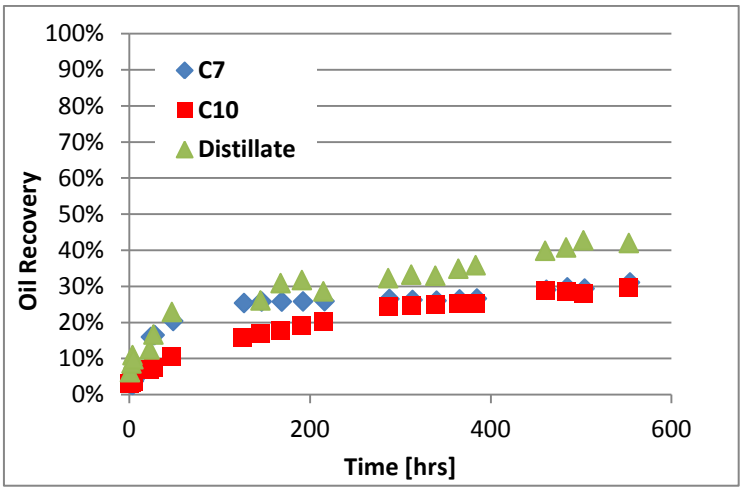

a) experiments 16, 17 and 18

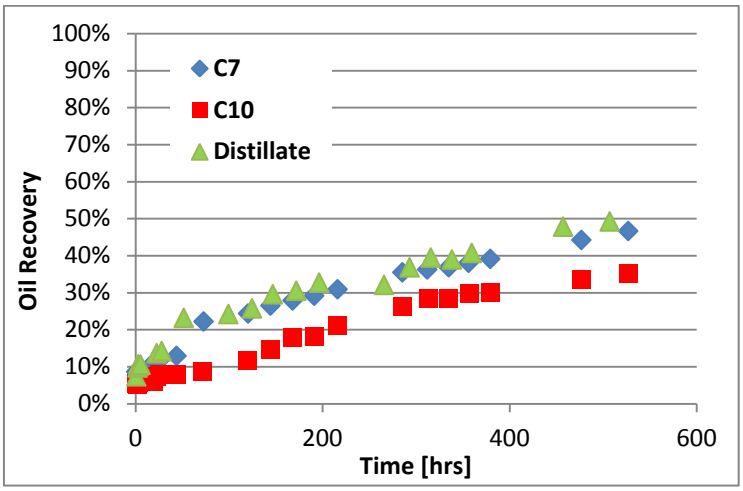

b) experiments 25, 26 and 27

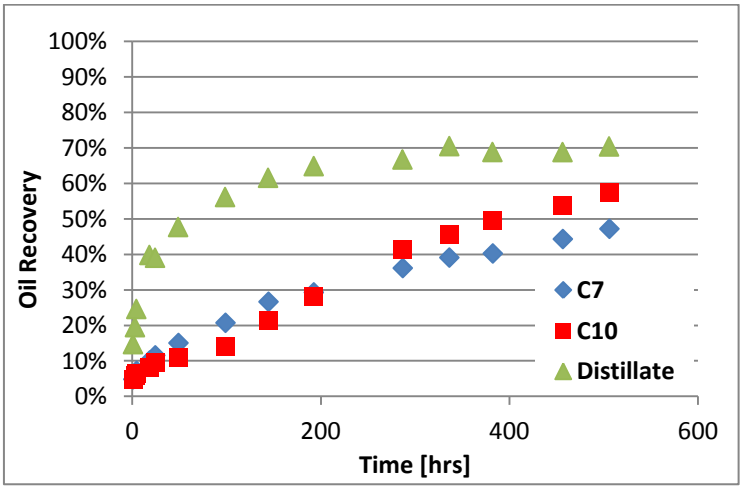

c) experiments 34, 35 and 36

Fig. 9: Recovery rates for cores saturated with Oil 2 with experiments run at a) 25°C, b) 50°C, and c) 80°C.

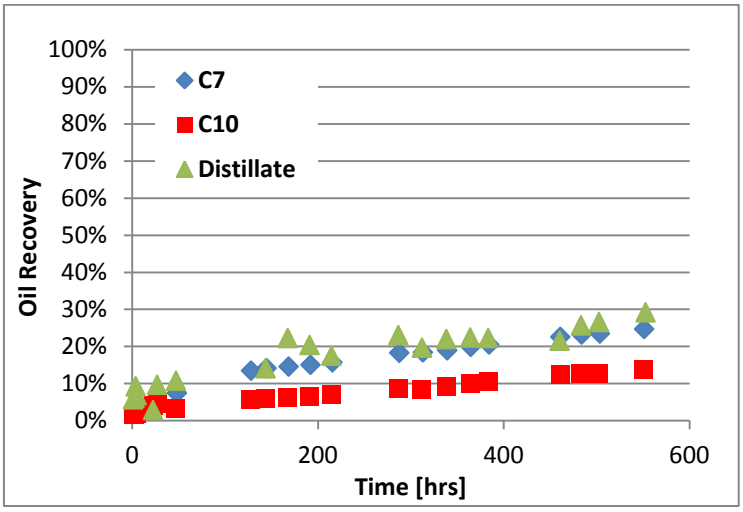

a) experiments 19, 20 and 21

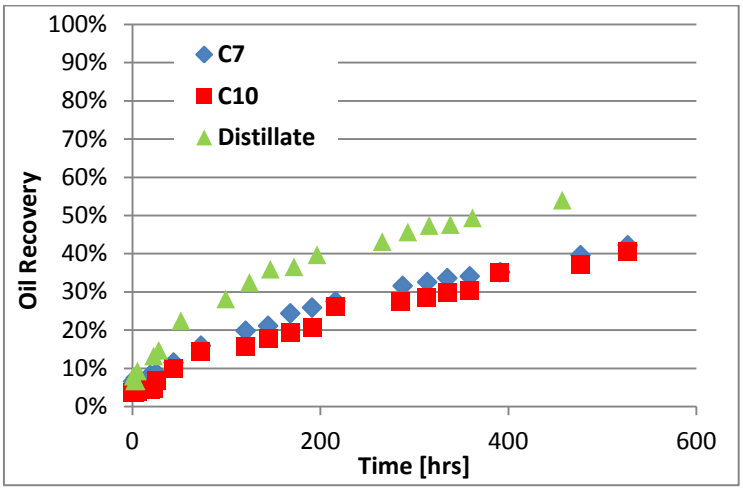

b) experiments 28, 29 and 30

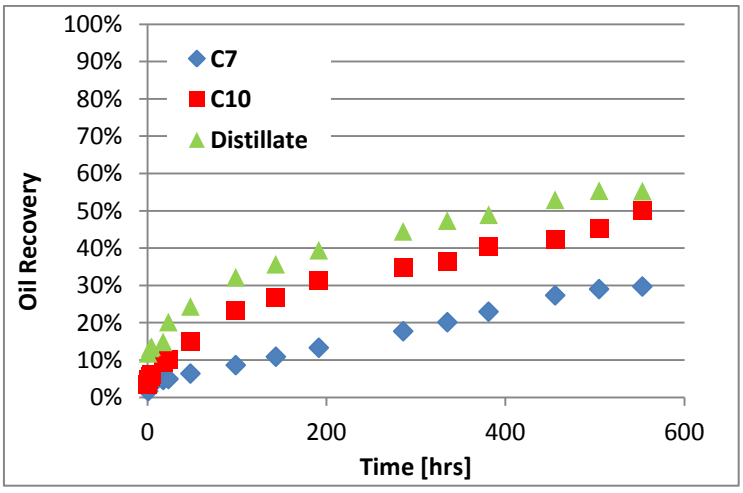

c) experiments 37, 38 and 39

Fig. 10: Recovery Rates for cores saturated with Oil 3 with experiments run at a) 25°C, b) 50°C, and c) 80°C.

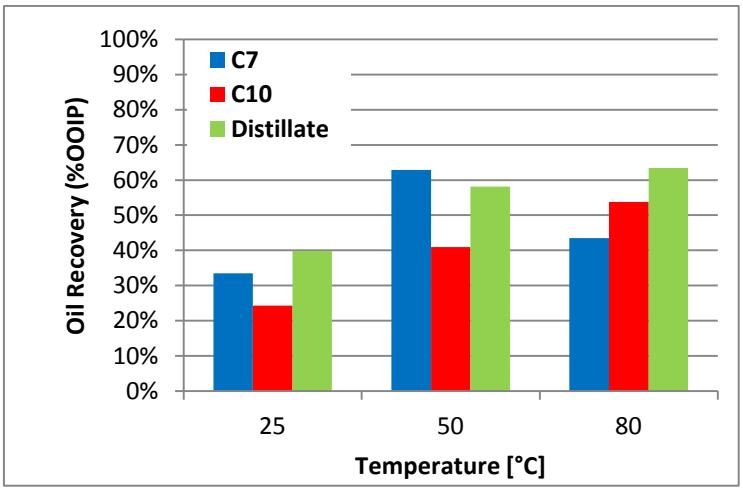

a) ultimate recovery of Oil 1

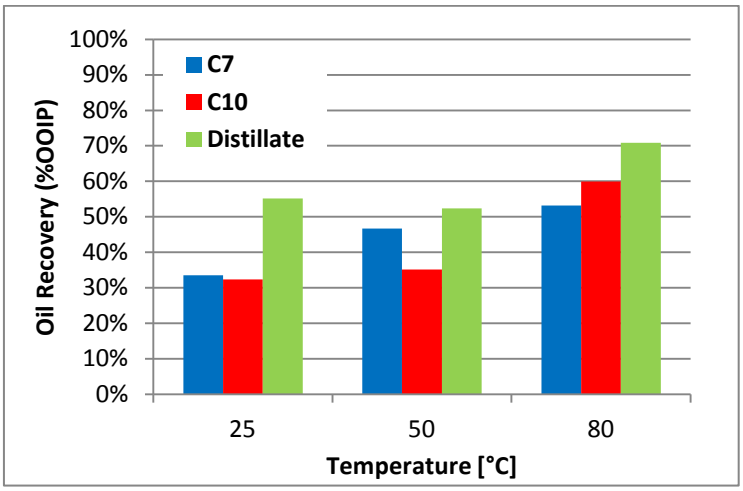

b) ultimate recovery of Oil 2

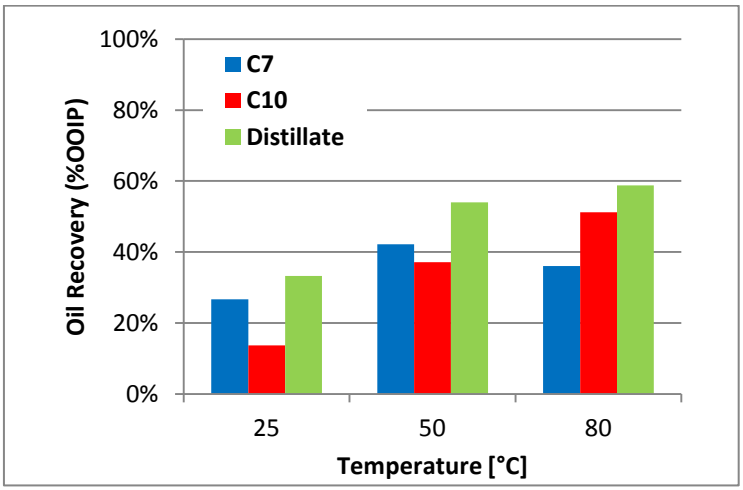

c) ultimate recovery of Oil 3

Fig. 11: Ultimate recovery summary.

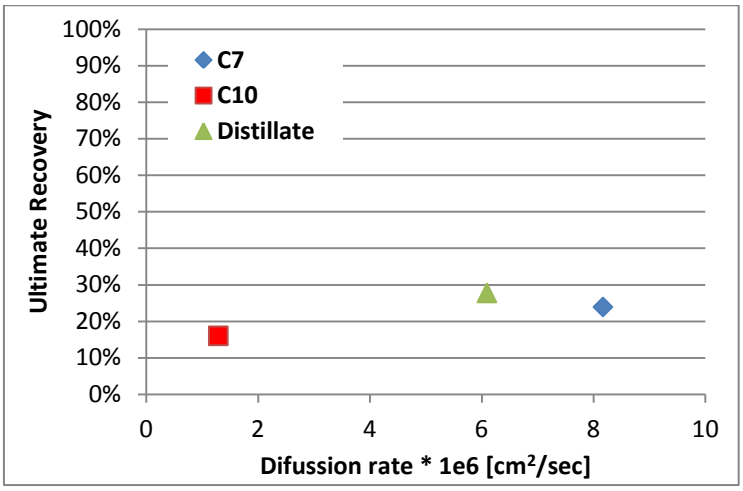

a) Molecular diffusion rate vs. ultimate recovery at low concentration of solvents in Oil 1 (exp 13, 14 and 15)

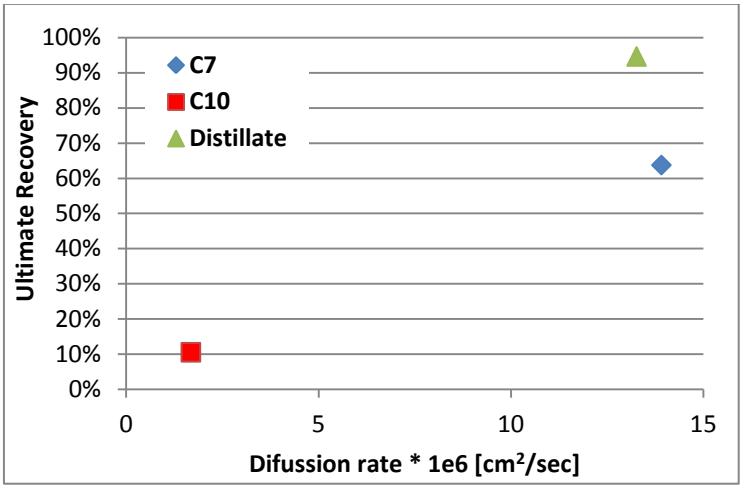

b) Molecular diffusion rate vs. ultimate recovery at high concentration of solvents in Oil 1 (exp 4, 5 and6)

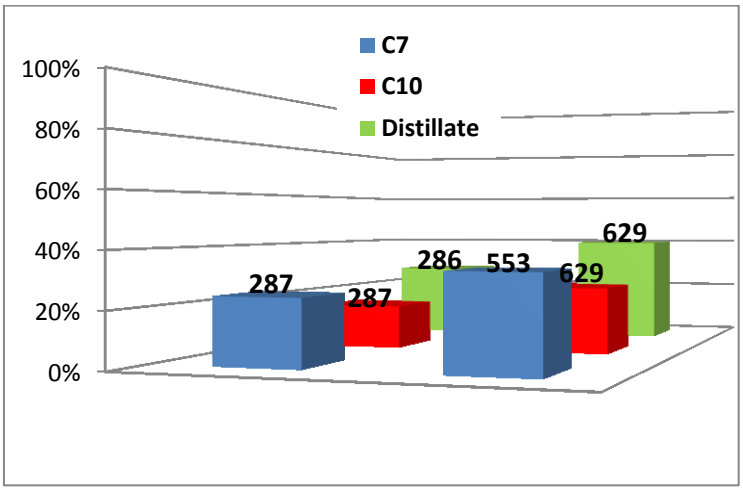

c) Soaking time effect (written in bold fonts on each bar in hours) on recovery for the experiments run at low concentration of solvent.

Fig. 12: Solvent concentration and soaking time effect on experiments run at 25°C for cores saturated in Oil 1.

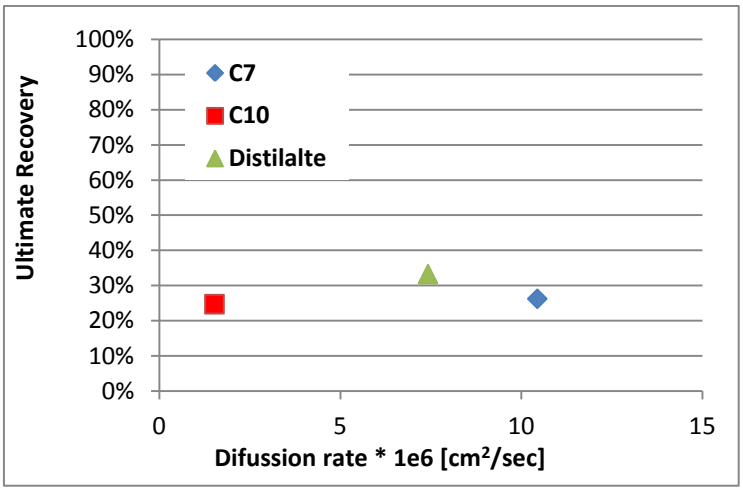

a) Molecular diffusion rate vs. ultimate recovery at low concentration of solvents in Oil 2 (exp 16, 17 and 18)

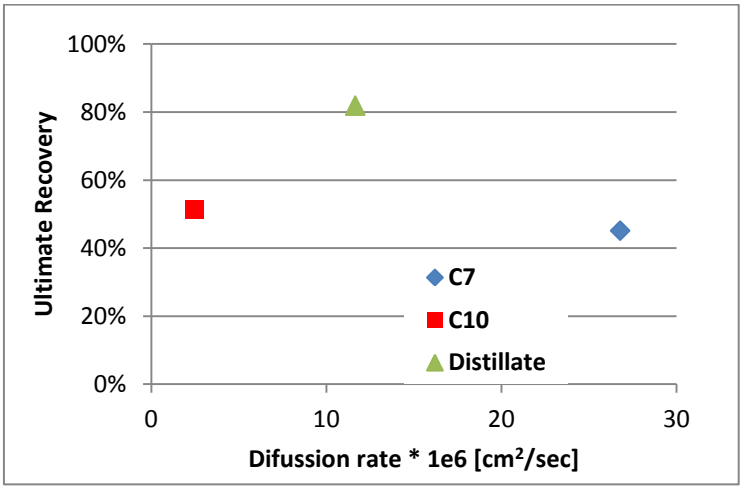

b) Molecular diffusion rate vs. ultimate recovery at high concentration of solvents in Oil 2 (exp 7, 8 and 9)

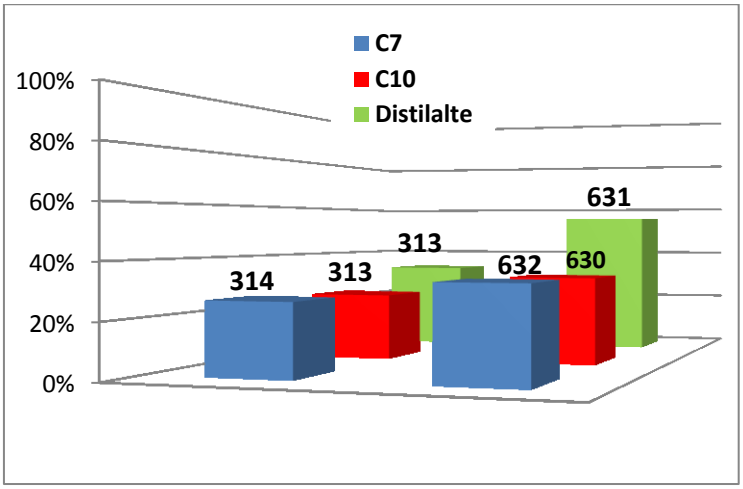

c) Soaking time effect (written in bold fonts on each bar) on recovery for the experiments run at low concentration of solvent.

Fig. 13: Solvent concentration and soaking time effect on experiments run at 25°C for cores saturated in Oil 2.

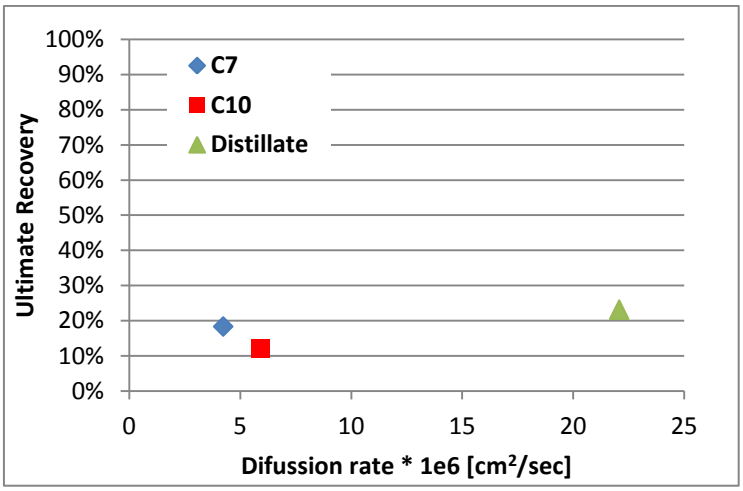

a) Molecular diffusion rate vs. ultimate recovery at low concentration of solvents in Oil 3 (exp 19, 20 and 21)

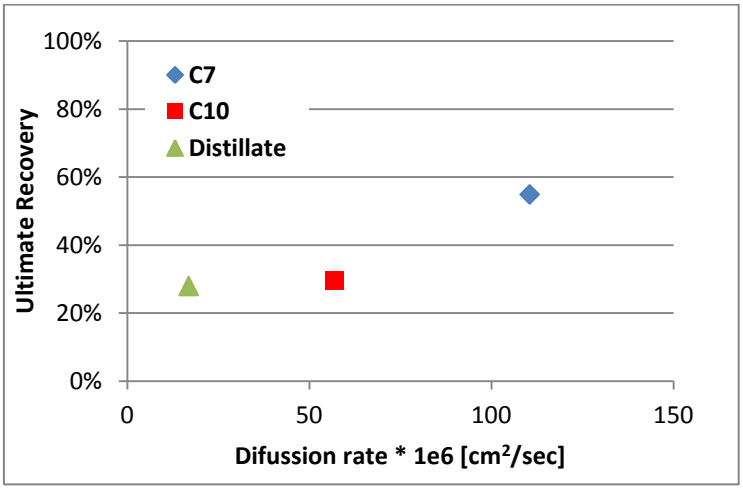

b) Molecular diffusion rate vs. ultimate recovery at high concentration of solvents in Oil 3 (exp 10, 11 and 12)

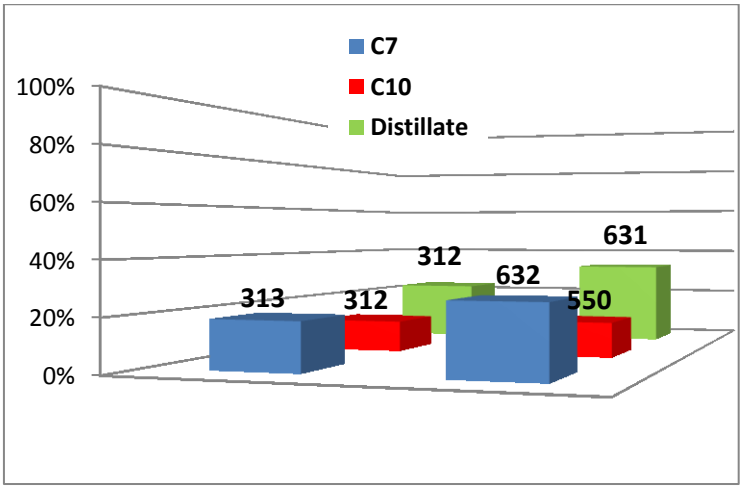

c) Soaking time effect (written in bold fonts on each bar) on recovery for the experiments run at low concentration of solvent.

Fig. 14: Solvent concentration and soaking time effect on experiments run at 25°C for cores saturated in Oil 3.

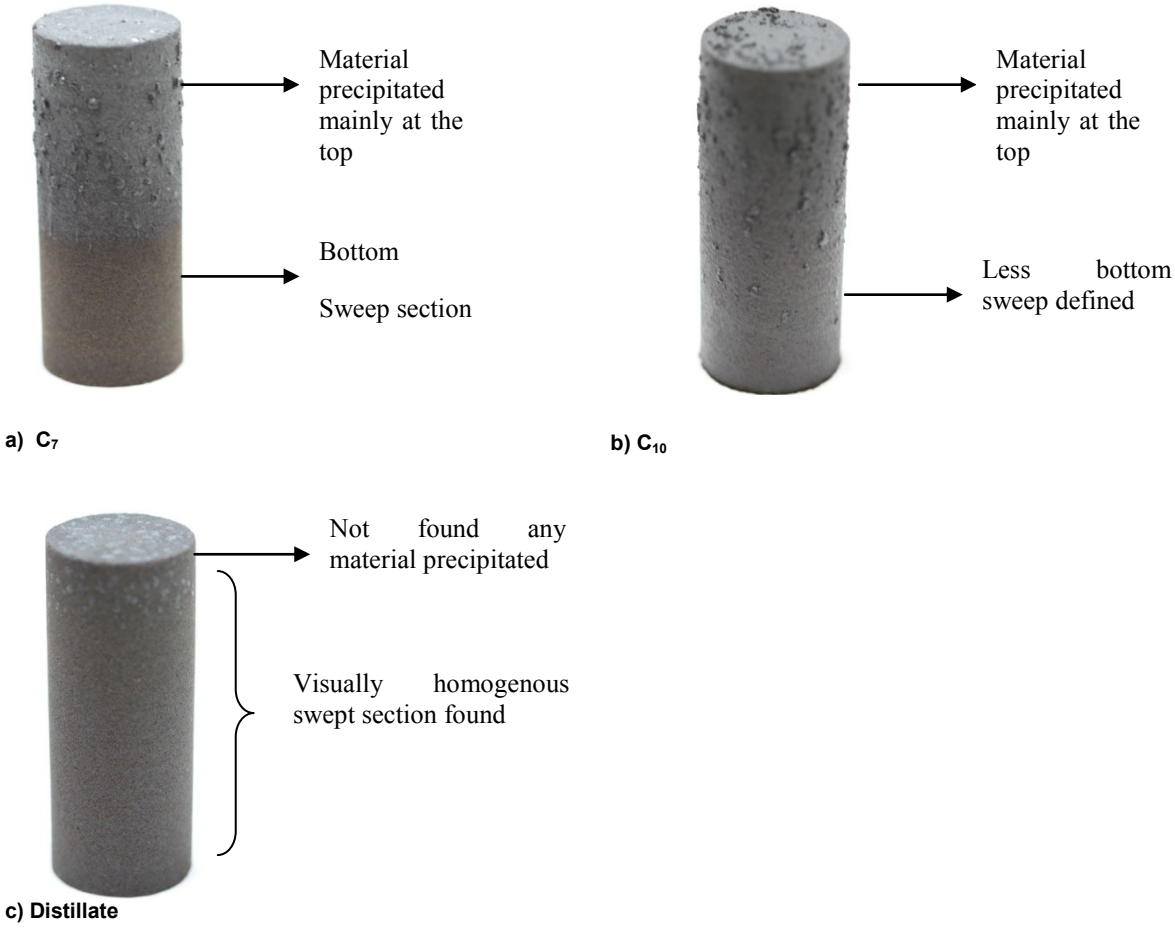

Fig. 15: Cores saturated with Oil 3 left after experiment at 50°C were run in experiments; a) 28, b) 29, and c) 30.

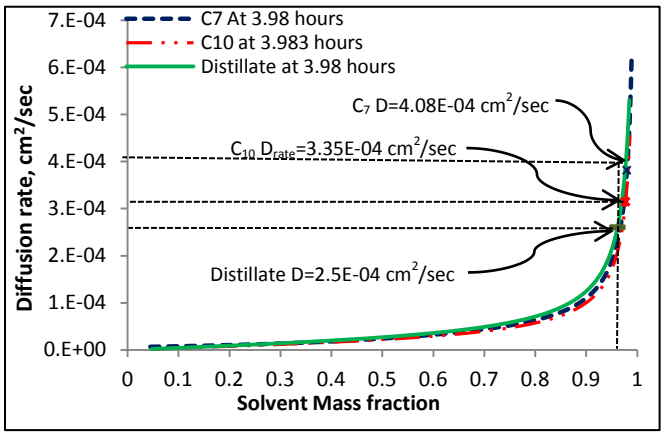

Fig. A1:Molecular diffusion coefficient vs. solvent concentration for mineral oil (modified from Fig. 9 of Marciales and Babadagli 2014).

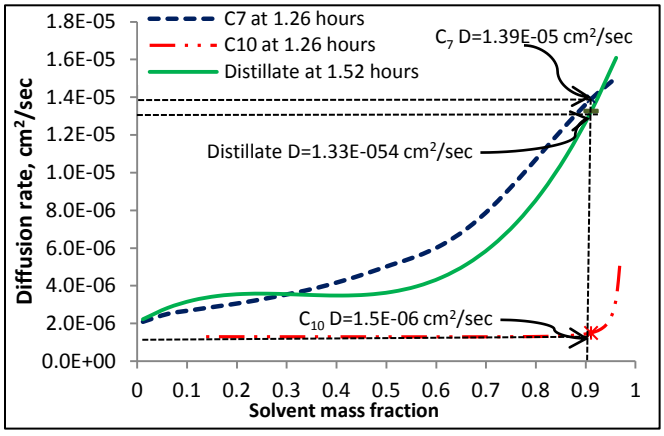

Fig. A2:Molecular diffusion coefficient vs. solvent mass fraction for Oil 1 (modified from Fig. 10 of Marciales and Babadagli 2014).

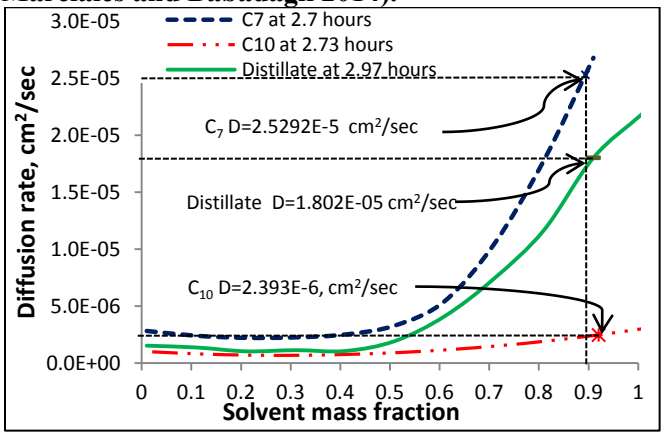

Fig. A3:Molecular diffusion coefficient vs. solvent concentration for Oil 2 (modified from Fig. 11 of Marciales and Babadagli 2014).

CHAPTER 4: PORE SCALE INVESTIGATIONS ON SOLVENT RETRIEVAL DURING HEAVY-OIL RECOVERY AT ELEVATED TEMPERATURES: A MICROMODEL STUDY

A version of this paper will be submitted to the International Journal of Heat and Mass Transfer

Preface

This work attempts to visualize the solvent recovery mechanisms at the pore scale using micro fluidic devices (also known as micromodels) at low pressure in order to understand the phenomena behind this process when applied to fractured reservoirs.

After the micromodels were saturated with dyed mineral oil, a certain amount of dyed solvent was injected. Once the solvent diffused inside the porous media, different parameters such as heating source, composition inside the fracture, solvent type, and porous wettability were studied to establish their impact on solvent retrieval mechanisms. Pore visualization was achieved through the use of UV light image analysis and the optimal recovery technique was found.

1. Introduction

The flow of two miscible fluids in porous media is commonly encountered in different anthropogenic and natural processes including enhanced oil and heavy-oil recovery, ground water contamination and nuclear waste disposal, and CO_2 sequestration. Over several decades, attention has been given to the use of solvents in heavy-oil recovery. Initial attempts were to inject solvents at isothermal conditions [1-4]. Later, solvent was considered as an additive to steam [5-8] or injected alternately with steam [9-16]. Injection of hydrocarbon gases and CO_2 under miscible conditions is also a common practice in the late stages of the recovery of lighter oils [17].

In all of these applications, the retrieval of expensive solvent is essential for the economics of the process. Optimal conditions were determined on the basis of selecting proper solvent type and amount [4,18-20] and setting up suitable operational schemes to maximize oil recovery while minimizing solvent retention in the reservoir [21-26].

All these previous attempts on the subject indicated that the use solvent in any type heavy oil recovery applications would not be viable without viable solvent retrieval design. This can be achieved by injecting water after solvent in light oil and homogeneous reservoirs. This is not practically viable in case of heavy-oil systems due to unfavorable mobility. If the reservoir is heterogeneous, caused by natural or hydraulic fractures, wormholes, and frequent occurrences of low and high permeability layers, the solvent retrieval is even more complicated.

Solvent retrieval, as a mandatory step in heavy-oil recovery applications, was investigated through theoretical and experimental research, and pilot scale field applications. Gupta et al. [18] studied the capillary adsorption in porous media as the key process for solvent retrieval and retention clarifying the impact of pore size distribution in the thermodynamics involved in the process. Other conceptual proposals at the field scale consist of a solvent recovery methodology through the employing solvents in sequence depending on their carbon size number. This sequence is based on the fact that heavier solvents should be injected first followed by lighter ones, which can be recovered through the reduction of

reservoir pressure [27]. Additionally, Gates and Gutek [28]improved this idea using the same principle giving more operational details to this methodology considering the efficient injection schemes of solvent.

Also, Léauté [8] proposed a new method called LASER (liquid addition to steam for enhancing recovery), which involves diluent oil injection with steam at the late stage cycles. The field scale pilot applications showed that 80% recovery of diluent is attainable through the use of proper separation facilities in the wellhead [29](Leaute and Carey 2007). Later on, Gupta and Gittins [21] and Gupta et al. [30] proposed a method for evaluating solvent recovery during the alternate injection of solvent and steam (SAP, solvent aided process) considering the heavy components of oil, deasphalting inside the reservoir by injected solvent, and the composition of produced oil.

In addition to these types of solvent retrieval options for heavy-oil recovery in homogeneous reservoirs, attempts were made for heterogeneous (fractured) systems. Babadagli and Al-Bahlani [31,32] patented a technology suggesting solvent retrieval by introduction of heat through steam or hot water injection at temperatures near the boiling point of the solvent. Al-Bahlani and Babadagli [11,12] and Mohammed and Babadagli (2013) showed that the solvent retrieval might reach 90% if the proper temperature range is selected during post steam/hot-water applications.

2. Statement of the Problem and Objectives

When solvent is injected into a fracture porous medium it diffuses into matrix while flowing in the fracture network. The matrix oil diluted through this process can be recovered by gravity drainage and convective transport [12,13,34,35]. Although the process is rather slow, the effectiveness of heavy-oil recovery can be improved by proper solvent selection [36,37]. To improve the efficiency of the process, the solvent must be retrieved at economically acceptable rates. This, however, may not be possible through the viscous or capillary displacement due to permeability contrast between the fracture and matrix. As mentioned in Section 1, Babadagli and Al-Bahlani [31,32] suggested injecting steam or hot-water to heat the matrix to the boiling point of the solvent. Hence, this

method is purely based on maintaining the suitable thermodynamic conditions; i.e., the boiling temperature of solvent for given pressure.

Numerous experimental work at the core scale have been presented to clarify the physics [12] and optimal operation conditions [11,12,14-16,19,20] of the solvent retrieval process. Further visual studies are needed to clarify the dynamics of the solvent retrieval at non-isothermal conditions and the reasons behind the solvent entrapment in the matrix. This is a crucial problem in heavy-oil recovery from the reservoirs with different types of heterogeneities including steam/solvent injection in fracture carbonates and post-CHOPS (cold heavy-oil production with sands) enhanced oil recovery applications.

This work introduces a micro scale analysis to clarify the dynamics of solvent retrieval from matrix under variable temperatures at atmospheric pressure. The reasons for the entrapment of the solvent during this process were also investigated for different wettability conditions, solvent type and heating process.

Although the work presented here is mainly qualitative, there are some thermodynamic concepts worth reviewing for a better understanding of the phenomena occurring during the micro scale experiments. We start with the review of the theory of the process in Section 3 and introduce experimental design and observations in Sections 4 and 5.

3. Theory: Effect of Pore Size in Phase Equilibrium-Kelvin Effect: Vapor Pressure and Boiling Point

When liquid or vapors are contained inside porous media, their phase equilibrium properties are not the same as they are in bulk conditions; i.e., over a flat surface. This is explained through the *Kelvin effect* [38].

Depending on the shape of the surface and the radius of the porous media containing it, the vapor pressure and boiling point may increase or decrease. For our specific case, wherein the solvent under consideration is mostly on the convex side of the surface, there was a set of equations to predict and quantify the change of the vapor pressure or boiling point given a specific pore size and other properties of the system.

$$P_r^s = P_\infty^s exp\left(-\frac{2\sigma v^L}{rRT}\right) \quad (1)$$

$$T_r^s = T_\infty^s exp\left(-\frac{2\sigma v^L}{r\lambda^{vap}}\right) \quad (2)$$

P_r^s Vapor pressure of the liquid in the porous media

P_∞^s Vapor pressure of the same liquid at the same temperature under bulk conditions

σ Surface tension at the given temperature

v^L Molar volume

r Pore size radius

R Gas constant

T System temperature

T_r^s Saturation temperature in the porous media

T_∞^s Saturation temperature of the same liquid at the same pressure under bulk conditions

λ^{vap} Heat of vaporization

Eq. 1, also known as the Kelvin equation, predicts the reduction in the vapor pressure when the pore size decreases at a constant temperature. For this case, the *Kelvin effect* describes the condensation of vapor into finely porous solids wet by the condensate at partial pressures below the equilibrium vapor pressure, also known as capillary condensation [38], or the capillary adsorption in which a liquid will desorb the larger pores earlier than the smaller ones when pressure is gradually lowered. After reducing the vapor pressure below the saturation pressure of a pure solvent contained in porous media, substantial amount of solvent will remain in the liquid phase [18]. On the other hand, Eq. 2, known as Thomson equation, shows that the boiling point becomes lower as the droplet or the pore gets smaller [38].

Is should be emphasized that Eqs. 1 and 2 are valid for a single pore size. As natural porous media contain variable sizes of pore, it is important to include pore size distribution when applying this set of equations for constructing desorption curves. Additionally, if

there is more than one substance saturating the porous media, the computation of the desorption curve for each specific case makes the calculations more complex [18].

The experimental data (Section 5) provided in the remaining part of the paper will shed light not only on the retrieval of solvent for practical applications but also provide the base to further develop the Thomson equation for variable pore sizes.

4. Experimental Methodology

All solvent retrieval experiments were carried out using a Berea sandstone replica model with a fracture. The dimensions of the matrix part of the model were 5x 5 cm, while the fracture dimensions are 1 x 5 cm. The depth of the model was nearly 40μm. The model, made of glass, was prepared through chemical etching techniques suggested by Naderi et al. [39] and Thai (2005).

The micromodel had the injection and production points at the left and right side of the fracture as shown in **Figure 1**. The picture area, used throughout the experiments, is the shadowed section in Figure 1 and its dimensions were approximately 1.9 x 2.7 cm.

The images were captured using a Canon (7D model) camera assembled with a 100mm macro lens and a filtered UV light. During the experiments, the oil and solvent phases were dyed with oil-wet solvents (DFSB-K175, DFSB-K43) from Risk Reactor [40]. A heating plate was employed to provide the heat source necessary to increase the temperature inside the micromodel. Temperature was monitored continuously using a thermocouple (fluke 53/54 II). The injection of oil and solvent into the micromodel was achieved by controlled syringe pump (Kant YA 12). The setup is illustrated in **Figure 2.**

The micromodel, made of borosilicate glass, was initially water-wet/mixed-wet. Later on, its wettability was altered to oil-wet/mixed-wet using dichlorooctamethyltetrasiloxane (Surfasil^{TM}) following the procedure suggested by Naderi and Babadagli [39].

The oil phase was composed by light mineral oil (LMO). Heptane (C7) and distillate oil were the solvents used in the experiments. Their boiling point, viscosity, and density are given in **Table 1** and **Figure 3**.

5. Experimental Procedure

The models were heated in two different ways, namely matrix (whole model including fracture) and fracture heating. The matrix heating refers to the tests in which the whole micromodel was heated uniformly during the experiment including matrix and fracture (the shaded area in **Figure 4a**). This mimics heating the matrix by a fracture totally in contact with one side of the matrix (planar heating). In fracture heating, heat was only applied to the fracture section of the model, as shown in **Figure 4-b.** This type of heating boundary condition refers to point heating rather than planar. Both cases result in different heat transfer processes and, thereby, different temperature distributions.

Table 2 summarizes the experimental conditions. In the experiments, different combinations of oil-solvent types and heating boundary conditions were applied. All experiments started with achieving full saturation of the micromodel by light mineral oil (LMO). The next step was to inject solvent to fill the fracture at a rate of 1.0 ml/hr (at 25°C). The production point was kept opened during the injection period until the fracture was fully filled with the solvent. At this point, the injection point was closed and the solvent was left to diffuse into the matrix at room conditions. This phase was continued until the equilibrium point is reached; i.e., solvent fingers stabilized inside the matrix. The third step was started with a progressive increase of heat to the model to start the solvent boiling process. The bubble forming process was videotaped. When no more bubbles were observed after a certain period of time, temperature was increased again. This duration of the last step depended on each specific case (boiling temperature of the solvent or other factors listed in Table 1).

The initial conditions in all experiments were the same, filling the fracture with the solvent before starting to heat the model. The exception was Experiment 2, in which the fracture was filled with LMO, assuming that before heating the process, oil was produced for a period of time resulting in the fill up of fractures with it.

6. Results

The parameters studied to analyze the mechanisms for solvent retrieval through the visualization experiments included a) heating boundary conditions, b) the fluid that filled the fracture before the heating period, c) solvent type, and d) wettability. All pictures included in the paper from this point on were taken out from the framed area (1.9 x 2.7 cm) in Figure 1. Some images show the whole area and a few of them were close-ups of the pores.

For observation purposes, the color of the dye used with solvent and oil was the same. The pores filled with pure solvent are displayed in cyan color, while brown areas represent pure LMO. Any variation between these two is a product of its mixture since both fluids are fully miscible in first contact in all proportions, and solvent and oil dye are oil-wet. Solvent in the vapor phase and micromodel grains were detailed for each specific case.

6 Effect of Heat Distribution: Experiments 1 and 3

6.1 *Results for Experiment 1.*

Figure 5 shows the micromodel after solvent saturation and before the heating step for Experiment 1. The first bubble appeared inside the fracture when temperature reached a value of 57.8°C, which is below the bulk boiling point of heptane. This could be explained by the Kelvin effect described by Eq. 2; however, the bubbles were not stable. Subsequently, temperature of the heating plate was increased to the next level, which caused a temperature rise to 75°C in the fracture and 55°C inside the matrix. A slow rate of bubble growing and expansion of solvent towards the horizontal edges and then vertically into the pores were observed (**Fig. 6)**.

In order to observe the vapor growth, the temperature was increased again until it reached a value of 75°C in the fracture and 63°C inside the matrix. At this time, all solvent was completely vaporized inside the fracture and drained out via the production point, and the bubbles continued growing in the vertical direction as shown in the images of **Figure 7a-d**.

Figure 8 shows the close-up images of the preferred route for the bubbles to expand and how solvent is retrieved during Experiment 1. It was observed that bubbles grew up together as a continuous phase in the matrix. Note that vapor solvent (black color

surrounded by a white line) in fracture flows toward the production end but the liquid solvent (or oil solvent mixture in cyan color) also fills the fracture adjacent to the matrix. This solvent re-enters the matrix and occupies the pores in the vicinity to the matrix (Figure 7d). Phase change also occurs in many sections of the system (circled areas in Figure 8b).

6.2 *Results for Experiment 3.*

After solvent diffusion is completed for Experiment 3 (**Figure 9a**), uniform heat was applied to the micromodel. This means matrix and fracture zones were heated at the same time (i.e., there was no temperature gradient throughout the whole model as in Experiment 1). Because of this, the matrix reached the solvent boiling point temperature faster compared to Experiment 1. Mixture quality between oil and solvent was also affected by temperature increase. When temperature of the model was increased from room conditions to 75°C, the matrix showed more homogeneous mixing, likely because of the Soret effect, which in this case refers to the contribution of the temperature gradient to the mass transfer [41] (Fig. 9b).

This test did not show nucleation or slow bubble growth from it. On the contrary, the bubbles developed spontaneously throughout the whole -observed- area and the fracture started to fill up by solvent vapor (Fig. 7j-l). Although this process was quicker, the efficiency of the solvent retrieval was not as effective as it was in Experiment 1 (point heating) as indicated by trapped liquid solvent (cyan color) surrounded by vapor (black color). At the same time, some solvent bubbles were trapped surrounded by the solvent present in liquid phase (**Figure 10**). However, these isolated bubbles were connected and created a continuous phase after a while (**Figure 11**), which facilitated solvent retrieval.

This run was useful to scrutinize the temperature effect in solvent recovery. After eight hours of uniform planar heating at a constant temperature, there was no significant change in bubble growth due to solvent evaporation; but, a slight improvement in solvent retrieval was achieved (**Figure 12**).

A visual comparison of solvent vaporization efficiency for this case is illustrated in Figure 7i-l**.** While solvent vaporization grew in vertical direction in Experiment 1, both vertical and horizontal growth of bubbles were observed at the same time due to planar heating.

6.3 *Effect of composition in the fracture in Experiment 2.*

Experiment 2 differs from the others because it contains only original oil (LMO) in the fracture. After completing the solvent injection phase, LMO was fed through the injection point to displace the solvent in the fracture and saturate the fracture with it. However, since the mobility ratio of LMO is higher than solvent (C_7) for this case, a degree of LMO intrusion into matrix was unavoidable (**Fig. 13a**). An improvement in oil-solvent mixture quality was observed (**Fig. 13b**) due to temperature increase to 75°C.

Solvent retrieval in this case was not achieved under the same temperatures (≤75°C) required to boil any solvent contained in the fracture or matrix as in all the other experiments. Even if the system was kept under these conditions for a period of time to produce any variation (1.5 hours). As in Experiment 3, it was found that composition of the phase in question is determinant to observe phase change. Despite no knowledge of the predominant hydrocarbon size mixture in the fracture, the temperature in the system was incrementally raised to observe any bubble forming. This was achieved when the fracture temperature reached 135°C and the temperature in the matrix was 88.6°C. Although this value is below the lowest boiling range distribution for LMO (Fig. 3), it is higher than the minimum required for boiling heptane as mentioned in Experiment 1. This deviation from the original values could be expected as a result of the Kelvin effect, and this temperature was needed to boil any of the lighter components present in the oil, which at least have a carbon size number twice that of heptane (Fig. 3).

Initially, a change was observed in the fracture in the vicinity of the production point and progressively developing toward the injection point (Figure 7e-h). After 6 hours of constant heating, only the fracture zone is vaporized (**Figure 14**).

Despite that the experiment was stopped before any bubble was observed inside the matrix, the bubbling expansion trend obtained here was similar to Experiment 1 and this could be attributed to the heat distribution, because, as in the previous case, only the fracture area was exposed to the heat source.

6.4 Effect of solvent type in Experiment 4.

Figure 15a shows the solvent (distillate) fingers (in cyan/green color) in the heavy oil medium (brown) right before the fracture was heated and mixture quality improved after 35 minutes (**Fig. 15b**). This corresponds to the time at which the fracture temperature was raised to 38.5°C and the matrix temperature was 31.3°C. In this case, solvent started boiling and the temperature in the fracture and matrix reached 75°C and 55°C, respectively. At this point, the solvent contained in the fracture quickly vaporized and drained toward the production well, and, at the same time, solvent vapor developed in the matrix started to feed the fracture and get retrieved (**Fig. 16)**.

Even though the heating transfer was only applied to the fracture zone (point heating), the bubble growth did not show a similar behavior as in the other cases (Experiments 1 and 2). This is due to the multiple components present in the solvent, which leads to faster desorption of solvent in some pores randomly. This could also be explained by the Kelvin effect. The components present in the distillate (Figure 3) lighter than C_7 started boiling as indicated by lower boiling temperature compared to the previous experiments, and draining via fracture (Fig. 16). The overall solvent vapor growth is shown in Figure 7m through p.

6.5 Effect of wettability in Experiment 5.

After modifying the wettability of the same micromodel to more oil-wet following the procedures suggested by Naderi and Babadagli [39], and Mohammed and Babadagli [33], Experiment 5 was implemented following the same procedure as described. **Figure 17** shows the micromodel after solvent injection phase was completed at room conditions (Figure 16**a**) and after the fracture was heated up to 57°C during 1 hour from the fracture zone until the first signal of solvent vaporization appeared (Fig. 17b).

During this experiment, the solvent vaporization started in the vicinity of the production well and expanded horizontally toward the injection point. At the same time, vapor blobs growing in the matrix near the production point expanded mainly in the west direction and displaced solvent toward the matrix (**Figure 18**). The Figure 7**q to t** provides a general view of the pattern growth.

The effect of wettability in the distribution of vapor bubbles and the preferred pathways in the matrix was explored using close up images (at the pore scale) (**Fig. 19**). Note that the

same heating conditions (experiment 4 and 5) were applied and the focus was on the same section of the micromodel (the red ovals for both cases in Fig. 19).

In the oil-wet case (Fig. 19b) it can be observed that some vapor bubbles invaded the pores with smaller pore throats compared to the water-wet case. This type of pore is indicated inside the small red circles in Figure 19a.

Although there is no water phase present in the experiments, having a vapor phase and two liquid phases (solvent and oil+solvent mixture) yielded two immiscible phases that makes the wettability critical in the stability of the porous medium. **Figure 20** shows the change in the distribution of boiled solvent for both cases under the same micro model area during the heating step for Experiments 4 (water-wet) and 5 (oil-wet). The shots were taken right after the bubbles invaded the pores and one minute later. As observed in Figure 20a, the vaporized solvent in this case was present as a thin film inside the thin diameter pores (circled area) and did not reach the pore walls. Although the phase seems to follow tortuous paths for the adjacent pores, the connections were not stable and broke in a very short time, as pointed in the circled area in Figure 20b, resulting in a discontinuity of the vapor phase. On the other hand, the oil-wet case showed a quite different behavior. The solvent bubbles filled the pores due to more oil-wet nature (Figure 20c), and created more stable (and continuous) vapor phase that lasted a longer period of time (Fig. 20d) compared to the water-wet case.

7. Conclusions and Remarks

Solvent retrieval during heavy-oil recovery applications in heterogeneous porous media was investigated visually at pore scale using micro models. Liquid solvents were used due to higher mixing capability yielding more ultimate oil recovery. The retrieval of this type of solvent was achieved by heating the system and increased the temperature up to the boiling point of the solvent inside the porous media. Solvent diffused into the matrix start bubbling and changed its phase to vapor from liquid. The expanding solvent was expected to flow into the fracture and retrieved by producing it via higher permeability fracture system. This process was analyzed in this paper taking into account the factors playing a role, including heating -boundary- conditions, solvent type, matrix wettability, initial

conditions in the fracture (fluid type occupying it), and temperature. The following conclusions can be withdrawn from this study:

1. Solvent vaporization was found to be more efficient for the case in which fracture (point) heating was applied. It showed less oil trapped inside the matrix surrounding by its vapor phase and vapor chamber moved more easily to the fracture.
2. Kelvin effect might explain why vaporization was achieved below its bulk boiling point value for all the micro model experiments.
3. Since boiling point is an intrinsic property of the hydrocarbons employed, the heavier the composition in the fracture, the higher its boiling point despite the Kelvin effect reduction. Therefore, for the case in which fracture was filled with oil, and under the operating conditions used in the experiment, no effective solvent recovery was achieved.
4. Bubbles break up and solvent trapped by this phenomena was more frequently observed for the original wettability case (glass model, which was water-wet) compared to the wettability altered case to more oil-wet, in which the vapor bubbles' communication remained weaker and discontinued.
5. The nucleation of bubbles and phase conversion from liquid to vapor followed different patterns for heptane and distillate oil. The nucleation process started earlier in the case of distillate, likely due to vaporization of lighter and aromatic components that pure heptane case. The bubble growth followed more discontinuous patterns in the distillate case. For more efficient solvent retrieval (i.e., the heavier components of the distillate), higher temperatures are needed. Considering distillate is more efficient in heavy-oil recovery due to its aromatic components as shown in earlier studies [19,36,37], it is worth expanding this research to estimate the optimal temperature range of the distillate for an efficient retrieval.

This outcome of this research would be useful in the solvent applications for heavy-oil recovery from fractured water or oil wet systems (especially carbonates), layered systems

showing distinct permeability contrast, unconsolidated oil sands that developed a wormhole network after a severe CHOPS process.

Acknowledgments

This research was conducted under Tayfun Babadagli's Natural Sciences and Engineering Research Council of Canada (NSERC) Industrial Research Chair in Unconventional Oil Recovery (the industrial partners are Canadian Natural Resources Limited, Suncor Energy Incorporated, Touchstone Exploration, Sherritt Oil, Apex Engineering Incorporated, Husky Energy, and Pemex) and an NSERC Discovery Grant (RES0011227).

References

[1] Farouq, S.G. Snyder, Miscible Thermal Methods Applied to a Two-Dimensional, Vertical Tar Sand Pack, With Restricted Fluid Entry, Journal of Canadian Petroleum Technology **12** (1973) 22-26.
[2] A.M Butler, I.J. Mokrys, Recovery of Heavy Oils Using Vaporized Hydrocarbon Solvents: Further Development of the Vapex Process. Journal of Canadian Petroleum Technology **32** (1993) 56-62.
[3] S.K. Das, R.M. Butler, Countercurrent Extraction of Heavy Oil and Bitumen, Paper SPE 37094 presented at the International Conference on Horizontal Well Technology (1996a) Calgary, Alberta, Canada, 18-20 November.
[4] S.K. Das, R.M. Butler, Diffusion Coefficients of Propane and Butane in Peace River Bitumen, Canadian Journal of Chemical Engineering **74** (1996b) 986-992.
[5] A. Farouq, Bitumen Recovery from Oil Sands, Using Solvents in Conjunction with Steam. Journal of Canadian Petroleum Technology **3** (1976).
[6] T.N. Nasr, G. Beaulieu, H. Golbeck, et al. Novel Expanding Solvent-SAGD Process "ES-SAGD," Journal of Canadian Petroleum Technology (technical note) **42** (2003) 13-16.
[7] T.N. Nasr, O.R. Ayodele, Thermal Techniques for the Recovery of Heavy Oil and Bitumen, Paper SPE 97488, SPE International improved Oil Recovery Conference in Asia Pacific, Kuala Lumpur, Malaysia, 2005.
[8] R.P. Léauté, Liquid Addition to Steam for Enhancing Recovery (LASER) of Bitumen with CSS: Evolution of Technology from Research Concept to a Field Pilot at Cold Lake, Paper number 79011, SPE/Petroleum Society of CIM/CHO International Operations and Heavy Oil Symposium and International Horizontal Well Technology Conference, Calgary, Alberta, Canada, 2002.
[9] L. Zhao, Steam Alternating Solvent Process, Paper SPE 86957, International Thermal Operations and Heavy Oil and Western Regional Meeting, Bakersfield, California, 2004.
[10] L. Zhao, T. Nasr, G. Huang, et al., Steam Alternating Solvent Process: Lab Test and Simulation, Journal of Canadian Petroleum Technology **44** (2005) 37-43.

[11] A.M. Al-Bahlani, T. Babadagli, Field Scale Applicability and Efficiency Analysis of Steam-Over-Solvent Injection in Fractured Reservoirs (SOS-FR) Method for Heavy-Oil Recovery. Journal of Petroleum Science and Engineering **78** (2011a) 338-346.
[12] A.M. Al-Bahlani, T. Babadagli, SOS-FR (Solvent-Over-Steam Injection in Fractured Reservoir) Technique as a New Approach for Heavy-Oil and Bitumen Recovery: An Overview of the Method. Energy and Fuels **25** (2011b) 4528-4539.
[13] A.M. Al-Bahlani, T. Babadagli, Visual Analysis of Diffusion Process During Oil Recovery Using Hydrocarbon Solvents and Thermal Methods, Chemical Engineering Journal **181-182** (2012) 557-569.
[14] V. Pathak, T. Babadagli, N.R. Edmunds, Experimental Investigation of Bitumen Recovery from Fractured Carbonates Using Hot-Solvents, Journal of Canadian Petroleum Technology **52** (2013) 289-295.
[15] V. Pathak, T. Babadagli, N.R. Edmunds, Mechanics of Heavy Oil and Bitumen Recovery by Hot Solvent Injection, SPE Reservoir Evaluation and Engineering **15** (2012) 182-194.
[16] V. Pathak, T. Babadagli, N.R. Edmunds, Heavy Oil and Bitumen Recovery by Hot Solvent Injection, Journal of Petroleum Science and Engineering **78** (2011) 637-645.
[17] T. Babadagli, Development of Mature Oil Fields – A Review. Journal of Petroleum Science and Engineering **57** (2007) 221-246.
[18] S. Gupta, S Gittins, P. Picherack, Insights into Some Key Issues with Solvent Aided Process, Journal of Canadian Petroleum Technology **43** (2003) 54-61.
[19] K. Naderi, T. Babadagli, G. Coskuner, Bitumen Recovery by the SOS-FR (Steam-Over-Solvent Injection in Fractured Reservoirs) Method: An Experimental Study on Grosmont Carbonates, Energy and Fuels **27** (2014) 6501-6517.
[20] K. Naderi, T. Babadagli, An Evaluation of Solvent Selection Criteria and Optimal Application Conditions for the Hybrid Applications of Thermal and Solvent Methods (2015), in review.
[21] S. Gupta, S. Gittins, Measurement of Recovered Solvent in Solvent Aided Process, Paper CSUG/SPE 136402, SPE Canadian Unconventional Resources & International Petroleum Conference, Calgary, Alberta, Canada, 2010.
[22] N. Edmunds, B. Maini, J. Peterson, Advanced Solvent-Additive Processes via Genetic Optimization (2009) Paper PETSOC 2009-115.
[23] M. Keshavarz, R. Okuno, T. Babadagli, Optimal Application Conditions for Steam-Solvent Coinjection, Paper SPE 165471, SPE Heavy Oil Conference, Calgary, Alberta, Canada, 2013.
[24] Reservoirs Using Hybrid Optimization Techniques. Journal of Canadian Petroleum Technology **51** (6) (2012a) 437-44.
[25] M. Al-Gosayir, T. Babadagli, J. Leung. Optimization of SAGD and Solvent Additive SAGD Applications: Comparative Analysis of Optimization Techniques with Improved Algorithm Configuration. Journal of Petroleum Science and Engineering 98-**99** (2012b) 61-68.
[26] M. Al-Gosayir, J. Leung, T. Babadagli. Optimization of SOS-FR (Steam-Over-Solvent Injection in Fractured Reservoirs) Method Using Hybrid Techniques: Testing Cyclic Injection Case. Journal of Petroleum Science and Engineering **110** (2013) 74-84.
[27] S. Gupta, S Gittins, Effect of Solvent Sequencing and Other Enhancements on Solvent Aided Process, Journal of Canadian Petroleum Technology **45** (2007) 57-61.
[28] I.D. Gates, A.M.H. Gutek, US Patent No. 7464756, 2008.

[29] R.P. Léatué, B.S. Carey, Liquid Addition to Steam for Enhancing Recovery (LASER) of Bitumen with CSS: Results from the First Pilot Cycle, Journal of Canadian Petroleum Technology. **46** (2007) 22-30.
[30] S. Gupta, S Gittins, S. Canas, Methodology for Estimating Recovered Solvent in Solvent-Aided Process, Journal of Canadian Petroleum Technology **51** (2012) 339-350.
[31] T. Babadagli, Al-Bahlani, Hydrocarbon Recovery Process for Fractured Reservoirs, U.S. Patent No. 8,813,846, 2014.
[32] T. Babadagli, Al-Bahlani. "Hydrocarbon Recovery Process for Fractured Reservoirs," Canadian Patent Application No: 2,681,823 filed on Oct. 5, 2009, granted on Feb. 5, 2015.
[33] M. Mohammed, T. Babadagli, Efficiency of Solvent Retrieval during Steam-Over-Solvent Injection in Fractured Reservoirs (SOS-FR) Method: Core Scale Experimentation, Paper SPE -165528-MS, SPE Heavy Oil Conference, Calgary, Alberta, Canada, 2013.
[34] C.U. Hatiboglu, T. Babadagli, Diffusion Mass Transfer in Miscible Oil Recovery: Visual Experiments and Simulation, Transport in Porous Media **74** (2008) 169-184.
[35] C.U. Hatiboglu, T. Babadagli, Lattice-Boltzmann Simulation of Solvent Diffusion into Oil Saturated Porous Media, Physical Review E **76** (2007) 066-309.
[36] A. Marciales, T. Babadagli, Selection of Optimal Solvent Type High Temperature Solvent Applications in Heavy-Oil and Bitumen Recovery, Paper SPE 170021, SPE Heavy Oil Conference, Calgary, Alberta, Canada, 2014a.
[37] A. Marciales, T. Babadagli, Solvent Selection Criteria Based on Diffusion Rate and Mixing Quality for Different Temperature Steam/Solvent Applications in Heavy-Oil and Bitumen Recovery, Paper SPE 169291, SPE Latin American and Caribbean Petroleum Engineering Conference, Maracaibo, Venezuela, 2014b.
[38] J. Berg, An Introduction to Interfaces and Colloids, The Bridge to Nanoscience, Singapore: World Scientific Publishing Co. Pte. Ltd, 2010.
[39] K. Naderi, T. Babadagli, Pore-Scale Investigation of Immiscible Displacement Process in Porous Media under High- Frequency Sound Waves, Journal of Fluid Mechanics **680** (2011) 336-360.
[40] Risk Reactor, Inc., www.riskreactor,com, accessed February 2014.
[41] W. Köhler, S. Wiegand, Thermal Nonequilibrium Phenomena in Fluid Mixtures, Lecture Notes in Physics **584** (2002).

Table 1. Oil and solvents properties.

Hydrocarbon samples	Density g/ml @ 25 °C	Viscosity, cP @ 25 °C	Refractive index, *n* @25°C	Boiling point, at 1 atm. , °C
Mineral Oil	0.8734	250	1.47635	TBP curve
Distillate	0.738	0.742	1.41025	TBP curve
Heptane	0.683	0.294	1.38418	98°C

Table 2. Oil (LMO-light mineral oil), solvent and heating type combinations applied during the experiments.

Experiment No.	Solvent type	Oil type	Fracture content	Heating section	Wettability
1	C_7	LMO	C_7	Fracture	Water wet
2	C_7	LMO	LMO	Fracture	Water wet
3	C_7	LMO	C_7	Matrix	Water wet
4	Distillate	LMO	Distillate	Fracture	Water wet
5	C_7	LMO	C_7	Fracture	Oil wet

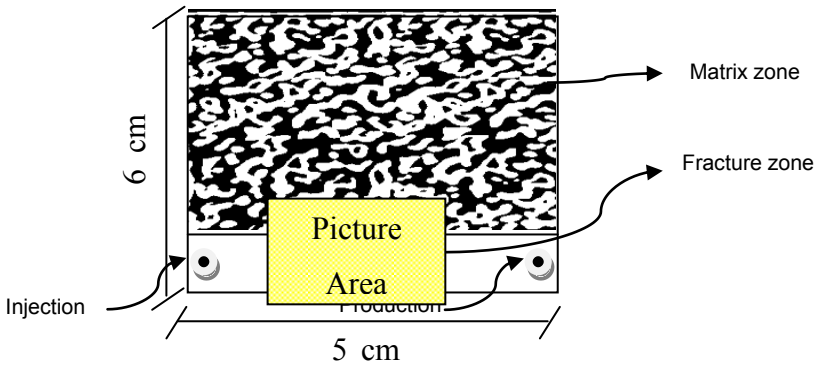

Figure 1: Micromodel scheme and picture area.

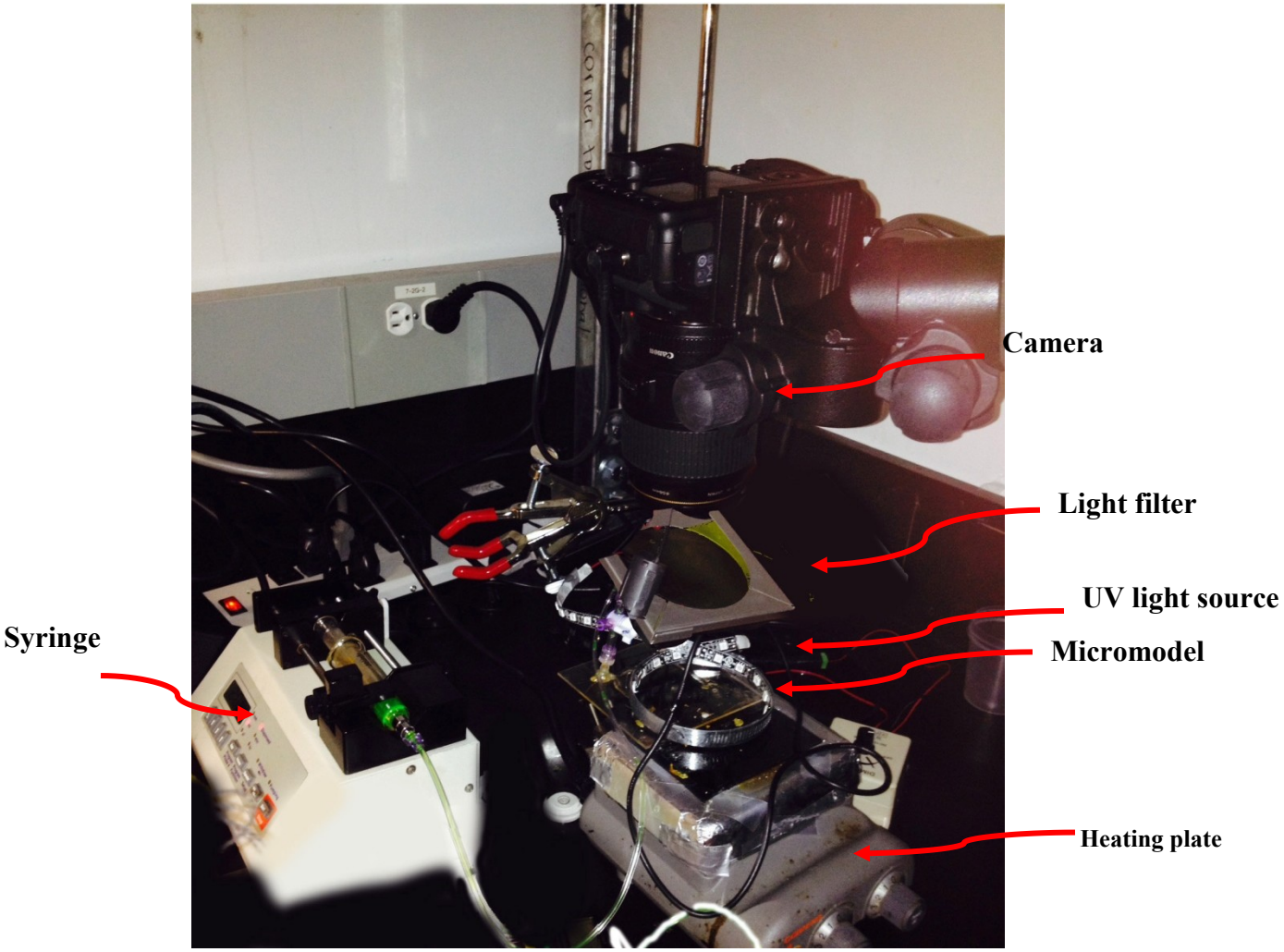

Figure 2: Experimental set up.

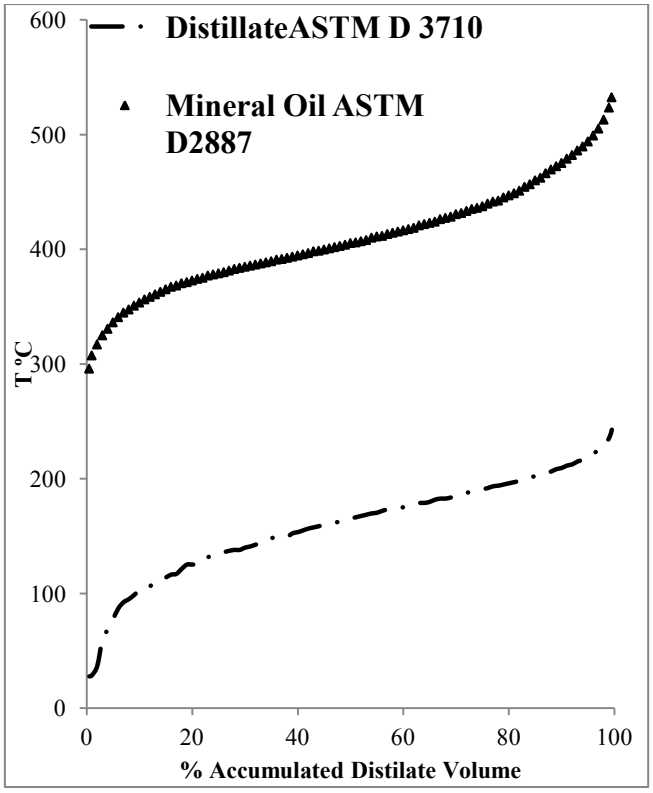

Carbon size number	FBP °C	Distillate	LMO
IBP-C_5	36.1	1.918	---
C_6 -C_{10}	173.9	56.122	---
C_{11}- C_{13}	235	40.937	---
C_{14}-C_{20}	344	---	1.5
C_{21}-C_{30}	449	---	55.9
C_{31}-C_{40}	522	---	40.3
C_{41}-C_{50}	575	---	---
C_{51}-C_{60}	615	---	---
C_{61}-C_{70}	647	---	---
C_{71}-C_{80}	675	---	---
C_{81}-C_{90}	700	---	---
C_{91}-C_{100}	720	---	---
C_{100+}	720+	---	---

Figure 3: Boiling range distribution for LMO and Distillate.

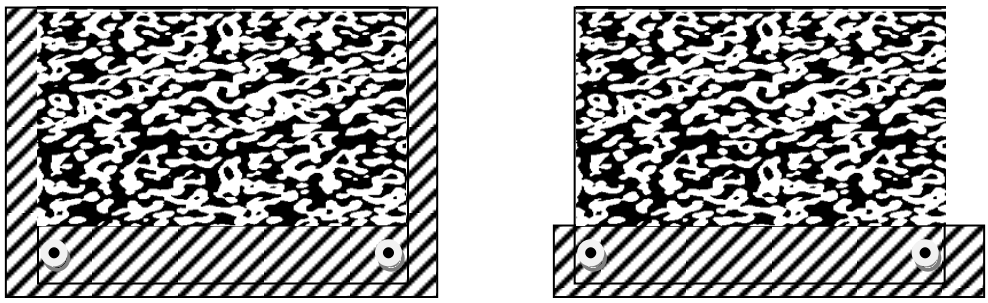

Figure 4: Schematic representation of heat distribution: a) matrix, b) fracture.

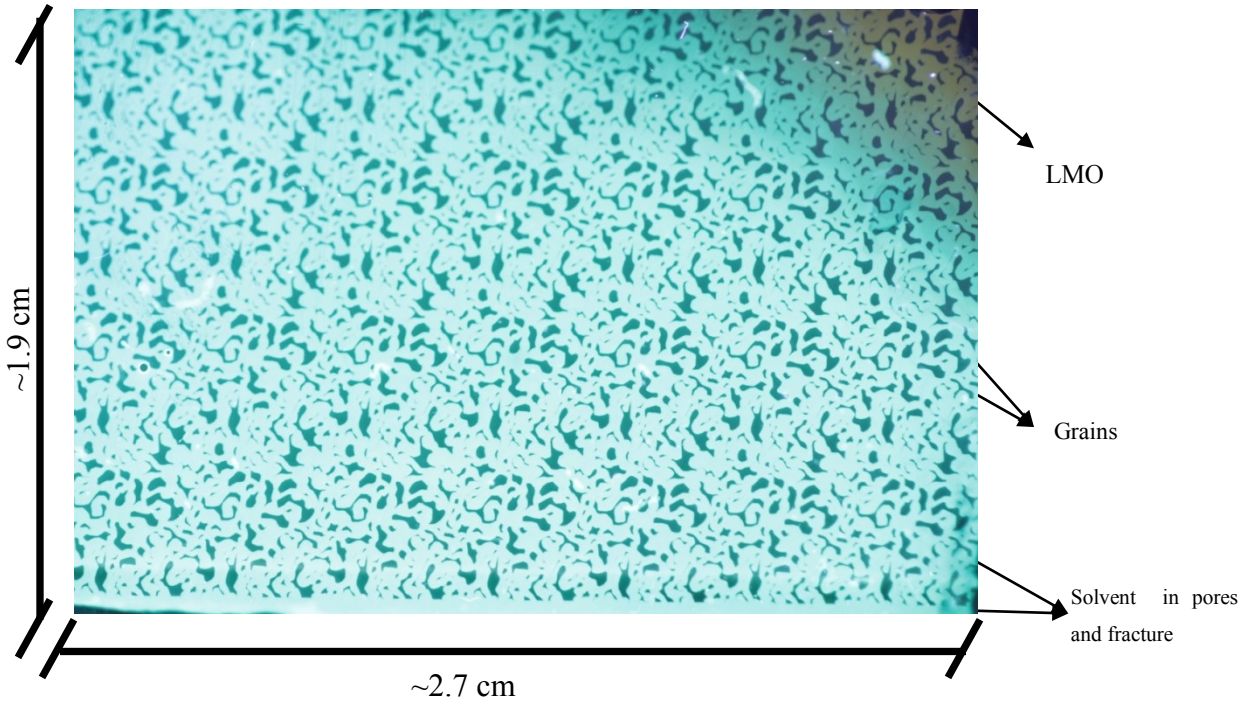

Figure 5: Micromodel after solvent saturation and before starting the heating step for Experiment 1.

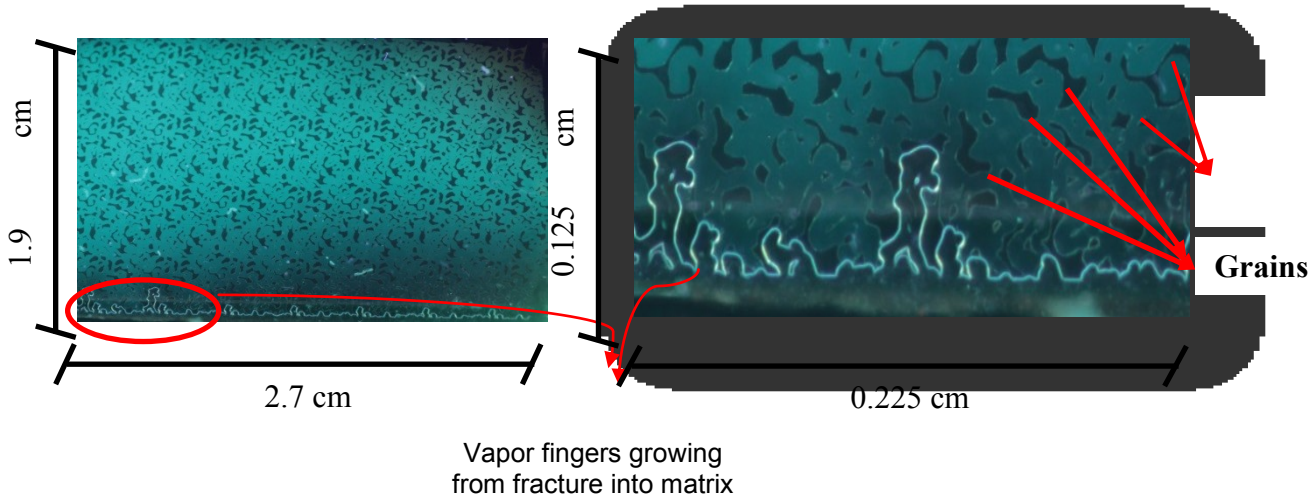

Figure 6: Bubble growth for fracture heating type in Experiment 1.

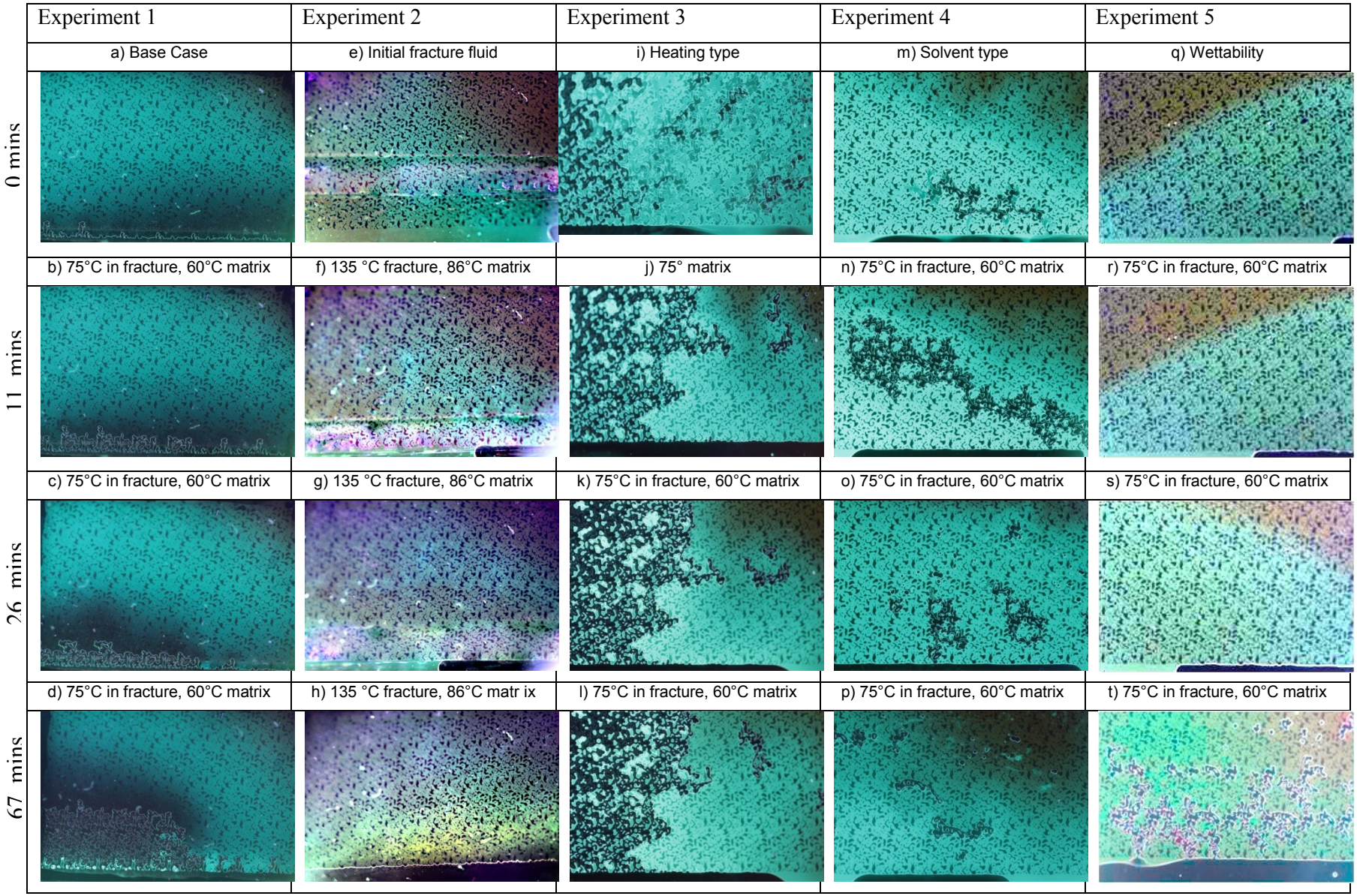

Figure 7: Macro visualization of solvent vaporization patterns for all the experiments at different times. "0 min" corresponds to the point first bubble is observed.

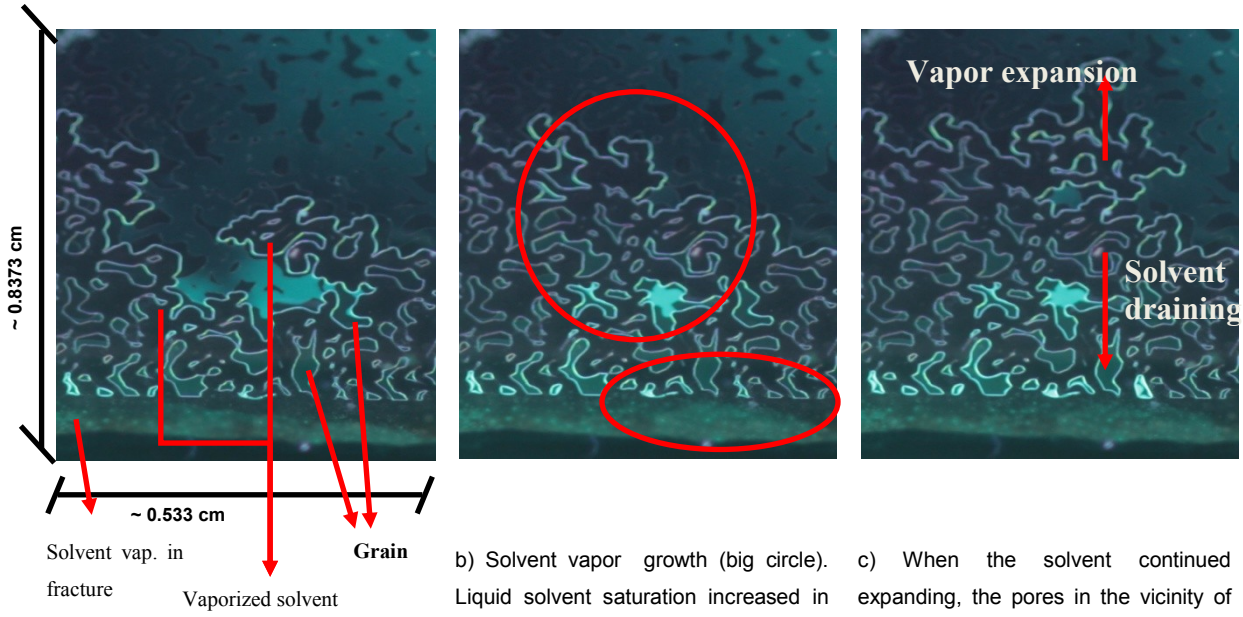

a) Initial condition.

b) Solvent vapor growth (big circle). Liquid solvent saturation increased in the pores adjacent to the fracture and fracture itself.

c) When the solvent continued expanding, the pores in the vicinity of the fracture showed increased saturation.

Figure 8; Solvent retrieval mechanism.

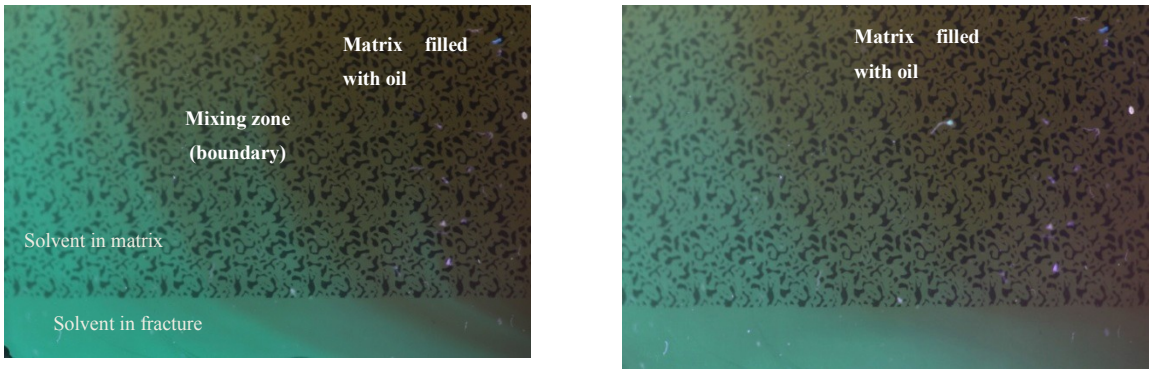

a) After solvent saturation and diffusion

b) Improve mixing due to heating

Figure 9: Micromodel before solvent phase change in Experiment 3.

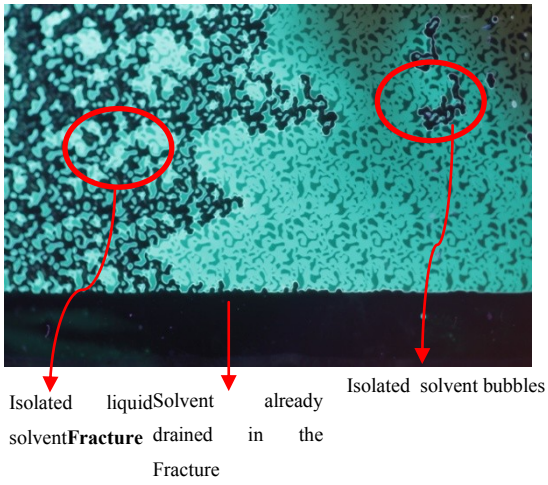

Figure 10: Phase change of solvent when homogeneous (whole system) heating is applied in Experiment 3.

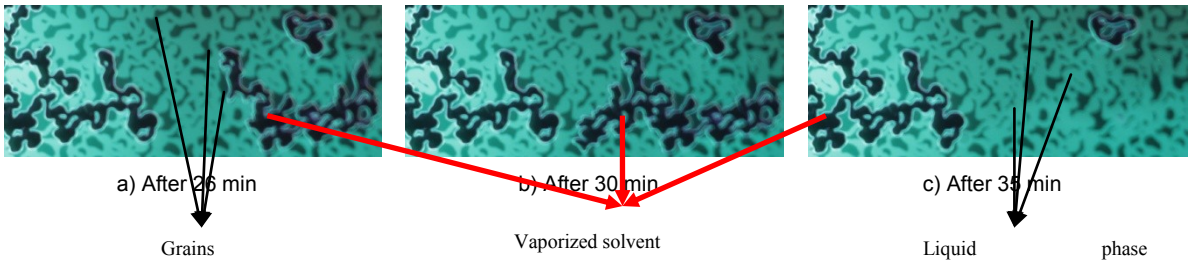

Figure 11: Recovery mechanisms and bubble migration in Experiment 3.

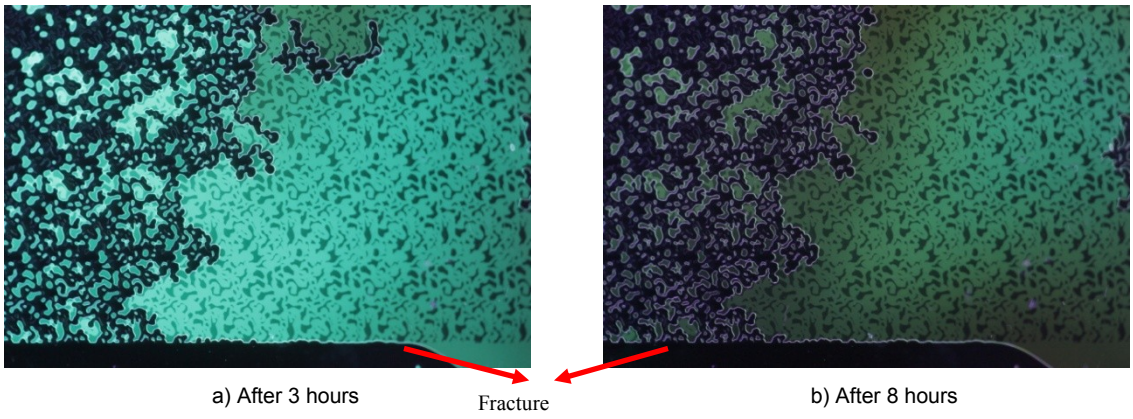

Figure 12; Time effect in homogeneous heating.

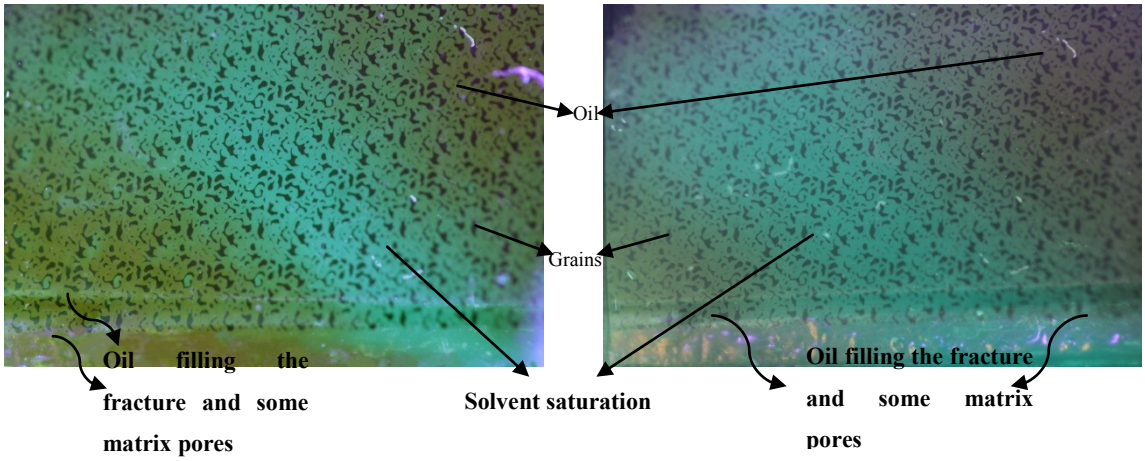

a) Micromodel before starting the heating step

b)Mixing quality improvement due heat transfer

Figure 13: Pore and matrix oil-solvent saturation before any phase change in Experiment 2.

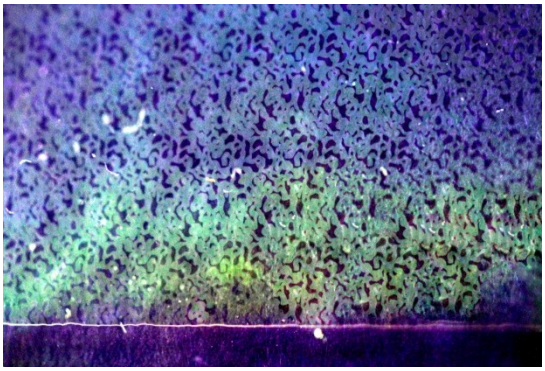

Figure 14: Solvent evaporation after 6 hours of constant heating.

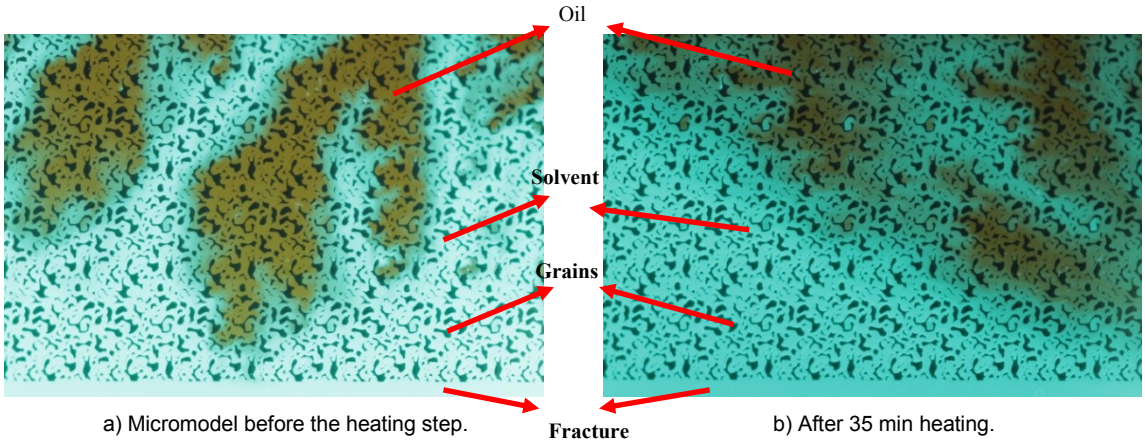

a) Micromodel before the heating step.

b) After 35 min heating.

Figure 15: Mixing quality improved due to temperature increase in Experiment 4.

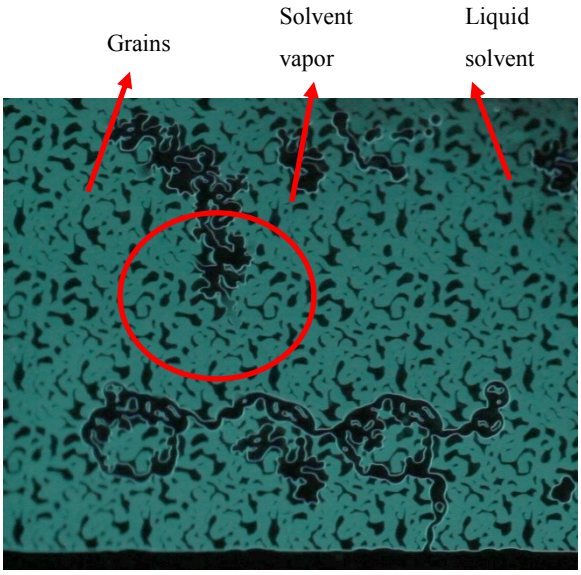

a) Initial system. t=0.

b)Upper vapourized solvent (arrowed circle) expands downward contracting lower vapor region and pushing solvent toward the fracture (dashed square) t=1 sec.

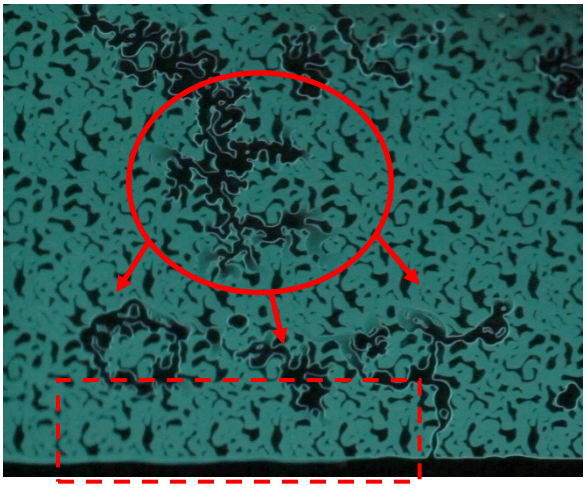

c) Upper solvent vapor continues it expansion by the displacement of the solvent downward. t=2 sec.

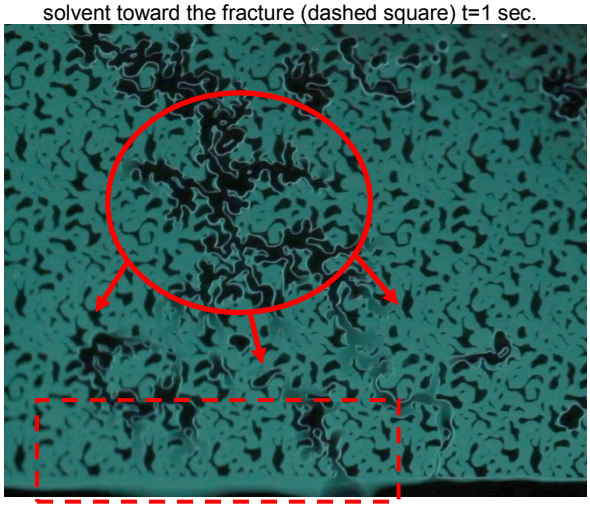

d) Some solvent is driven through the fracture. t=3 sec.

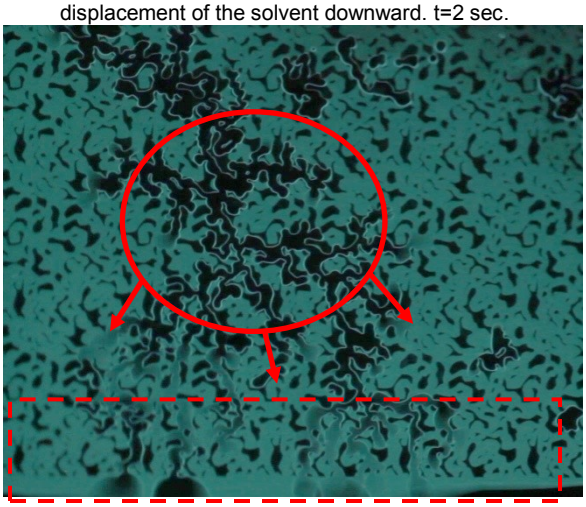

e) Solvent continues producing in the fracture. t=4 sec.

f) Vapor phase growth toward the fracture. t=5 sec.

g) Vapor phase grows and expands starts communicating the fracture. t=6 sec.

h) Vapor communication starts with the fracture. t=7 sec.

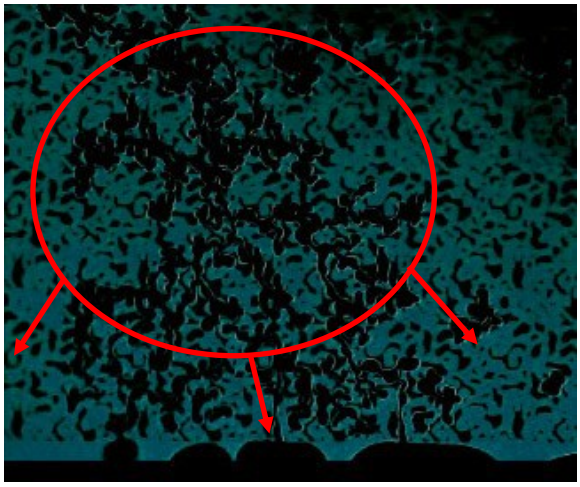

i) More bubbles are connected to the fracture. t=8 sec.

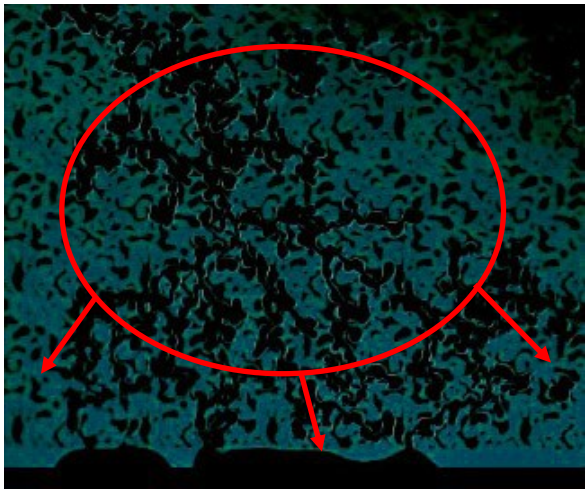

j) Vaporized solvent is drained via fracture by the existent vapor channels and through liquid solvent displacement. t=9 sec.

Figure 16: Solvent recovery mechanism for Experiment 4.

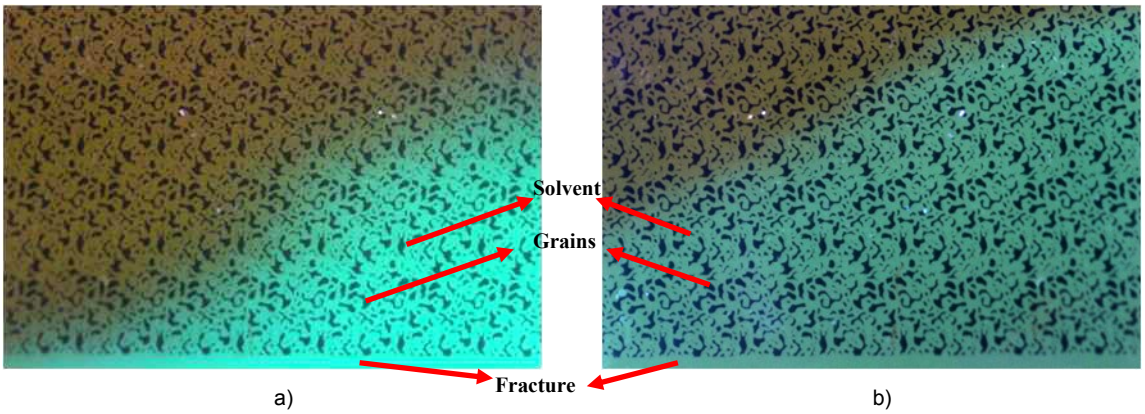

a) b)

Figure 17.:Matrix oil-solvent mixing before a) temperature increase and b) phase change in Experiment 5.

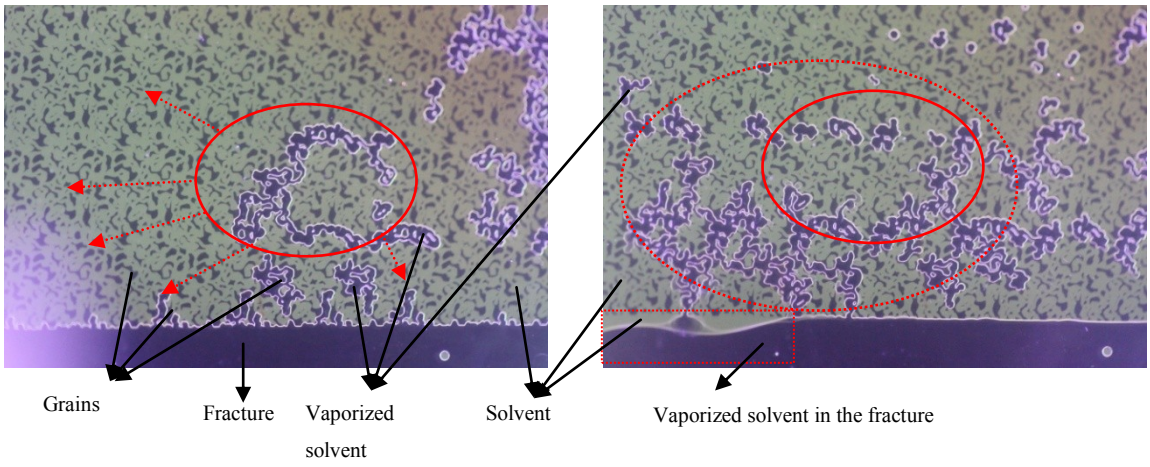

a) Initial condition. Dashed arrows points the direction of bubble growing.

b) Dashed oval indicates the region for vapor expansion and bubbles break up. Dash square shows the solvent produced in the fracture.

Figure 18: Recovery mechanism in Experiment 5.

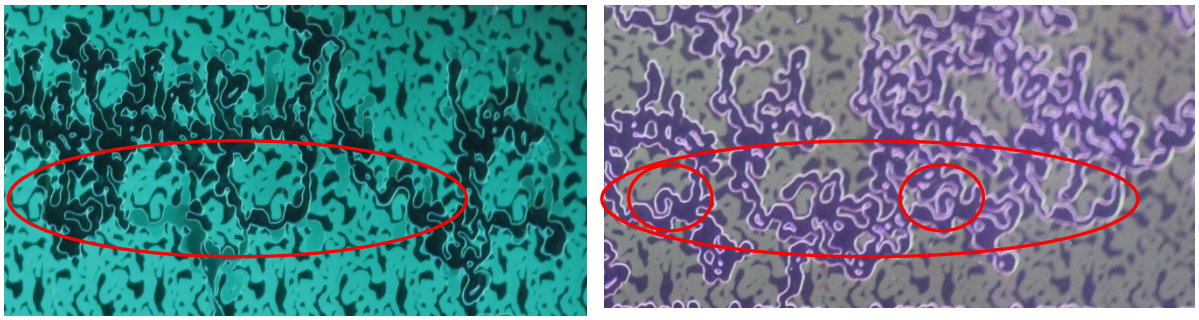

a) Water-wet

b) Oil-wet

Figure 19: Water-wet vs. oil-wet case.

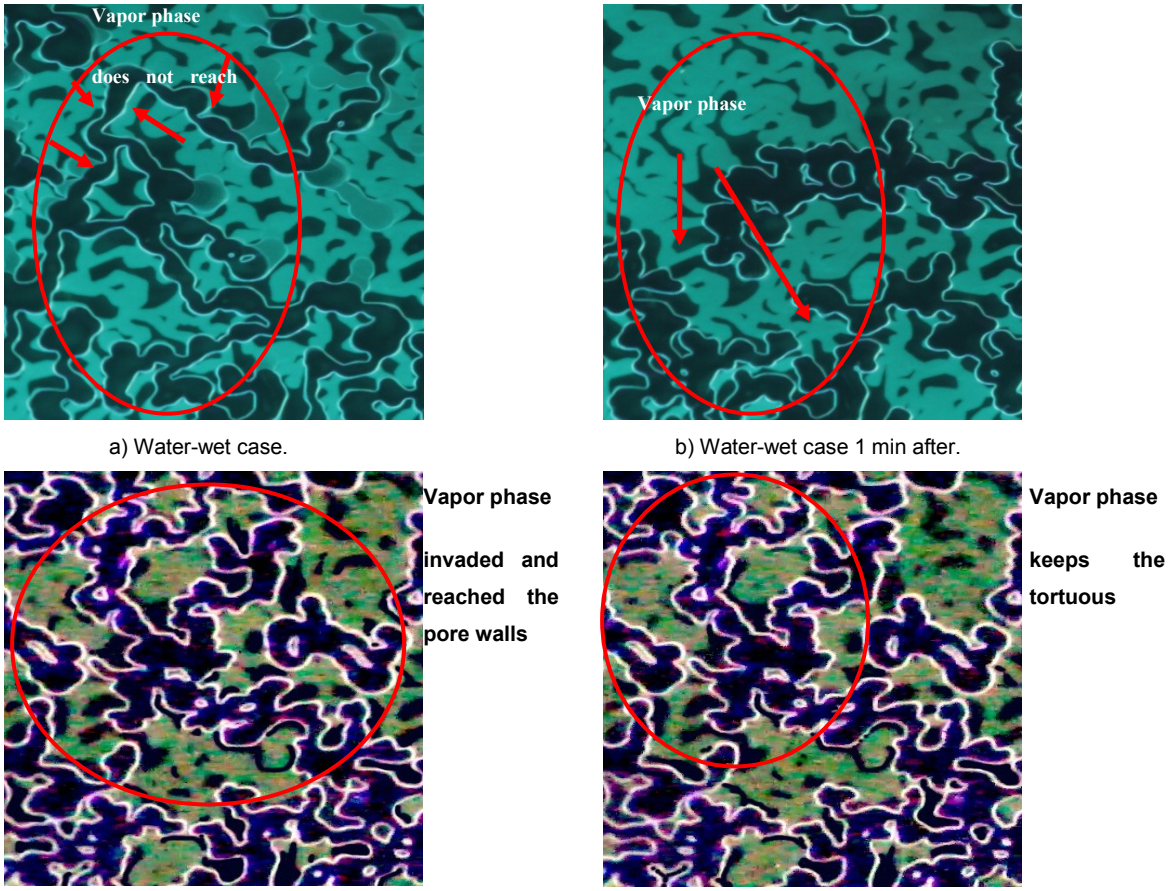

a) Water-wet case. b) Water-wet case 1 min after.

c) Oil-wet case. d) Oil-wet case 1 min after.

Figure 20: Vapor phase stability water-wet (a and b) vs. oil-wet case (c and d).

CHAPTER 5: CONTRIBUTION AND RECOMMENDATIONS

Major Conclusions and Contributions

1. A case study representing different possible combinations of solvent-oil pairs with varying composition was established to propose the optimal solvent type considering both mixing quality and diffusion rate. The oil samples employed have viscosities between 40–460.000 cP at 25°C, different carbon size number and densities. Also, a wide range of -liquid- solvent types, C_7, C_{10} and a mixture from C_6 to C_{14} with aromatic components (distillate oil) were tested.

2. The molecular or bulk diffusion rate for the liquid-liquid experiments was determined for different solvent types. The UV light method was applied to mineral oil samples and X-ray CAT scanning was applied when heavy crude oil samples were examined. Both methods were improved through image processing using MATLAB® (for the first case) and DataViewer® (for the second case).

3. Viscosity and density reduction at different concentration of solvents at different temperatures were analyzed along with asphaltene titration tests. It was shown that the lighter the molecular weight of the solvent, the faster the diffusion rate, the higher the density and viscosity reduction, and the higher asphaltene precipitation. Optimal solvent concentration was defined (to be in the range of 20–40 % volume in the mixture) in order to obtain a drastic reduction of original oil viscosity and density while minimizing asphaltene precipitation.

4. The bulk solvent characteristics (fluid-fluid interaction) related to mixing quality and diffusion rate were shown to be consistent with the oil recovery through solvent-oil-rock interaction experiments. The lower the molecular weight of the solvent, the higher the diffusion rate and, hence, the recovery rate. The lower the asphaltene precipitation of the solvent, the higher ultimate recovery. Additionally, suitable solvent types and critical solvent concentrations were defined for an efficient oil recovery process.

5. Temperature was a critical factor impacting oil recovery efficiency. When it came closer to the boiling point of the solvent, its efficiency decreased due to lower mixing quality caused by solvent evaporation inside the pores and pore blocking due to precipitated material. When high concentration of solvent is employed, oil recovery is faster than the case of its half amount is employed in a longer period of time. Hence, starting with high concentrations of solvent with a high diffusion rate solvents is a plausible approach.

6. Non iso-thermal solvent injection application in heterogeneous porous media was studied at the pores scale using micromodels. The solvent retrieval process from matrix (low permeability part) at variable temperatures was qualitatively analyzed for different wettability, reservoir heating conditions, and solvent type. Also observed was the variation of the thermodynamic properties of the solvents in porous media due to the phenomenon called the Kelvin effect. Due to this effect, the solvent vaporized inside the micro pores around 20°C lower than its bulk boiling

point.

7. The information collected during the experiments run in Chapters 1 and 2 would be useful since it provides data of representative oil and solvent types for its consolidation into fitting equations provided in literature and being used as input data for oil simulation programs, in both upstream and downstream industry.

Recommendations and Future Work

1. Molecular diffusion rate was measured at room conditions and temperature effect was observed indirectly through rock-solvent experiments. However, bulk diffusion test, in which solvent and oil are placed at the same temperature value, would contribute to clarifying this issue.

2. The experiments run in Chapters 2 and 3 suggested that solvent application sequence starting with light solvent and progressively increasing its molecular size to heavier one. However, this set of experiments could not be achieved in this thesis. More work is needed to propose optimal sequence of different types of solvents and their concentrations. In conjunction with this, pore plugging due to asphaltene deposition needs to be studied as lighter solvents used in the beginning of the process would cause severe asphaltene precipitation.

3. The experiments run in Chapters 2 and 3 showed how recovery efficiency by heptane and decane decreased when temperature of the experiment is increased closer to its boiling point. But this value was much lower than its bulk boiling point. This phenomenon can be explained by the Kelvin effect mentioned in Chapter 4. Hence, it is suggested to extend this study by using an average pore size of the Berea sandstone cores estimated through X-ray CAT scanning and interfacial tension values for the solvents measured at the experimental temperatures. When this information is collected, the Thompson equation can be also used to estimate the boiling point of the solvents in the porous media to propose suggested temperature ranges for optimal solvent retrieval.